REMARKS

Claims 88, 90, 91, and 94-98 are under examination in this case. These claims stand rejected under 35 U.S.C. § 112, first paragraph, and 35 U.S.C. § 102(b). Claims 88 and 90 have been cancelled. Applicants reserve the right to pursue this subject matter in this or a future, related application. As applied to claim 91 and its dependent claims, the rejections are addressed below.

Rejections under 35 U.S.C. § 112, first paragraph

Claims 88, 89, 91, and 94-98 stand rejected under 35 U.S.C. § 112, first paragraph, as failing to comply with the written description requirement. Claims 88 and 89 have been cancelled. As applied to amended claim 91 and its dependent claims, this rejection is respectfully traversed.

As amended, claim 91 requires that a modification be located directly adjacent to at least one amino acid of the seven sequence locations recited in claim 91. Applicants' specification provides a clear written description of this subject matter, and, with respect to the current claims, the Office's assertion that the claims fail to provide a "sufficient recitation of distinguishing identifying characteristics" cannot be maintained. Indeed, the sites for AAV modifications are recited with complete specificity. Neither can it be asserted that the "large genus is not adequately defined by a structure/function correlation." Applicants have identified sites in the AAV capsid sequence amenable to modifications using their inventive approach of studying structure and protein alignments of different parvoviruses, such as AAV2, CPV, and B19, and choosing appropriate positions for modification. Applicants have demonstrated the general success of this approach in the present specification. Moreover, sites identified by Applicants and covered by claim 91 have also been confirmed by others as positions amenable to modification without destroying infectivity, and, where tested, modifications that reduce antigenicity.

In particular, Applicants submit herewith a number of references, published after Applicants' priority date, relevant to the current claims. Of these references, Wu et al. (*J. Virol.* 74: 8635-8647, 2000; copy enclosed) demonstrates that insertions at three of Applicants' claimed positions are well tolerated and further that every site encompassed by Applicants' claims that was tested by Wu was amenable to modification without destruction of infectivity. In particular, Wu states, at page 8645, left col., that:

> Of the positions identified as being on the surface of the capsid, we found six that potentially are capable of accepting foreign epitope or ligand insertions for retargeting the viral capsid to alternative receptors. These are...the loop I region (aa 266), the loop IV region (near aa 447 and 591)...

These positions correspond to modification sites, SEQ ID NO: 2 (amino acids 257-266), SEQ ID NO: 4 (amino acids 443-452), and SEQ ID NO: 8 (amino acids 583-592) of Applicants' claims. (The remaining four sites specified by Applicants were not tested by Wu, as indicated by Table 1). Further evidence of the workability of Applicants' approach and recited AAV modification sites is provided by Shi (*Human Gene Ther.* 12: 1697-1711, 2001; copy enclosed) and Bartlett (US 2002/0192823; copy enclosed), each of which confirms that insertions at amino acid 587 (SEQ ID NO: 8) do not destroy AAV infectivity, as well as Shi and Bartlett (*Molecular Therapy* 7:515, 2003; copy enclosed), which extends this finding to amino acids 584 and 588. The Shi and Bartlett reference states that "insertions following amino acids 139, 584, or 588 were well tolerated and did not affect titer appreciably." Again, insertions at amino acid 584 and 588 are encompassed by SEQ ID NO: 8. In addition, the Office is directed to the very recent publication by Maheshri et al. (*Nature Biotech.* 24: 198, 2006; copy enclosed) and the review of that article by Asokan and Samulski (*Nature Biotech.* 24: 158, 2006; copy enclosed). These references describe experiments demonstrating that mutations produced by error-prone PCR at AAV positions 258 (SEQ ID NO: 2), 567 (proximal to SEQ ID NOS: 6, 7), 587 (SEQ ID NO: 8), 713 (SEQ ID NO: 9), and 716 (SEQ ID NO: 9) reduce AAV antigenicity, with dramatic reductions in antigenicity resulting from modifications

at positions 587 (SEQ ID NO: 8) and 716 (SEQ ID NO: 9) (Table 1, Figure 6A, p. 202, col. 2). This reference therefore confirms that of the seven locations specified in claim 91, four are amenable to modification and result in reduced antigenicity.

In view of the above evidence, Applicants request withdrawal of the rejections under 35 U.S.C. § 112, first paragraph. Applicants have provided scientific evidence that a number of different types of modifications, including insertion and PCR-based mutations (likely missense mutations and/or small deletions) can be made in the AAV capsid sequence at the sites particularly specified in claim 91 without destroying infectivity. In particular, of the seven recited positions, Applicants or others have demonstrated that modifications can successfully be made at five of those sites. Moreover, the submitted reference by Maheshri confirms that modifications at four of the seven sites reduce viral antigenicity. These results demonstrate not only that these particular sites are useful for generating infectious AAV having reduced antigenicity in a host but also confirming the general workability of Applicants' approach to identifying capsid positions amenable to modifications and useful for reducing antigenicity. This evidence is nowhere contradicted by reasoning or scientific publications provided by the Office. Applicants' current scope of protection is justified, and the rejections under 35 U.S.C. § 112, first paragraph should be withdrawn.

Rejection under 35 U.S.C. § 102

Claims 88, 90, 91, and 94-98 stand further rejected under 35 U.S.C. § 102(a) as being anticipated by Mamounas. Claims 88 and 90 have been cancelled. As applied to the current claims, this rejection is respectfully traversed.

The current rejection is based on the statement by the Office that Applicants' previous claim 91 was unclear as to the positions of the modifications. By the present amendment, Applicants have introduced clarifying claim language consistent with the teaching of the present specification, requiring that a modification be located directly

adjacent to one of a list of specifically recited amino acid locations. As the Office apparently agrees that these particular modification sites are nowhere disclosed by Mamounas, this basis for the rejection may be withdrawn.

In addition, Applicants wish to correct the record regarding previous arguments made in connection with the Mamounas reference. In Applicants' Reply mailed December 28, 2005, Applicants stated that the Mamounas reference failed to teach a structural protein of AAV that was capable of particle formation. Applicants now believe that statement to be in error in view of Table 2 of Mamounas, disclosing NCI 187 cells transduced with AAV/Ad vp1 hydro SCF, an AAV vector with an SCF insert, that apparently produces virus. Applicants note that this argument is unnecessary for supporting the patentability of the present claims.

CONCLUSION

Applicants submit that the claims are now in condition for allowance, and such action is respectfully requested. If there are any charges or any credits, please apply them to Deposit Account No. 03-2095.

Respectfully submitted,

Date: 22 May 2006

Karen L. Elbing, Ph.D.
Reg. No. 35,238

Clark & Elbing LLP
101 Federal Street
Boston, MA 02110
Telephone: 617-428-0200
Facsimile: 617-428-7045

treating group A *Streptococcus* with proteolytic enzymes such as trypsin destroyed the M protein antigen and thus altered the organism's antigenic composition.

Taking their cue from Lancefield's studies, Rodriguez-Ortega *et al.* treated serotype M1 group A *Streptococcus* strain SF370 with either trypsin or proteinase K, resulting in release of cell-surface protein fragments. Subsequently, these fragments were concentrated, analyzed by tandem mass spectrometry and identified using bioinformatics interrogation of the publicly available genome sequence of this strain. Seventy-two proteins were identified, including 43 proteins deduced from trypsin-cleaved peptides, 18 from proteinase K–released peptides and 11 proteins from peptides obtained from both proteases. Importantly, only 4 of the 72 proteins were predicted by PSORT to be cytoplasmic proteins, which means that the technique was highly specific for secreted and/or surface-associated proteins. These results were confirmed by fluorescence-activated cell sorting analysis using mouse polyclonal antibodies specific for 51 of the 72 identified proteins.

But the real beauty of this paper lies in the fact that the investigators did not rest on their technical accomplishments. Rather, they asked the logical next question: is there gold in the ore mined from cell-surface proteins? Based on the observation that 7 of the 11 previously reported group A *Streptococcus* protective antigens were identified successfully by their analysis, they tested the hypothesis that additional protective antigens were present among the 72 proteins identified. To do this, they first needed to define the cell-surface proteins of serotype M23 strain DSM2071, an organism (unlike strain SF370) that is highly virulent in mice. Seventeen proteins were identified in strain DSM2071, all of which have a homolog in strain SF370.

Turning next to the tried-and-true reverse vaccinology strategy pioneered by Chiron, 14 of the 17 proteins were overexpressed in recombinant form and used to immunize mice. Intranasal challenge of the immunized mice with strain DSM2071 revealed that two of the proteins conferred immunity in this model: M protein and a putative cell-envelope proteinase with a typical LPXTG cell-surface anchor motif. M protein has been known for decades to be a protective antigen[6], whereas the protective ability of the putative proteinase had not been previously described.

Lest we be accused of unbridled enthusiasm, let us note some limitations of the study. First, the analysis was conducted with group A *Streptococcus* grown *in vitro* in a rich medium and harvested at a single growth phase. Inasmuch as group A *Streptococcus* is known to significantly remodel its transcriptome and proteome under different growth conditions (including *in vitro* versus *in vivo*) and at different growth phases[8], the data presented are undoubtedly only a chapter rather than the whole book describing group A *Streptococcus* cell-surface proteins. Second, much of the work was done with strain SF370, an organism now known to be genetically divergent from the major M1 subclone responsible for the vast majority of contemporary infections[9]. Third, the authors identified only a relatively small proportion of the total number of proteins predicted by bioinformatics methods to be cell-anchored, lipoprotein, transmembrane-spanning and secreted. Especially noteworthy was the identification of only 6.5% of predicted transmembrane proteins. These issues should not be viewed as major flaws; rather, they are stimuli to conduct more extensive experiments that may produce additional discoveries.

What should be done next? From a broad perspective, clearly the strategy of Rodriguez-Ortega *et al.* can and should be applied to many other human and veterinary bacterial pathogens for which we lack efficacious vaccines. For example, *Staphylococcus aureus* continues to cause widespread human and animal disease. Undoubtedly, the strategy described by Rodriguez-Ortega *et al.* will be adopted rapidly by many investigators, and new vaccine candidates will be identified.

Several antigens have been reported to protect mice from experimental challenge with group A *Streptococcus*, generally in models of invasive infection[10]. It is recognized that a successful group A *Streptococcus* vaccine must be able to protect humans from pharyngotonsillitis caused by an extensive array of genetically diverse strains. Inasmuch as the cynomolgus macaque is the best animal model of this disease[11], it will be important to test candidate antigens for their ability to protect monkeys from pharyngotonsillitis. Once that important milestone has been achieved and appropriate safety tests have been conducted, it will be imperative to move vaccine candidates rapidly to clinical testing.

1. Scarselli, M. *et al. Trends Biotech.* **23**, 84–91 (2005).
2. Rodriguez-Ortega, M.J. *et al. Nat. Biotechnol.* **24**, 191-197 (2006).
3. Pizza, M. *et al. Science* **287**, 1816–1820 (2000).
4. Maione, D. *et al. Science* **309**, 148–150 (2005).
5. Carapetis, J.R. *Lancet Infect. Dis.* **5**, 685–694 (2005).
6. Lancefield, R.C. *Harvey Lectures*, **36**, 251 (1940–1941).
7. Lancefield, R.C. *J. Exp. Med.* **78**, 465–476 (1943).
8. Musser, J.M. & DeLeo, F. *Am. J. Pathol.* **167**, 1461–1472 (2005).
9. Sumby, P. *et al. J. Infect. Dis.* **192**, 771–782 (2005).
10. Bisno, A.L. *et al. Clin. Infect. Dis.* **41**, 1150–1156 (2005).
11. Virtaneva, K. *et al. Proc. Natl. Acad. Sci. USA* **102**, 9014–9019 (2005).

AAV does the shuffle

Aravind Asokan & R Jude Samulski

Directed evolution of adeno-associated virus (AAV) yields mutant vectors that can evade neutralizing antibodies.

DNA shuffling and related recombination techniques can dramatically accelerate the evolution of genetic mutations and enhance phenotypic traits. Such technology has been exploited to evolve proteins with improved stability and processing yields, enzymes with novel catalytic features, vaccines with increased immunogenicity and hybrid retroviruses[1,2]. In this issue, Maheshri *et al.*[3] extend error-prone PCR and a staggered extension process (analogous to DNA shuffling) into the realm of recombinant AAV vectors. The study not only adds to a rapidly growing vector tool kit but also sheds light on structural aspects of the AAV capsid that may inspire strategies for the rational design of novel AAV vectors.

Recombinant AAV vectors are rapidly becoming the reagents of choice for therapeutic gene transfer. To date, eleven different serotypes, dubbed AAV1–11, and over 100 variants have been isolated from human or nonhuman primate tissues[4]. After the establishment of the first infectious clone of AAV2 in 1982, recombinant AAV2 (rAAV2) vectors rapidly gained popularity in gene therapy applications owing to their lack of pathogenicity, expanded tropism and ability to establish long-term transgene expression. Recombinant AAV2 vectors have been tested in preclinical studies for the treatment of hemophilia, alpha-1 anti-trypsin deficiency, cystic fibrosis, Duchenne muscular

Aravind Asokan and R. Jude Samulski are at the Gene Therapy Center, 7113 Thurston Building, University of North Carolina at Chapel Hill, Chapel Hill, North Carolina 27599, USA.
e-mail: rjs@med.unc.edu

dystrophy, rheumatoid arthritis and many other diseases. Moreover, at least 20 clinical trials have been conducted with rAAV2 vectors carrying different transgenes in over 200 patients[5].

Yet despite the well-established safety and efficacy of rAAV2 vectors for *in vivo* gene transfer, several challenges remain. For example, several studies have focused on the issue of AAV's limited packaging capacity[6]. Other studies have been concerned with modulating AAV-receptor interactions to facilitate targeted delivery of therapeutic transgenes to specific tissue types[7]. Another major obstacle that can attenuate the efficacy of AAV vectors *in vivo* is the prevalence of preexisting neutralizing antibodies in humans previously exposed to AAV[8].

With these challenges in mind, Maheshri *et al.* generated a large ($>10^6$) AAV2 library with randomly distributed capsid mutations and used a high-throughput approach to select for AAV variants with altered receptor-binding ability and with the ability to evade neutralizing antibodies (**Fig. 1**). To assess the functional diversity of their capsid library, the entire population of AAV2 mutants was subjected to heparin affinity column chromatography. Not surprisingly, this simple experiment, which exploits the well-known interaction between wild-type AAV2 and its primary receptor, heparan sulfate, yielded mutants with a range of affinities for heparin.

Intriguingly, none of the amino acid changes in the low-affinity mutants overlap with previously generated AAV2 mutants with reduced affinity for heparin[9,10] or correspond to analogous positions on other AAV serotype capsids. Such mutant AAV2 vectors with low affinity for heparan sulfate are likely to be useful in applications requiring rapid dissemination of vector from the injection site.

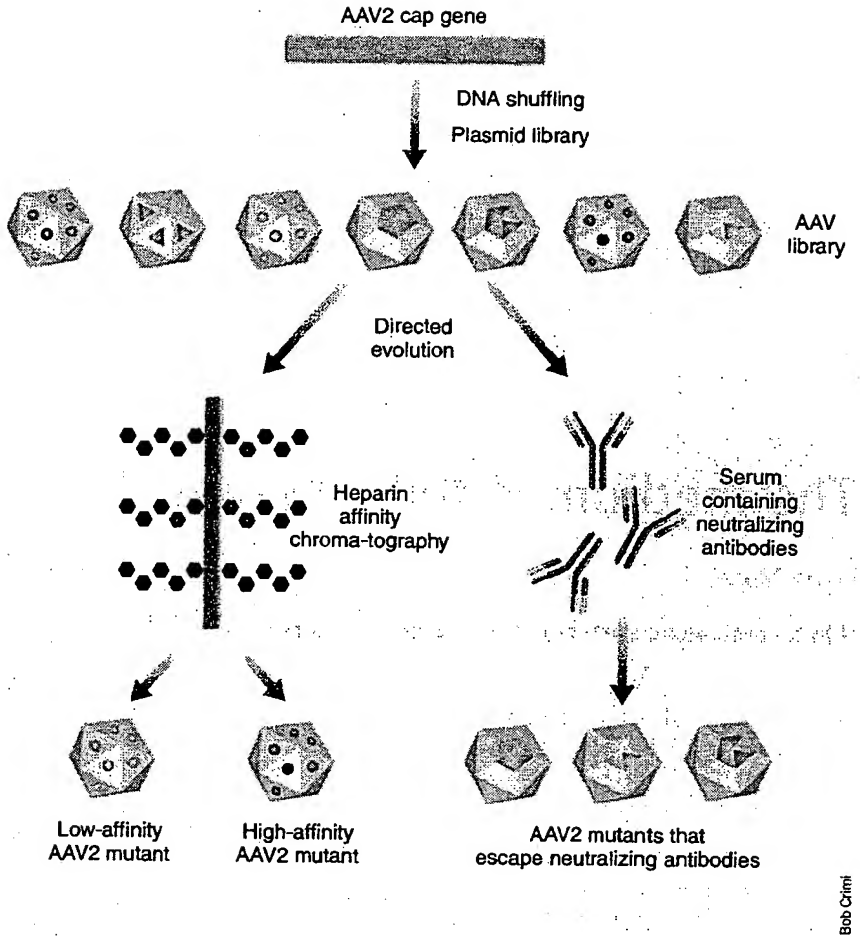

Figure 1 Generation of an AAV library by a recombination technique analogous to DNA shuffling followed by directed evolution. Novel AAV variants with varying receptor-binding affinities were isolated by subjecting the library to heparin affinity column chromatography. Neutralizing-antibody escape mutants were obtained by selection and amplification of infectious clones in the presence of wild-type AAV2 antisera.

On the other end of this spectrum, the authors isolated a mutant with higher affinity for heparin than wild-type AAV2. The amino acid changes in this high-affinity mutant capsid are rather sporadic, with one mutation resulting in 100-fold lower virus yields, underlining the structural complexity of the AAV virion shell. Although such high-affinity mutants might offer structural insight into capsid-receptor interactions, their potential applications in gene delivery are as yet unclear.

Having validated the applicability of this combinatorial approach for isolating novel AAV variants, the authors then cleverly exploit the same to resolve a clinically relevant problem, namely, preexisting immunity to AAV in the human population. The strategy involved repeated amplification of AAV2 mutants that retained infectivity in the presence of antisera with increasing neutralizing antibody titer. This approach yielded several neutralizing antibody–evading variants, including one remarkable mutant, dubbed r2.15, with the ability to transduce cells with moderate efficiency in the presence of a 1:2 antiserum dilution. More importantly, r2.15 vectors preincubated with neutralizing antisera and encapsidating the erythropoietin transgene afforded significantly enhanced serum levels of erythropoietin *in vivo* compared with unmodified recombinant AAV2 vectors.

As the authors note, further evaluation of the transduction efficiency of the r2.15 neutralizing-antibody escape mutant in the presence of pooled human sera and in animal models preimmunized with wild-type AAV2 is warranted. These exciting results validate the enormous utility of this high-throughput approach in generating AAV variants that can overcome the onslaught of physiological barriers *in vivo*.

Finally, the authors carried out structural analysis of the different neutralizing-antibody escape variants. This work revealed several unique mutations as yet unidentified by site-directed mutagenesis and two critical amino acid changes—one in the threefold heparin binding spike region (N587I) and the other in the twofold dimple region (T716A)—that appear to impart the neutralizing-antibody escape phenotype. The latter region has previously been identified as immunogenic[11], and the T716A change is also seen in AAV type 4, which is only weakly neutralized by AAV2 antisera. Interestingly, the N587 site and a novel R471A mutation have been recently identified through site-directed mutagenesis as potential sites for manipulation to facilitate neutralizing-antibody evasion[11]. As crystal structures of other AAV serotypes[12] and their corresponding neutralizing antibodies become available, a comparison of immunogenic regions on the surface of AAV serotype capsids will become feasible.

Taken together, these findings highlight the tremendous potential of combining high-throughput, directed-evolution approaches with conventional rational mutagenesis to elucidate structure-function correlates of the AAV capsid. Future molecular breeding among AAV serotypes should not only yield novel AAV mutants selected for a specific phenotype but also enable the identification of 'hot spots' within capsid subunits that can be subject to rational manipulation. The study by Maheshri *et al.* is thus a clear step towards the ultimate goal of engineering AAV vectors tailored to individual patient or disease profiles.

1. Ness, J.E. *et al. Adv. Protein Chem.* **55**, 261–292 (2000).
2. Soong, N.W. *et al. Nat. Genet.* **25**, 436–439 (2000).
3. Maheshri, N. *et al. Nat. Biotech.* **24**, 198–204 (2006).
4. Gao, G. *et al. Curr. Gene Ther.* **5**, 285–297 (2005).
5. Romano, G., *Drug News Perspect.* **18**, 311–316 (2005).
6. Duan, D. *et al. Mol. Ther.* **4**, 383–391 (2001).
7. Muzyczka, N. & Warrington, K.H. Jr. *Hum. Gene Ther.* **16**, 408–416 (2005).
8. Zaiss, A.K. & Muruve, D.A. *Curr. Gene Ther.* **5**, 323–331 (2005).
9. Wu, P. *et al. J. Virol.* **74**, 8635–8647 (2000).
10. Lochrie, M.A. *et al. J. Virol.* **80**, 821–834 (2005).
11. Moskalenko, M. *et al. J. Virol.* **74**, 1761–1766 (2000).
12. Padron, E. *et al. J. Virol.* **79**, 5047–5058 (2005).

The medium is the message

Harry Moore

Human embryonic stem cell lines are derived under defined conditions.

Before clinical trials of human embryonic stem (hES) cells can be contemplated, it will be necessary to create cell lines according to Good Manufacturing Practice standards of reproducibility and safety. In this issue, Ludwig *et al.*[1] report the derivation of two new hES cell lines under the most defined conditions to date, using feeder-independent culture with recombinant extracellular matrix components and other specific factors. This is welcome news for those centers wanting to generate hES cell lines for clinical applications. The new findings also raise some intriguing questions about the culture requirements for hES cells and how they may adapt or undergo further selection *in vitro*.

The culture of mammalian cells sometimes seems more like a cross between gardening and cooking rather than science. The 'green-fingered' expert in the lab will favor a particular culture medium, feeder-cell type and serum supplements to nurture his or her precious cells. A standard protocol can evolve from a hunch and practical necessity with a pinch of serendipity, rather than from basic principles. It may defy logic yet remain effective. Culture media can stay poorly defined for years or decades even when they cause considerable experimental error. Eventually, however, fully defined culture conditions are essential to provide a robust platform for a field.

Human embryonic stem cells are a classic case. Their derivation was based initially on methods for mouse ES cells, but we now know that factors such as leukemia inhibiting factor and bone morphogenic proteins, which support mouse ES cells, fail to exert the same effects in hES cells. The elucidation of factors that support hES cell growth has remained unresolved partly because of the reliance of many researchers on ill-defined, proprietary medium formulations and a continuing requirement for inactivated feeder cells.

Perhaps contrary to popular belief, hES cells are neither particularly difficult to derive nor particularly difficult to maintain. Yet consistency of culture has remained a real bugbear and is a serious obstacle to scaling up production and to high-throughput screening. Small differences in culture medium and especially in serum or serum-free supplements (which may be nominally serum-free but usually contain undefined animal and human products extracted from serum or plasma) can dramatically alter cell differentiation. Moreover, any suboptimal conditions lead to stochastic differentiation effects that make characterization and comparison of, say, cell surface markers or mRNA expression patterns particularly problematic.

Although incremental improvements for maintaining and deriving hES cells in the last few years have led to serum- and feeder-free conditions, these reports are deceptive[2] as so-called defined conditions still rely on various combinations of commercial, proprietary serum-free supplements, conditioned medium from feeder cells or extracellular basement membrane matrix products (such as Matrigel). Hence, a key recommendation from the inaugural meeting last year of the International Stem Cell Forum[3], a consortium of labs analyzing over 75 hES cell lines, was to develop a fully defined generic medium that could be used throughout the field and would provide a rational foundation for determining the signaling pathways that drive hES cell self-renewal and differentiation.

Since animal products can contaminate and modify hES cells, they may pose a risk in any future clinical situations and should be avoided if at all possible. (This concern may be overstated as many vaccines are produced with animal cells, but bovine products are a clear risk factor.) With this in mind, Ludwig *et al.* returned to first principles and, using a simple approach, tested some of their existing hES cell lines with a fully defined basal medium formulation to which growth factors (selected on the basis of known hES cell receptor expression) were systematically added. Having identified the best combination of factors to maintain established hES cell lines on Matrigel, they then generated an artificial human extracellular matrix with a combination of collagen IV, fibronectin, laminin and vitronectin to support hES cells through multiple passages. These conditions completely eliminated the use of animal products such as nonhuman sialic acid, Neu5Gc, which is a significant step forward in addressing some Good Manufacturing Practice issues. Lastly, they used the defined medium and matrix to derive two new cell lines, which was achieved efficiently from just five blastocysts.

As might be expected from previous studies, fibroblast growth factor, bFGF, was found to be the most important supplementary factor for maintaining hES cells, but LiCl, γ-aminobutyric acid (GABA), pipecolic acid and transforming growth factor β (TGFβ) were all beneficial. Significantly, these factors are different from those shown to maintain mouse ES cells in culture.

So far so good, but the study has a sting in the tail. Both hES cell lines generated were karyotypically abnormal. One line was XXY, either because it originated from an embryo having Klinefelter syndrome or because it acquired this abnormality in early culture. The second cell line was initially diploid but converted to trisomy 12 between 4 and 7 months in passage.

Was this purely bad luck or could some-

Harry Moore is at the Center for Stem Cell Biology, University of Sheffield, Western Bank, Sheffield, S10 2TN, UK.
e-mail: h.d.moore@shef.ac.uk

nature biotechnology

Directed evolution of adeno-associated virus yields enhanced gene delivery vectors

Narendra Maheshri[1], James T Koerber[1], Brian K Kaspar[2] & David V Schaffer[1]

Adeno-associated viral vectors are highly safe and efficient gene delivery vehicles. However, numerous challenges in vector design remain, including neutralizing antibody responses, tissue transport and infection of resistant cell types. Changes must be made to the viral capsid to overcome these problems; however, very often insufficient information is available for rational design of improvements. We therefore applied a directed evolution approach involving the generation of large mutant capsid libraries and selection of adeno-associated virus (AAV) 2 variants with enhanced properties. High-throughput selection processes were designed to isolate mutants within the library with altered affinities for heparin or the ability to evade antibody neutralization and deliver genes more efficiently than wild-type capsid in the presence of anti-AAV serum. This approach, which can be extended to additional gene delivery challenges and serotypes, directs viral evolution to generate 'designer' gene delivery vectors with specified, enhanced properties.

AAV is a 4.7-kilobase, single-stranded DNA virus that contains two genes[1]. *Rep* encodes four proteins necessary for genome replication (Rep78, Rep68, Rep52 and Rep40), whereas *cap* expresses three structural proteins (VP1–3) that assemble to form the viral capsid. AAV depends upon a helper virus such as an adenovirus for active replication and in the absence of a helper establishes a latent state in which its genome is maintained episomally or integrated into the host genome. A number of homologous human and nonhuman primate AAV serotypes have been identified[2–5]; of these, AAV2 is the best characterized as a gene delivery vehicle and the only one that has been used in clinical trials[6–8].

Recombinant gene delivery vector systems (rAAV), first generated based on AAV serotype 2 in the 1980s[9], have been shown to offer numerous major advantages. First, rAAV vectors are safe, as wild-type AAV is nonpathogenic[10]. In addition, rAAV offers the capability for efficient gene delivery and sustained transgene expression in numerous tissues, including muscle[11], lung[12], liver[13,14] and central nervous system[15,16]. Furthermore, rAAV has enjoyed some success in human clinical trials[6–8].

Despite these successes, several problems remain. For example, the majority of the human population has already been exposed to various AAV serotypes, and as a result a significant fraction of any patient population harbors neutralizing antibodies that block gene delivery[17–21]. Additional problems with rAAV vectors include limited tissue dispersion for serotypes that bind heparan sulfate (for example, AAV2 and AAV3)[3,22]; poor infection of refractory cell types such as stem cells[23,24]; challenges with high-efficiency, targeted gene delivery to specific cell populations; and a finite transgene carrying capacity[25].

Because these problems arise from the capsid proteins that mediate gene delivery, the capsid must be reengineered to overcome them. Site-directed point and insertional mutagenesis of the AAV2 *cap* genes indicate that the viral capsid can tolerate some limited modifications and maintain its infectious properties[26,27]. Furthermore, peptide insertion into discrete capsid locations has been successfully applied to generate rAAV2 vectors with some cell-selective gene transfer capabilities[28–31]. However, the molecular basis of some viral properties, such as antibody neutralization[18,19] and virus-cell interactions[2,4,32], is distributed throughout the primary sequence of the capsid; these properties are unlikely to be efficiently modulated by serial site-directed capsid modifications even if the AAV structures are available[33,34]. Therefore, a higher-throughput approach would aid the design of vectors with functional enhancements.

Nature's approach to functional diversification has been the evolution of numerous AAV serotypes[2,4,5], and detailed examination of these types will undoubtedly yield both a wealth of basic AAV virology information and delivery vectors with new properties. However, it would be advantageous to develop a complementary vector-engineering approach that can create novel vehicles with a desired set of specified properties. Directed evolution has been used to generate enzymes with novel catalytic features[35,36], antibodies with enhanced binding affinities[37,38] and retroviruses with new properties[39]. We have built upon this work to develop an efficient and high-throughput method to generate rAAV vectors with improved capabilities. Furthermore, we have applied this method to create rAAV2-based vectors that evade neutralizing antibodies *in vitro* and *in vivo* and that have altered receptor-binding properties.

[1]The Department of Chemical Engineering and The Helen Wills Neuroscience Institute, The University of California, Berkeley, California 94720-1462, USA. [2]Department of Gene Therapy and Division of Molecular Medicine Columbus Children's Research Institute and The Ohio State University, Columbus, Ohio 43205, USA. Correspondence should be addressed to D.V.S. (schaffer@berkeley.edu).

Received 31 October 2005; accepted 30 November 2005; published online 22 January 2006; doi:10.1038/nbt1182

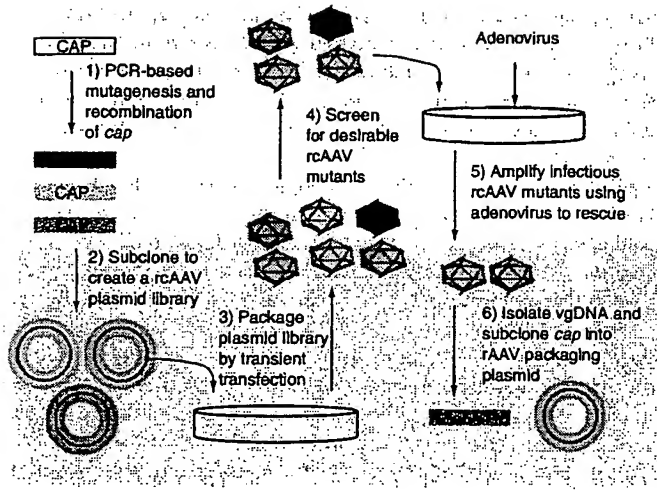

Figure 1 A forward genetics approach to creating 'designer' rAAV vectors. The entire *cap* gene was subjected to (1) mutagenesis and recombination using PCR-based methods. The mutant DNA was then (2) inserted into a rcAAV packaging plasmid to created a viral plasmid library. A viral particle library was created by (3) AAV helper-free transfection of the viral plasmid library into HEK 293 cells. This library was then (4) selected to isolate mutants with a desired set of properties. The resulting pools were (5) added to HEK 293 cells and rescued by the addition of adenovirus to select for only infectious particles and to amplify the small number of choice mutants. Several rounds of selection and amplification can be conducted to enrich the pool of choice mutants. Finally, (6) vector genome (vgDNA) from these mutants was extracted, amplified via PCR, and cloned into a rAAV helper plasmid to package 'designer' rAAV vectors. This enriched mutant pool can also be subjected to additional rounds of mutagenesis and selection, if desired.

RESULTS

Library generation

To generate a library of *cap* mutants with point mutations randomly distributed throughout VP1–3, we performed error-prone PCR followed by the staggered extension process[40]. Cloning the fragments yielded a viral plasmid library, pSub2Cap2*, with $>10^6$ independent clones (that is, bacterial colonies) after transformation. This plasmid diversity is large, although the resulting viral library diversity could potentially be smaller due to some nonsense or missense mutations yielding abnormal VP1–3 production. The viral plasmid was significantly diluted and packaged into AAV virions essentially as previously described[16]. The resulting AAV library can be selected for any variety of new properties or functions, and because the genotype of these variants is physically linked to their phenotype, the novel capsid sequence can readily be recovered by DNA sequence analysis of the encapsidated AAV genome (**Fig. 1**).

Heparin-binding mutants

As an initial gauge of how the library's sequence diversity translated into capsid functional diversity, we subjected CsCl-purified library particles to heparin affinity chromatography. Wild-type AAV elutes between 450 and 550 mM NaCl (**Fig. 2a**)[41]. In stark contrast, the AAV mutant library elutes at a wide range of salt concentrations, from the 150 mM load to the final 750 mM fraction, demonstrating that the library encompasses significant functional diversity. To generate mutants with either low or high heparin affinity, the 150 mM and 600–650 mM NaCl elution fractions were separately amplified by low multiplicity of infection (MOI) of human embryonic kidney epithelial (HEK) 293 cells, followed by adenovirus serotype 5 (Ad5) infection to

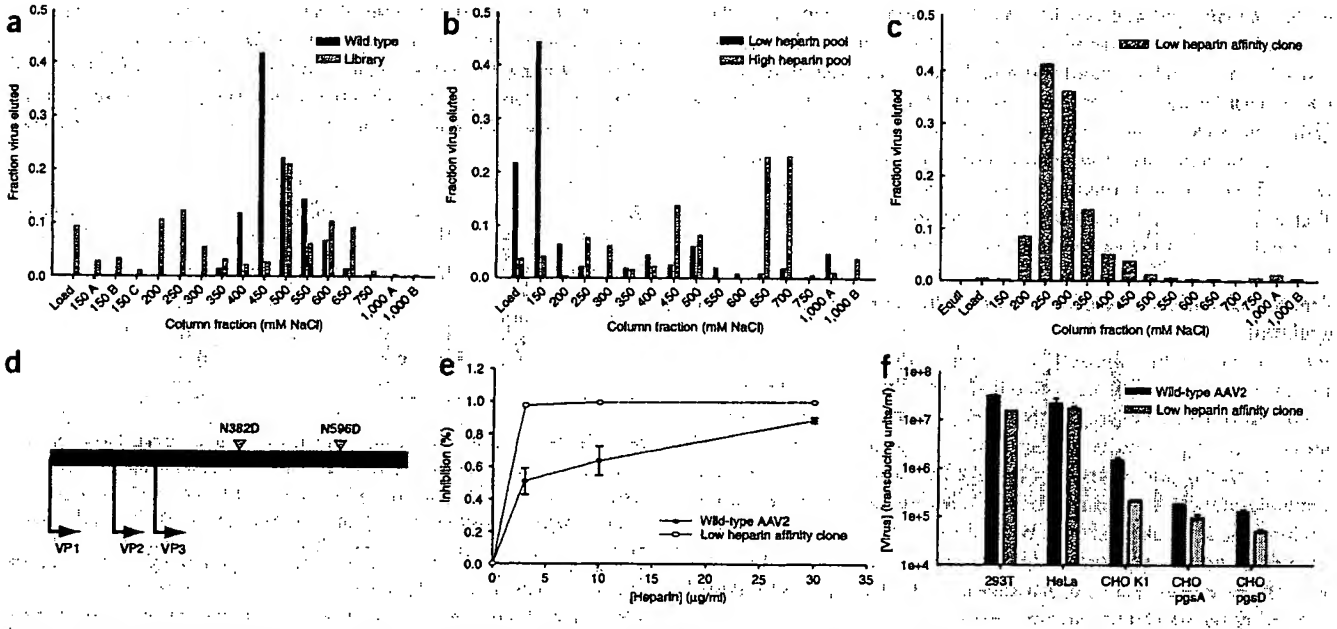

Figure 2 Heparin-binding characteristics of wild-type AAV versus the viral library. (**a**) The heparin affinity column chromatogram of wild-type AAV and the mutant library is shown, where virus gradually eluted from the column as the NaCl concentration was increased. Pools of virus from the load fraction and the 600-650 mM fractions were amplified by infection of HEK 293 cells followed by addition of adenovirus. (**b**) Chromatograms of the resulting pools from the mutant library are shown, and individual clones were subsequently isolated from the load and 700 mM fractions. (**c**) One clone exhibited reduced heparin affinity, and its (**d**) sequence data revealed numerous novel mutations. (**e**) Infection of HEK 293 cells by rAAV-GFP packaged in mutant or wild-type capsid revealed that the mutant is significantly more susceptible to inhibition by soluble heparin. (**f**) Infection of wild-type CHO cells and two variant lines expressing reduced heparan sulfate levels with rAAV-GFP packaged with wild-type or mutant capsid revealed that the low-affinity heparin-binding mutant was more sensitive to lower heparan sulfate levels.

Table 1 Neutralizing antibody titer of antibody-evading mutants

Clone	Neutralizing antibody titer reciprocal serum dilution
(+)	1,520
r1.2	482
r1.3	556
r1.4	583
r1.5	743
r2.1	606
r2.3	545
r2.4	536
r2.5	625
r2.15	15.8

The neutralizing antibody (NAB) titer for each clone was determined by fitting data in Figures 4a–b to a simple exponential decay. NAB titers are reported as the reciprocal of the volume fraction of serum necessary to reduce infectivity to 37% of the value measured in the absence of serum.

induce AAV replication and refractionation on the heparin column. After two such rounds of enrichment, the two resulting viral pools eluted from the column predominantly at 150 mM or 750 mM (Fig. 2). Notably, because each enrichment round involved viral infection and replication, these pools were composed of infectious virus.

Individual capsid clones were isolated from the two pools, inserted into a rAAV helper plasmid for recombinant vector production[42] and sequenced (Fig. 2d and Supplementary Fig. 1 online). rAAV-green fluorescent protein (GFP) produced from the clones was fractionated on a heparin column to verify their modified heparin affinity, and one high-titer clone eluted at 250 mM NaCl (Fig. 2c), significantly lower than the wild-type capsid. This mutant's transduction properties were further analyzed by infection of both HEK 293 cells in the presence of soluble heparin, as well as wild-type Chinese hamster ovary (CHO) cells and two mutant lines expressing reduced heparan sulfate levels[43]. When heparan sulfate binding became limiting, transduction with the low-heparin-affinity mutant was reduced (Figs. 2e,f). Other low-and high-affinity clones were obtained, but some failed to package high-titer recombinant virus (Supplementary Fig. 4 online). The ability to isolate diverse heparin-binding mutants from the AAV mutant library after only one round of mutagenesis demonstrates the utility of this approach for creating vectors with novel properties.

Creation of antibody-evading mutants after one and two rounds of evolution

We next applied this approach to a significant clinical problem: vector inactivation by neutralizing antibodies. Rabbit anti-AAV2 neutralizing serum with a neutralizing antibody titer (defined as the amount of serum necessary to reduce infectivity to 37%, or 1/e) for wild-type AAV of 1:1,500 was produced (Table 1), comparable to neutralizing antibody titers in human serum[17,18,20] (Supplementary Note online). Preimmune sera collected from two animals before rAAV inoculations, as well as serum depleted of IgG protein through incubation with protein A beads, had no neutralizing effect (data not shown), indicating IgG-dependent neutralization.

To isolate antibody-evading mutants, we selected the library against neutralizing serum. Wild-type, library or selected virus from the previous step was preincubated with varying antiserum amounts, added to HEK 293 cells and rescued by adenovirus (Fig. 3). The serum level was escalated after each step. After three selection steps, the virus pool maintained infectivity even after preincubation with a 1:30 dilution of serum. Viral genomic DNA was extracted from the selected antibody-evading mutant pool, and the *cap* sequence was PCR-amplified and inserted into both pSub2, to produce replication-competent AAV (rcAAV), and pXR2, to produce recombinant vectors. Five clones were sequenced and packaged. Four were packaged successfully and were tested for their ability to evade neutralization. In the absence of serum, infectious titers for these clones were equivalent to normal rAAV-GFP (Supplementary Table 1 online). However, in the presence of serum, all four clones had neutralizing antibody titers that were ~threefold improved over wild-type capsid (Fig. 4a and Table 1). Moreover, a substantial (>1%) fraction of cells were still transduced at a 1:37.5 dilution of serum. Although each clone had distinct mutations, they all shared a T716A mutation near the C terminus of VP3. In fact, the r1.3 clone had only the T716A mutation, indicating that this mutation was likely responsible for most, if not all, of the antibody-resistant phenotype. The packaged rcAAV mutants also showed enhanced ability to evade neutralization (data not shown). Therefore, one mutagenesis and three selection steps generated mutant capsids with a threefold improved neutralizing antibody titer as compared to wild-type capsid and a ~7.5% infectivity at serum levels that completely neutralized wild-type infectivity.

To further improve the antibody-evading property of the mutants, we subjected the previous pool to a second round of evolution, that is, mutagenesis followed by three selection steps. In contrast to the first evolution round (Fig. 3a), we were able in the second round to rapidly escalate the levels of serum used (Fig. 3b). After amplification of *cap* from the selected library and insertion into pXR2, seven mutants isolated from a pool generated rAAV-GFP, which exhibited only partial neutralization at a 1:15 serum dilution. Infectious titers of five clones were very similar to that of wild-type capsid, whereas two mutants had titers 100- to 1,000-fold lower than wild-type capsid and were thus not pursued (Supplementary Table 1 online). Antibody neutralization analysis revealed that four clones had neutralizing antibody titers similar to those isolated in the first round (Fig. 4b). However, clone r2.15 was only mildly neutralized, and when we repeated the neutralization assay using up to a 1:2.35 serum dilution (Fig. 4c), the neutralizing antibody titer of r2.15 was 96-fold improved compared to wild type (Table 1). Over 10% of virus remained

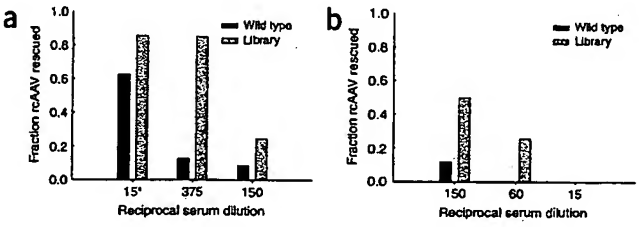

Figure 3 Selection of antibody-escape mutants from generated viral capsid libraries. AAV viral particles were incubated with various amounts of anti-AAV2 antiserum before addition to HEK 293T cells. Viral particles that productively infected cells were rescued by addition of Ad5 and quantified by QPCR. The fraction rescued was calculated at each serum dilution (that is, selection stringency) by normalizing the rescued AAV titer in the presence of serum by the rescued AAV titer in the absence of serum. (a) The first selection step in the first round of evolution indicated the viral capsid library is more infectious even in aggregate as compared to wild type, at a 1:375 serum dilution. The asterisk denotes that the first serum sample was primary antiserum, collected after only the first inoculation of rabbits with AAV. (b) In the second round of evolution, over 50% of the library was rescued at the 1:150 serum dilution as compared to the 10% in the first round, indicating progress over the first round. In both panels a and b, the viral pools rescued at the highest stringencies were amplified and subjected to two additional selection steps.

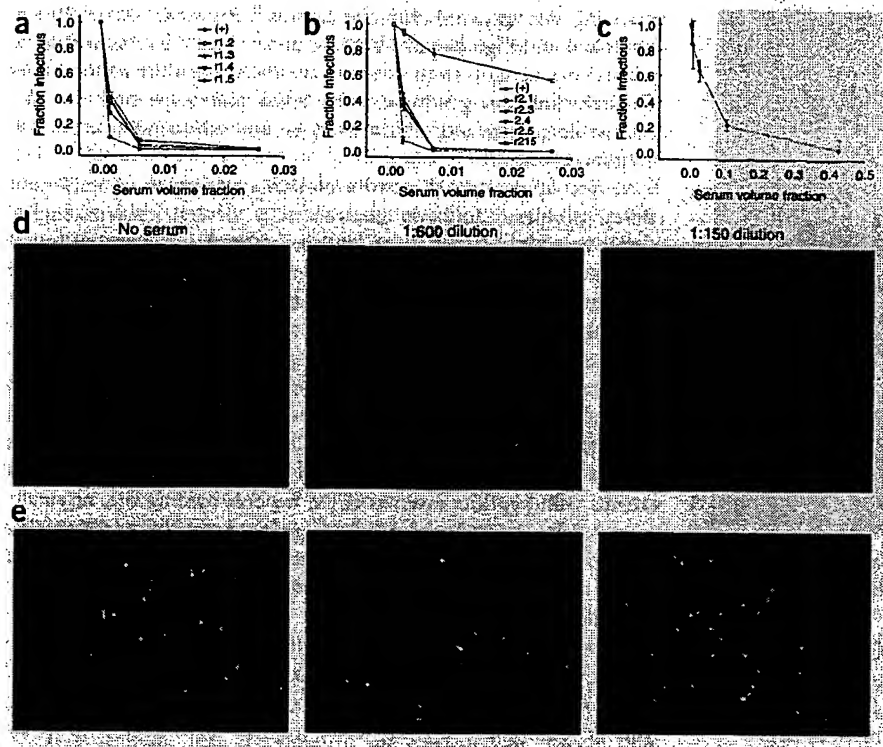

Figure 4 Neutralization profiles of antibody-evading mutants. (a) Antibody-evading mutants isolated after one round of mutagenesis were used to package high-titer rAAV-GFP and incubated with anti-AAV2 rabbit polyclonal serum before addition to HEK 293 cells at an MOI of 1. The fraction of infectious particles remaining was determined by fluorescence flow cytometry and normalized by the infectious titer in the absence of serum. The neutralizing antibody titer was determined by fitting these points to an exponential curve. (b) Of the five antibody-evading mutants isolated after a further round of mutagenesis, r2.15 exhibited a significant further improvement in antiserum evasion. Error bars indicate the standard deviation of triplicate samples, and trend lines are shown for clarity. (c) Further characterization of the r2.15 mutant neutralization profile was conducted using larger amounts of serum to determine a 96-fold improved antiserum evasion (that is, neutralizing antibody). (d) Representative panels of HEK 293 cells showed reduced GFP expression when infected with wild-type rAAV-GFP in the presence of serum. (e) In contrast, delivery of r2.15 mutant AAV GFP yielded no reduction in GFP expression at the same serum levels.

infectious at a serum dilution of 1:7, and 3% persisted at a 1:2.35 serum dilution.

In vivo analysis of antibody evasion

We next conducted an *in vivo* assay in which high-titer rAAV-Epo vector based on the r2.4 and r2.15 mutants was produced, preincubated with antiserum and analyzed for its ability to mediate erythropoietin gene delivery after injection in the mouse hind limb. This represented a rigorous assay where high concentrations of antibody were allowed to fully bind and opsonize virus before injection. Notably, with no serum, the two mutants yielded a higher hematocrit than wild-type capsid, a result that may be further investigated (**Fig. 5**). However, as serum was increased, r2.4 yielded increased hematocrits at 1–2 orders of magnitude higher serum concentrations, and r2.15 at 2–3 orders of magnitude higher serum concentrations, compared to wild-type capsid. A serum-only control did not increase hematocrits (data not shown).

Sequencing revealed that the mutations in r2.4 were identical to r2.15, except for two additional substitutions at T567S and N587I (**Fig. 6a**). Because N587 lies in the heparin-binding domain, we analyzed the heparin affinity of r2.15, along with r1.2, r1.5 and r2.3. The three latter clones had a wild-type binding phenotype, whereas r2.15 showed a slight reduction in heparin affinity (**Supplementary Fig. 2** online). To ensure that the selected mutants could evade the neutralizing responses of more than one animal, vector was tested against the serum of the second rabbit immunized against AAV2 and evaded the neutralizing responses of this serum to a similar extent (**Supplementary Fig. 3** online).

DISCUSSION

There has been major progress in the development of safe, efficient and therapeutically relevant adeno-associated virus vectors[6,9,11,12,15,16]. However, many challenges remain, including widespread preexisting immunity against human serotypes, targeted and efficient delivery, limited packaging capacity[25] and infection of nonpermissive cell types[23,24]. These problems are not surprising, since the parent AAVs are products of natural evolutionary pressures that select for survival rather than for performance in human gene therapy. To overcome these and other problems, the viral capsid must be modified. We have accordingly developed a high-throughput approach to engineer AAV variants with improved properties. Specifically, large ($>10^6$) AAV2 libraries with randomly distributed capsid mutations were

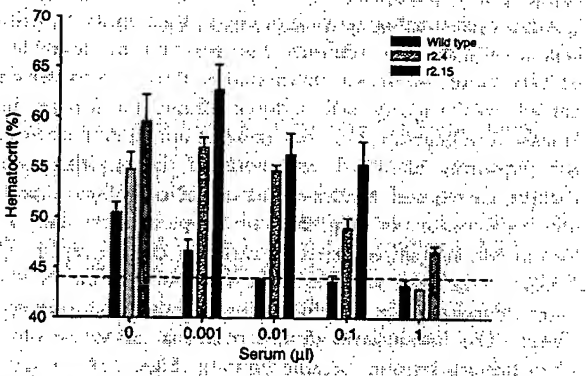

Figure 5 rAAV-Epo was produced with wild-type, r2.4 and r2.15 capsids. Vector was preincubated with varying levels of potent rabbit antiserum (1:6,000 neutralizing antibody), which allowed anti-AAV2 antibodies to opsonize vector particles before vector injection into the hind-limb muscle of adult mice. Two weeks after injection, hematocrit levels were measured and revealed that gene delivery mediated by the two antibody-evading mutants persists at serum levels that completely neutralize wild-type rAAV-Epo ($P < 0.005$). Error bars indicate the standard deviation of $n = 4$ samples, and the dotted line represents the basal hematocrit value. Results 3 weeks after injection were quantitatively similar (data not shown).

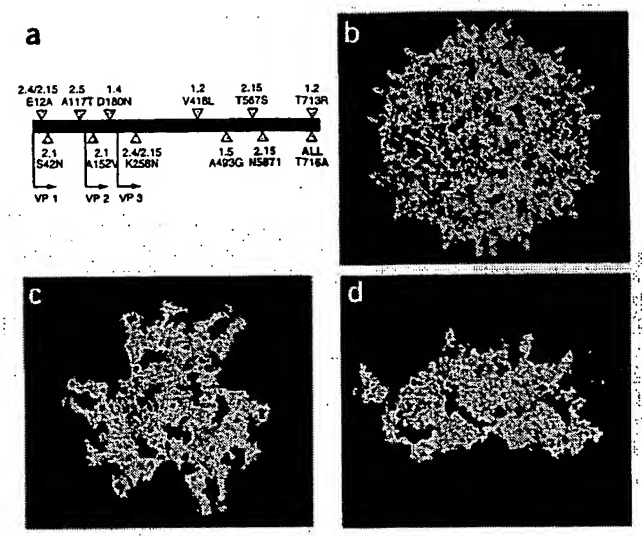

Figure 6 Mutation profile of neutralizing antibody-evading mutants. (a) Sequence data indicate that all nine mutants that had neutralizing titers threefold better than wild type contain the T716A mutation. The r2.15 mutant, which had a neutralizing titer 96-fold better than wild type, has two mutations absent from any other mutant. T567S is a conservative mutation that lies in a minor epitope associated with the A20 monoclonal antibody[19], whereas N587I lies in the heparin-binding domain[50], whose disruption has been shown to confer limited escape from neutralization by serum from certain human patients[44]. Therefore, the N587I mutation may be responsible for improvement from the first to the second round. (b) A molecular model of the full AAV2 capsid, based on the solved structure[34], is shown using Raswin. (c) Surface mutations found in the r2.15 mutant are labeled on a VP2 hexamer, with the phenotypically key N587I and T716A mutations shown in red and the other mutations in blue (see text for details). Mutated residues have been slightly exaggerated for clarity. (d) Several previously identified antigenic regions[18,19] as well as the heparin-binding site (HBS)[50] are labeled using various colors on a side view of the VP2 hexamer.

generated and selected for altered receptor binding and evasion of antibody neutralization.

Affinity chromatography selection yielded mutants with altered heparin affinity. Lower-affinity mutants may be desirable as gene delivery vectors when wide dissemination through a tissue or region is needed. AAV variants with reduced affinity for heparin have previously been generated[27,32], but none of our mutations overlap with any previously identified, and none of the resulting amino acid changes correspond to the sequences of orthologous positions in other AAV serotypes (**Fig. 2d** and **Supplementary Fig. 4** online). Two mutations that occurred on surface-accessible regions of VP3—N382D on the inner shoulder of the threefold spike and N596D on the outer shoulder of the threefold spike—resulted in a gain of negative charge. The low-heparin-affinity mutant's efficiency was reduced when heparin binding became limiting (**Figs. 2e,f**). A high-affinity mutant yielded low-titer vector but could enable insights into receptor-binding mechanisms.

The heparin-selection results confirm two key attributes of the method. First, the heparin chromatograms (**Fig. 2a**) demonstrate that the viral library contains considerable functional diversity. Second, the library was packaged by substantial dilution of mutant viral genome DNA, but a fraction of cells could have received multiple plasmids and therefore generated undesired chimeric mutant particles. A previous study that generated AAV peptide-display libraries used an additional packaging step to avoid chimeric capsids[30]. However, our ability to enrich low-and high-heparin-binding pools (**Figs. 2b,c**) as well as to isolate clonal variants from these pools indicates that the method does effectively link *cap* genotype with capsid phenotype and that the conceivable presence of chimeras does not substantially affect the evolution process.

We next applied the directed evolution approach to an important clinical problem: antibody neutralization. Several epidemiological studies have found that from 35–96% of the human population is seropositive for AAV1–5, and 18–67% harbors antibodies capable of significantly neutralizing rAAV1–5 gene delivery[12,17–20]. Therefore, preexisting immunity from 'accidental vaccination' by the parent virus could render AAV2 gene therapy ineffective in as much as two-thirds of the population. Mapping of dominant neutralizing epitopes has revealed the presence of both linear and complex conformation epitopes[18,19], rendering the rational design of variants that can escape antibody neutralization difficult. One study found that variants with peptides inserted at the heparin-binding site, originally generated for targeted gene delivery[28], reduced sensitivity to neutralizing antibodies[44]. However, success varied with the particular serum sample used, and infectious titer was reduced 10- to 1,000-fold, depending on the inserted peptide. Thus, disrupting one epitope can reduce antibody neutralization, but several mutations may be necessary to create a general neutralization-free vector. In addition, our more modest point mutations could achieve antibody-evasion without significantly altering vector tropism for situations in which maintaining heparin binding is desired.

Selecting the AAV2 library for efficient gene delivery in the presence of neutralizing antiserum yielded numerous successful variants, including one with a 96-fold improvement and the ability to mediate moderate gene delivery even at a ~1:2 serum dilution. This reduced neutralization is similar to the neutralization of other AAV serotypes by anti-AAV2 serum[4,45]. We further demonstrated that two mutants, r2.4 and r2.15, evaded antibody neutralization *in vivo* at serum levels several orders of magnitude greater than those required to neutralize delivery with the wild-type capsid. Surprisingly, both mutants also mediated enhanced gene delivery compared with wild type in the absence of serum (**Fig. 5**). Analysis of mutations present in 12 different clones suggests two key mutations in VP3, N587I and T716A, are largely responsible for the antibody-evasion phenotype. The N587I mutation lies on the surface of the threefold spike within the heparin-binding site[32] (**Figs. 6c,d**) but maintains high infectivity and only slightly reduces heparin affinity (**Supplementary Fig. 2** online). Interestingly, antibody-escape mutants in a number of picornaviruses also occur in receptor-binding sites with no change in receptor binding[46]. The T716A mutation found in all antibody-evading mutants lies on the surface of the twofold dimple region (**Figs. 6c,d**), previously identified as an immunogenic region[18]. Interestingly, AAV4 (only weakly neutralized by anti-AAV2 serum[45]) also has an alanine at position 716, raising the possibility that directed evolution could mirror some changes generated by natural evolution.

Our directed evolution approach can readily be extended to additional AAV gene delivery challenges. Future efforts may evolve AAV variants to escape neutralization by pooled human sera representative of a potential patient population. Furthermore, the mutant library may contain variants capable of more efficient delivery to problematic cells, such as stem cells resistant to all AAV serotypes attempted[23,24], provided that the problems reside in the capsid structure. In addition, variants could be selected to overcome specific blocks in the intracellular AAV gene delivery pathway[47]. Moreover, because the gene transfer characteristics of alternate AAV serotypes

vary in properties such as their cell surface receptors[43,48], tissue tropism[3] and overall delivery efficiency[3], they offer rich starting material for additional evolution.

In summary, we present a high-throughput approach to evolve AAV viral variants with advantageous gene delivery properties, and we have applied this approach to generate AAV2 mutants with altered receptor binding and neutralizing antibody-evasion properties. This method allows one to stipulate the criteria a designer vector must satisfy rather than attempting to identify a natural variant that likely meets only some of those needs. Furthermore, no initial mechanistic knowledge of the capsid properties is needed, and analysis of the results enhances our understanding of the capsid's structure-function relationships. For example, as more useful variants are isolated, pooling their sequence information with natural AAV serotypes should lead to the identification of adaptable regions in the capsid that can be tailored without compromising transduction. This approach therefore has potential to enhance knowledge of both AAV basic virology and vector engineering.

METHODS

Library generation and vector packaging. An AAV2 *cap* ORF genetic library was generated by error-prone PCR followed by the staggered extension process as described[40], using 5′-GCGGAAGCTTCGATCAACTACGC-3′ and 5′-GG GGCGGCCGCAATTACAGATTACGAGTCAGGTATCTGGTG-3′ as forward and reverse primers, respectively. To construct pSub2, a 1.8 kilobase linear fragment was generated by PCR using 5′-GCGGAAGCTTCGATCAACTACGC-3′ and 5′-GATGCCGGGAGCAGACAAGCCCGTCAGGGC-3′ with pSub201 (ref. 9) as template. Both this fragment and pSub201 were digested with *Hin*dIII and *Cla* I, and the products were ligated to create the 5.7-kb rcAAV packaging plasmid, pSub2, into which the resulting *cap* product could be inserted after *Hin*dIII/*Not* I digestion. AAV was produced and purified by CsCl centrifugation essentially as previously described[16]. Briefly, in a ~75% confluent 15-cm dish of HEK 293 (ATCC) cells, 25 μg of pHelper (Stratagene) or pXX6, 25 μg of pBluescript (Stratagene), and 7 or 70 ng of the pSub2Cap2* plasmid library were transfected by the calcium phosphate method. This 1:2 × 10^{-4} molar ratio was calculated such that > 90% of cells received approximately one member of the pSub2Cap2* plasmid library, assuming each cell receives ~50,000 total plasmids[49]. Viral libraries were harvested as described[16], and virus was purified using CsCl density centrifugation. In the case of selection for antibody evasion, the above procedure was repeated using viral genomic DNA from a selected pool of mutant rcAAV as the template for error-prone PCR.

For all experiments, the AAV genomic titer was determined by extracting vector DNA as previously described[16] followed by quantification using real time PCR on a Bio-Rad iCycler using SYBR Green dye (Molecular Probes).

Heparin column chromatography. Approximately 10^{12} AAV library particles were loaded onto a 1-ml HiTrap heparin column (Amersham) previously equilibrated with 0.15 M NaCl and 50 mM Tris at pH 7.5. Washes were performed using 0.75 ml volumes of Tris buffer with increasing increments of 50 mM NaCl up to 750 mM, followed by a 1 M wash. As a control, rAAV-GFP was also subjected to this chromatography. Mutant virus from both a combined pool of the load and 150-mM fraction (low heparin affinity) and the 650-mM fraction (high heparin affinity) were added to 10^7 HEK 293T cells at a genomic MOI of 1–10. Cells were superinfected with adenovirus serotype 5 (Ad5) 2 d after infection, and virus was harvested 3 d later. Both crude lysates and viral particles precipitated by ammonium sulfate were characterized by heparin column chromatography as above. To isolate individual viral clones from library fractions that eluted at different salt concentrations, viral DNA was extracted from the fractions, amplified by PCR, and inserted into pSub2Cap2. These single clone rcAAV mutants were then packaged as previously described, subjected to heparin column chromatography to verify their phenotype, and then sequenced at the UC Berkeley DNA Sequencing Facility.

***In vitro* transduction assays.** Either wild-type or mutant rAAV-GFP particles were added to HEK 293T, HeLa, CHO K1, CHO pgsA and CHO pgsD cell lines at a genomic MOI of 3,000. After 48 h, the fraction of green cells was quantified by flow cytometry at the UC Berkeley Cancer Center (Beckman-Coulter EPICS). Heparin inhibition studies were performed identically, except that viral particles were preincubated with varying amounts of heparin (0–30 μg/ml) in 75 μl of PBS (pH 7.4) for 1 h at 37 °C before addition to HEK 293T cells. The medium was changed 1 h later. After 48 h, the fraction of green cells was quantified by flow cytometry.

Antiserum generation and library antibody neutralization screen. Polyclonal sera containing neutralizing antibodies against AAV2 were generated in two New Zealand White rabbits in accordance with the UC Berkeley Animal Care and Use Committee and National Institutes of Health (NIH) standards for laboratory animal care. Briefly, 5 × 10^{10} CsCl-purified rAAV2 particles carrying β-galactosidase cDNA were mixed with 0.5 ml TiterMax adjuvant (CytRx) and injected into the anterior hind-limb muscle. Two boosts were performed at 3-week intervals using the same AAV dosage, followed by antiserum collection. Adjuvant was not used in the last boost.

One round of evolution consisted of *cap* mutagenesis followed by three selection steps against neutralizing serum. Both wild-type and a mutant rcAAV library were incubated with varying amounts of serum (0–7.5 μl) in 75 μl of PBS (pH 7.4) for 30 min at 25 °C, followed by addition to 2.5 × 10^5 HEK 293 cells in a 6-well format. After 48 h, AAV was rescued from infected cells by addition of Ad5, and cells were harvested 24 h later. The rescued rcAAV was subjected to two additional infection-and-rescue steps in the presence of increasing amounts of serum.

Clonal antibody neutralization screen. Individual viral clones from the library fraction that successfully infected cells even in the presence of neutralizing antibody were inserted into the pXR2 rAAV packaging plasmid[42], and rAAV-GFP was produced as above. To assess the extent of neutralization of these antibody-evading rAAV variants, they were incubated with varying amounts of rabbit sera as above, followed by addition to 2.5 × 10^5 HEK 293 cells in 12 well format at an MOI of 1. At 48 h after infection, the fraction of green cells was quantified by flow cytometry. Iodixanol gradient purified rAAV mutants[41] were subjected to heparin column chromatography as above.

***In vivo* neutralization assay.** pXR2 containing wild-type, 2.4 or 2.15 *cap* were used to package pAAV-CB-mEpo, a vector expressing murine erythropoietin under the control of the chicken β-actin enhancer/cytomegalovirus promoter (a kind gift of J. Wilson, University of Pennsylvania). High-titer rAAV-Epo was produced and purified as described[16]. 2.0 × 10^{10} rAAV-Epo particles were incubated with varying amounts of high-titer rabbit sera (Supplementary Fig. 3 online) for 30 min, then injected into the hind-limb muscle of 8-week-old female BALB/c mice (Jackson Laboratories, $n = 4$). Beginning 14 d after infection, animals were retroorbitally bled and hematocrits determined every 7 d. Animal studies were approved by the UC Berkeley Animal Care and Use Committee and conducted in accordance with NIH guidelines on laboratory animal care.

Note: Supplementary information is available on the Nature Biotechnology website.

ACKNOWLEDGMENTS

We thank Wilson Mok, Diana Chai, Kirti Magudia, and Robert Teachnor for technical assistance. This work was funded by National Science Foundation Graduate Fellowships (to N.M. and J.K.), Project A.L.S. funding (to B.K.), and Whitaker Foundation and ALS Association funding (to D.S.).

COMPETING INTERESTS STATEMENT

The authors declare that they have no competing financial interests.

Published online at http://www.nature.com/naturebiotechnology/
Reprints and permissions information is available online at http://npg.nature.com/reprintsandpermissions/

1. Srivastava, A., Lusby, E.W. & Berns, K.I. Nucleotide sequence and organization of the adeno-associated virus 2 genome. *J. Virol.* **45**, 555–564 (1983).
2. Chiorini, J.A., Kim, F., Yang, L. & Kotin, R.M. Cloning and characterization of adeno-associated virus type 5. *J. Virol.* **73**, 1309–1319 (1999).
3. Davidson, B.L. *et al.* Recombinant adeno-associated virus type 2, 4, and 5 vectors: transduction of variant cell types and regions in the mammalian central nervous system. *Proc. Natl. Acad. Sci. USA* **97**, 3428–3432 (2000).

4. Gao, G.P. *et al.* Novel adeno-associated viruses from rhesus monkeys as vectors for human gene therapy. *Proc. Natl. Acad. Sci. USA* **99**, 11854–11859 (2002).
5. Gao, G. *et al.* Adeno-associated viruses undergo substantial evolution in primates during natural infections. *Proc. Natl. Acad. Sci. USA* **100**, 6081–6086 (2003).
6. Kay, M.A. *et al.* Evidence for gene transfer and expression of factor IX in haemophilia B patients treated with an AAV vector. *Nat. Genet.* **24**, 257–261 (2000).
7. Manno, C.S. *et al.* AAV-mediated factor IX gene transfer to skeletal muscle in patients with severe hemophilia B. *Blood* **101**, 2963–2972 (2003).
8. Moss, R.B. *et al.* Repeated adeno-associated virus serotype 2 aerosol-mediated cystic fibrosis transmembrane regulator gene transfer to the lungs of patients with cystic fibrosis: a multicenter, double-blind, placebo-controlled trial. *Chest* **125**, 509–521 (2004).
9. Samulski, R.J., Chang, L.S. & Shenk, T. Helper-free stocks of recombinant adeno-associated viruses: normal integration does not require viral gene expression. *J. Virol.* **63**, 3822–3828 (1989).
10. Berns, K.I. & Linden, R.M. The cryptic life style of adeno-associated virus. *Bioessays* **17**, 237–245 (1995).
11. Xiao, X., Li, J. & Samulski, R.J. Efficient long-term gene transfer into muscle tissue of immunocompetent mice by adeno-associated virus vector. *J. Virol.* **70**, 8098–8108 (1996).
12. Halbert, C.L., Rutledge, E.A., Allen, J.M., Russell, D.W. & Miller, A.D. Repeat transduction in the mouse lung by using adeno-associated virus vectors with different serotypes. *J. Virol.* **74**, 1524–1532 (2000).
13. Koeberl, D.D., Alexander, I.E., Halbert, C.L., Russell, D.W. & Miller, A.D. Persistent expression of human clotting factor IX from mouse liver after intravenous injection of adeno-associated virus vectors. *Proc. Natl. Acad. Sci. USA* **94**, 1426–1431 (1997).
14. Snyder, R.O. *et al.* Persistent and therapeutic concentrations of human factor IX in mice after hepatic gene transfer of recombinant AAV vectors. *Nat. Genet.* **16**, 270–276 (1997).
15. McCown, T.J., Xiao, X., Li, J., Breese, G.R. & Samulski, R.J. Differential and persistent expression patterns of CNS gene transfer by an adeno-associated virus (AAV) vector. *Brain Res.* **713**, 99–107 (1996).
16. Lai, K., Kaspar, B.K., Gage, F.H. & Schaffer, D.V. Sonic hedgehog regulates adult neural progenitor proliferation in vitro and in vivo. *Nat. Neurosci.* **6**, 21–27 (2003).
17. Erles, K., Sebokova, P. & Schlehofer, J.R. Update on the prevalence of serum antibodies (IgG and IgM) to adeno-associated virus (AAV). *J. Med. Virol.* **59**, 406–411 (1999).
18. Moskalenko, M. *et al.* Epitope mapping of human anti-adeno-associated virus type 2 neutralizing antibodies: implications for gene therapy and virus structure. *J. Virol.* **74**, 1761–1766 (2000).
19. Wobus, C.E. *et al.* Monoclonal antibodies against the adeno-associated virus type 2 (AAV-2) capsid: epitope mapping and identification of capsid domains involved in AAV-2-cell interaction and neutralization of AAV-2 infection. *J. Virol.* **74**, 9281–9293 (2000).
20. Sun, J.Y., Anand-Jawa, V., Chatterjee, S. & Wong, K.K. Immune responses to adeno-associated virus and its recombinant vectors. *Gene Ther.* **10**, 964–976 (2003).
21. Peden, C.S., Burger, C., Muzyczka, N. & Mandel, R.J. Circulating anti-wild-type adeno-associated virus type 2 (AAV2) antibodies inhibit recombinant AAV2 (rAAV2)-mediated, but not rAAV5-mediated, gene transfer in the brain. *J. Virol.* **78**, 6344–6359 (2004).
22. Nguyen, J.B., Sanchez-Pernaute, R., Cunningham, J. & Bankiewicz, K.S. Convection-enhanced delivery of AAV-2 combined with heparin increases TK gene transfer in the rat brain. *Neuroreport* **12**, 1961–1964 (2001).
23. Smith-Arica, J.R. *et al.* Infection efficiency of human and mouse embryonic stem cells using adenoviral and adeno-associated viral vectors. *Cloning Stem Cells* **5**, 51–62 (2003).
24. Hughes, S.M., Moussavi-Harami, F., Sauter, S.L. & Davidson, B.L. Viral-mediated gene transfer to mouse primary neural progenitor cells. *Mol. Ther.* **5**, 16–24 (2002).
25. Dong, J.Y., Fan, P.D. & Frizzell, R.A. Quantitative analysis of the packaging capacity of recombinant adeno-associated virus. *Hum. Gene Ther.* **7**, 2101–2112 (1996).
26. Hermonat, P.L., Labow, M.A., Wright, R., Berns, K.I. & Muzyczka, N. Genetics of adeno-associated virus: isolation and preliminary characterization of adeno-associated virus type 2 mutants. *J. Virol.* **51**, 329–339 (1984).
27. Rabinowitz, J.E., Xiao, W. & Samulski, R.J. Insertional mutagenesis of AAV2 capsid and the production of recombinant virus. *Virology* **265**, 274–285 (1999).
28. Girod, A. *et al.* Genetic capsid modifications allow efficient re-targeting of adeno-associated virus type 2. *Nat Med.* [published erratum appears in *Nat. Med.* 1999 Dec;5(12):1438] **5**, 1052–1056 (1999).
29. Shi, W., Arnold, G.S. & Bartlett, J.S. Insertional mutagenesis of the adeno-associated virus type 2 (AAV2) capsid gene and generation of AAV2 vectors targeted to alternative cell-surface receptors. *Hum. Gene Ther.* **12**, 1697–1711 (2001).
30. Müller, O.J. *et al.* Random peptide libraries displayed on adeno-associated virus to select for targeted gene therapy vectors. *Nat. Biotechnol.* **21**, 1040–1046 (2003).
31. Perabo, L. *et al.* In vitro selection of viral vectors with modified tropism: the adeno-associated virus display. *Mol. Ther.* **8**, 151–157 (2003).
32. Opie, S.R., Warrington, Jr., K.H., Jr., Agbandje-McKenna, M, Zolotukhin, S. & Muzyczka, N. Identification of amino acid residues in the capsid proteins of adeno-associated virus type 2 that contribute to heparan sulfate proteoglycan binding. *J. Virol.* **77**, 6995–7006 (2003).
33. Walters, R.W. *et al.* Structure of adeno-associated virus serotype 5. *J. Virol.* **78**, 3361–3371 (2004).
34. Xie, Q. *et al.* The atomic structure of adeno-associated virus (AAV-2), a vector for human gene therapy. *Proc. Natl. Acad. Sci. USA* **99**, 10405–10410 (2002).
35. Stemmer, W.P. Rapid evolution of a protein in vitro by DNA shuffling. *Nature* **370**, 389–391 (1994).
36. May, O., Nguyen, P.T. & Arnold, F.H. Inverting enantioselectivity by directed evolution of hydantoinase for improved production of l-methionine. *Nat. Biotechnol.* **18**, 317–320 (2000).
37. Boder, E.T. & Wittrup, K.D. Yeast surface display for screening combinatorial polypeptide libraries. *Nat. Biotechnol.* **15**, 553–557 (1997).
38. Daugherty, P.S., Chen, G., Iverson, B.L. & Georgiou, G. Quantitative analysis of the effect of the mutation frequency on the affinity maturation of single chain Fv antibodies. *Proc. Natl. Acad. Sci. USA* **97**, 2029–2034 (2000).
39. Soong, N.W. *et al.* Molecular breeding of viruses. *Nat. Genet.* **25**, 436–439 (2000).
40. Zhao, H., Giver, L., Shao, Z., Affholter, J.A. & Arnold, F.H. Molecular evolution by staggered extension process (StEP) in vitro recombination. *Nat. Biotechnol.* **16**, 258–261 (1998).
41. Zolotukhin, S. *et al.* Recombinant adeno-associated virus purification using novel methods improves infectious titer and yield. *Gene Ther.* **6**, 973–985 (1999).
42. Rabinowitz, J.E. *et al.* Cross-Packaging of a Single Adeno-Associated Virus (AAV) Type 2 Vector Genome into Multiple AAV Serotypes Enables Transduction with Broad Specificity. *J. Virol.* **76**, 791–801 (2002).
43. Summerford, C. & Samulski, R.J. Membrane-associated heparan sulfate proteoglycan is a receptor for adeno-associated virus type 2 virions. *J. Virol.* **72**, 1438–1445 (1998).
44. Huttner, N.A. *et al.* Genetic modification of the adeno-associated virus type 2 capsid reduce the affinity and the neutralizating effects of human serum antibodies. *Gene Ther.* **10**, 2139–2147 (2003).
45. Gao, G. *et al.* Clades of Adeno-associated viruses are widely disseminated in human tissues. *J. Virol.* **78**, 6381–6388 (2004).
46. Hewat, E. & Blaas, D. in *Antibodies in Viral Infections*, vol. 260 (ed. Burton, D.R.) 29–44, (Springer-Verlag, Berlin, 2001).
47. Hansen, J., Qing, K., Kwon, H.J., Mah, C. & Srivastava, A. Impaired intracellular trafficking of adeno-associated virus type 2 vectors limits efficient transduction of murine fibroblasts. *J. Virol.* **74**, 992–996 (2000).
48. Walters, R.W. *et al.* Binding of adeno-associated virus type 5 to 2,3-linked sialic acid is required for gene transfer. *J. Biol. Chem.* **276**, 20610–20616 (2001).
49. Batard, P., Jordan, M. & Wurm, F. Transfer of high copy number plasmid into mammalian cells by calcium phosphate transfection. *Gene* **270**, 61–68 (2001).
50. Kern, A. *et al.* Identification of a heparin-binding motif on adeno-associated virus type 2 capsids. *J. Virol.* **77**, 11072–11081 (2003).

JOURNAL OF VIROLOGY, Sept. 2000, p. 8635–8647
0022-538X/00/$04.00+0

Vol. 74, No. 18

Mutational Analysis of the Adeno-Associated Virus Type 2 (AAV2) Capsid Gene and Construction of AAV2 Vectors with Altered Tropism

PEI WU,[1,2] WU XIAO,[2,3] THOMAS CONLON,[2,4] JEFFREY HUGHES,[2,3] MAVIS AGBANDJE-McKENNA,[5,6,7] THOMAS FERKOL,[8] TERENCE FLOTTE,[1,2,4] AND NICHOLAS MUZYCZKA[1,2,6]*

Department of Molecular Genetics and Microbiology,[1] Department of Pediatrics,[4] Department of Molecular Pharmaceutics,[3] Department of Biochemistry,[5] Powell Gene Therapy Center,[2] UF Brain Institute,[6] and Center for Structural Biology,[7] University of Florida, Gainesville, Florida 32610-0266, and Division of Pediatric Pulmonology, Rainbow Babies and Children's Hospital, Cleveland, Ohio 44106-6006[8]

Received 1 March 2000/Accepted 8 June 2000

Adeno-associated virus type 2 (AAV2) has proven to be a valuable vector for gene therapy. Characterization of the functional domains of the AAV capsid proteins can facilitate our understanding of viral tissue tropism, immunoreactivity, viral entry, and DNA packaging, all of which are important issues for generating improved vectors. To obtain a comprehensive genetic map of the AAV capsid gene, we have constructed 93 mutants at 59 different positions in the AAV capsid gene by site-directed mutagenesis. Several types of mutants were studied, including epitope tag or ligand insertion mutants, alanine scanning mutants, and epitope substitution mutants. Analysis of these mutants revealed eight separate phenotypes. Infectious titers of the mutants revealed four classes. Class 1 mutants were viable, class 2 mutants were partially defective, class 3 mutants were temperature sensitive, and class 4 mutants were noninfectious. Further analysis revealed some of the defects in the class 2, 3, and 4 mutants. Among the class 4 mutants, a subset completely abolished capsid formation. These mutants were located predominantly, but not exclusively, in what are likely to be β-barrel structures in the capsid protein VP3. Two of these mutants were insertions at the N and C termini of VP3, suggesting that both ends of VP3 play a role that is important for capsid assembly or stability. Several class 2 and 3 mutants produced capsids that were unstable during purification of viral particles. One mutant, R432A, made only empty capsids, presumably due to a defect in packaging viral DNA. Additionally, five mutants were defective in heparan binding, a step that is believed to be essential for viral entry. These were distributed into two amino acid clusters in what is likely to be a cell surface loop in the capsid protein VP3. The first cluster spanned amino acids 509 to 522; the second was between amino acids 561 and 591. In addition to the heparan binding clusters, hemagglutinin epitope tag insertions identified several other regions that were on the surface of the capsid. These included insertions at amino acids 1, 34, 138, 266, 447, 591, and 664. Positions 1 and 138 were the N termini of VP1 and VP2, respectively; position 34 was exclusively in VP1; the remaining surface positions were located in putative loop regions of VP3. The remaining mutants, most of them partially defective, were presumably defective in steps of viral entry that were not tested in the preliminary screening, including intracellular trafficking, viral uncoating, or coreceptor binding. Finally, in vitro experiments showed that insertion of the serpin receptor ligand in the N-terminal regions of VP1 or VP2 can change the tropism of AAV. Our results provide information on AAV capsid functional domains and are useful for future design of AAV vectors for targeting of specific tissues.

Adeno-associated virus type 2 (AAV2) belongs to the human parvovirus family, which requires a helper virus for productive replication (5, 7, 8). The nonenveloped capsid adopts an icosahedral structure with a diameter of approximately 20 nm. Packaged within the capsid is a single-stranded DNA genome of 4.7 kb that contains two large open reading frames (ORFs), *rep* and *cap* (35). Three structural proteins, designated VP1, VP2, and VP3, are encoded in the *cap* ORF and made from the p40 promoter by use of alternative splicing and alternative start codons. The three proteins share the same ORF and end at the same stop codon. The C-terminal regions common to all three capsid proteins fold into a β-barrel structure that is present in several viruses (31). Their molecular masses are 87, 73, and 62 kDa, and their relative abundances within the capsid are approximately 5, 5, and 90%, respectively (26). Recently, AAV has attracted a significant amount of interest as a vector for gene therapy (6, 26). It has a number of unique advantages that are potentially useful for gene therapy applications, including the ability to infect nondividing cells, a lack of pathogenicity, and the ability to establish long-term gene expression.

Early genetic studies on deletion mutants of AAV revealed that capsid proteins were required for accumulation of single-stranded DNA and production of infectious particles (19, 38). Mutations in the C-terminal region common to all three proteins also abolished virion formation and failed to accumulate single-stranded DNA (32). VP1 was thought to be important for virus infectivity or stability because mutations in the N-terminal region unique to VP1 produced DNA-containing particles with significantly reduced infectivity (19, 38). In vitro

* Corresponding author. Mailing address: Department of Molecular Genetics and Microbiology, P.O. Box 100266, College of Medicine, University of Florida, Gainesville, FL 32610. Phone: (352) 392-5913. Fax: (352) 392-5914. E-mail: muzyczka@mgm.ufl.edu.

assembly studies (33) and capsid initiation codon mutagenesis studies (25) suggested that both VP2 and VP3 were required for capsid formation and production of infectious particles, and either VP1 or VP2 was required for nuclear localization of VP3. Recently, Hoque et al. (19b) have shown that the VP2 N-terminal residues 29 to 34 are sufficient for nuclear translocation and suggested that the major function of VP2 is to translocate VP3 into the nucleus. A recent insertional mutation study on AAV capsid protein revealed that mutations in the capsid gene could affect AAV capsid assembly and infection (30). Since the crystal structure of AAV was still unavailable, the functional domains of the AAV capsid proteins were mostly predicted based on information derived from other related autonomous parvoviruses, canine parvovirus (CPV), feline panleukopenia virus, and B19, whose crystal structures were available (1, 2, 40, 41). Sequence comparison of AAV to these viruses revealed a few conserved functional domains (9, 10), but the exact functions of these domains were not clear.

While certain groups of cells cannot be transduced by AAV (22, 27), AAV can transduce a wide variety of tissues, including brain, muscle, liver, lung, vascular endothelial, and hematopoietic cells (12–14, 16, 21, 45, 48). Recently, Summerford and Samulski (37) reported that heparan sulfate proteoglycan is the primary cellular receptor for AAV, and their group further revealed that the binding site lies within VP3 (30). In addition, human fibroblast growth factor receptor 1 and $\alpha_v\beta_5$ integrin were identified as coreceptors for AAV (28, 36). Attempts to alter the AAV capsid also have been made in order to expand the tropism of AAV. Yang et al. (47) showed improved infectivity of hematopoietic progenitor cells by generating a chimeric recombinant AAV (rAAV) having the single-chain antibody against human CD34 protein. Girod et al. (15) showed that insertion of the L14 epitope into the capsid coding region can expand the tropism of this virus to cells nonpermissive for AAV infection that bear the L14 receptor. However, in both cases the normal AAV tropism was not disrupted. Ideally, for the purpose of retargeting, the normal AAV receptor binding would need to be modified so that rAAV infects only targets bearing the receptors for the engineered epitope.

In this study, we used site-directed mutagenesis to mutate the capsid ORF. Initially, 48 alanine scanning mutations were made in which two to five charged amino acids in the AAV capsid ORF were mutated to alanine residues by site-directed mutagenesis. We reasoned that since the mutations were an average of 15 to 20 amino acids (aa) apart and spanned the whole capsid gene, some of them would inevitably fall in or near the functional domains of AAV capsid. In addition, over 40 substitution and insertion mutations were made in a search for regions that could tolerate insertions for the purpose of retargeting AAV vectors. By analyzing these mutants, we obtained a preliminary functional map of the AAV capsid protein. Our results identified critical regions within the capsid that were potentially responsible for receptor binding, DNA packaging, capsid formation, and infectivity. In addition, we identified sites that were suitable for epitope insertions that might be useful for targeted gene delivery.

MATERIALS AND METHODS

Cell culture. Low-passage-number (passages 27 to 38) HFK 293 cells (17) and HeLa cells were grown in Dulbecco's modified Eagle's medium supplemented with 10% fetal calf serum, penicillin (100 U/ml), and streptomycin (100 U/ml) at 37°C and 5% CO_2. IB3 cells were propagated as described elsewhere (34).

Construction of AAV capsid mutant plasmids. Plasmid pIM45 (previously called pIM29-45 [23]) was used as the template for all mutant constructions. Mutagenesis was achieved by using the Stratagene site-directed mutagenesis kit according to the supplier's manual. For each mutant, we designed two PCR primers which contained the sequence of alanine substitution or insertion plus a unique endonuclease restriction site flanked by 15 to 20 homologous bp on each side of the substitution or insertion. The restriction site was designed to facilitate subsequent DNA sequencing of the mutants and for potential insertion of tags or foreign epitopes. The PCR products were digested with endonuclease *Dpn*I to eliminate the parental plasmid template and were propagated in *Escherichia coli* XL-Blue (Stratagene). Miniprep DNAs were extracted from ampicillin-resistant colonies and were screened by restriction endonuclease digestion. Positive clones were sequenced in the capsid ORF region. The capsid ORF was then subcloned back into the pIM45 backbone with *Sma*I and *Sph*I to eliminate background mutations. The same mutagenesis strategy was used for peptide substitution and insertion mutant constructions.

Production of rAAV particles. To produce rAAV with mutant capsid proteins, we transfected 293 cells with three plasmids: (i) pIM45, which supplied either wild-type (wt) or mutant capsid proteins (23); (ii) pXX6, which contained the adenovirus (Ad) helper genes (46); and (iii) pTRUF5, which contains the green fluorescent protein (*gfp*) gene driven by the cytomegalovirus (CMV) promoter and flanked by the AAV terminal repeats (22). In some experiments, pTRUF5 was substituted with CBA-AT, a recombinant AAV plasmid that contains the human α1-antitrypsin (hAAT) gene under the control of the CMV–β-actin promoter. The plasmids were mixed at a 1:1:1 molar ratio. Plasmid DNAs used for transfection were purified by the QIAGEN Maxi-prep kit according to the supplier's manual.

The transfections were carried out as follows. 293 cells were split 1:2 the day before the transfection so that they could reach 75% confluency the next day. Ten 15-cm-diameter plates were transfected at 37°C, using calcium phosphate as described elsewhere (51), and incubated at 37°C. Forty-eight hours after transfection, cells were harvested by centrifugation at 1,140 × *g* for 10 min, the pellets were resuspended in 10 ml of lysis buffer (0.15 M NaCl, 50 mM Tris-HCl [pH 8.5]), and viruses were released by freezing and thawing three times. The crude rAAV lysates were treated with Benzonase (pure grade; Nycomed Pharma A/S) at a final concentration of 50 U/ml at 37°C for 30 min. The crude lysates were clarified by centrifugation at 3,700 × *g* for 20 min, and the supernatant was subjected to further purification by iodixanol step gradient and heparan sulfate affinity purification as previously described (51).

To determine whether any of the mutants were temperature sensitive, the transfections were done in six-well dishes as duplicates at 39.5 and 32°C. Viruses were resuspended in 250 μl of lysis buffer. All crude rAAV preparations were stored at −80°C until their titers were determined.

Gel electrophoresis, immunoblotting, and immunoprecipitation. Crude or purified rAAV samples were analyzed on sodium dodecyl sulfate (SDS)–10% polyacrylamide gels. The samples were mixed with sample buffer and boiled at 100°C for 5 min before loading. For immunoblotting, the proteins were transferred to a Nitro-bond membrane at 4°C, and the membrane was probed with monoclonal antibody (MAb) B1, directed against the capsid proteins (43). The capsid bands were visualized by peroxidase-coupled secondary antibodies using ECL (enhanced chemiluminescence detection) (Amersham) as suggested by the supplier.

For immunoprecipitation, heparan column-purified rAAV samples were diluted in 10 volumes of NETN buffer (0.1 M NaCl, 1 mM EDTA, 20 mM Tris-HCl [pH 7.5], 0.5% Nonidet P-40) and incubated overnight at 4°C in the presence of a MAb to the hemagglutinin (HA) epitope conjugated to Sepharose beads (BAbCo). For a negative control, MAb AU1-conjugated beads (BAbCo) were used. AU1 is a commonly used epitope, DTYRYI. After incubation, the samples were centrifuged for 5 min at 17,600 × *g* at 4°C. The beads were washed three times with 1 ml of NETN for 10 min at room temperature and resuspended in protein loading buffer. After centrifugation, the supernatant was precipitated with 15% trichloroacetic acid on ice for 1 h and centrifuged for 45 min at 4°C, and the pellet was resuspended in loading buffer. The samples then were boiled in sample buffer and analyzed by Western blotting with MAb B1 as described above.

Virus titers. The infectious titers of rAAV-containing wt and mutant capsids were measured at two temperatures, 39.5 and 32°C, for the alanine scanning mutants and at 37°C for all other mutants by using the fluorescent cell assay, which detects expression of the *gfp* gene. This was done essentially as described previously by Zolotukhin et al. (51). Briefly, 293 cells were seeded in a 96-well dish the day before infection so that they would reach about 75% confluence the next day. Serial dilutions of wt and mutant rAAV-GFP crude preparations were added to the cells in the presence of Ad5 at a multiplicity of infection (MOI) of 10. The cells and viruses were incubated at 37°C (or 32° and 39.5°C) for 48 h, and the titers were determined by counting the number of green cells with the fluorescence microscope. For each mutant, the infections were done twice and the average was taken. For mutants that contained a packaged CBA-AT gene, infectivity was measured by the infectious center assay on 293 cells as previously described (51) and by enzyme-linked immunosorbent assay (ELISA) measurement of hAAT secreted into culture media from infected cells as described elsewhere (34).

To determine the rAAV physical particle titer, we used the A20 ELISA kit (American Research Bioproducts). The crude rAAV stocks were serially diluted and incubated with the A20 kit plate. The readings that fell into the linear range were taken, and the titers were read off the standard according to the manufacturer's instructions. The A20 antibody detects both full and empty particles (44).

To determine the titer of rAAV physical particles that were full (i.e., contained

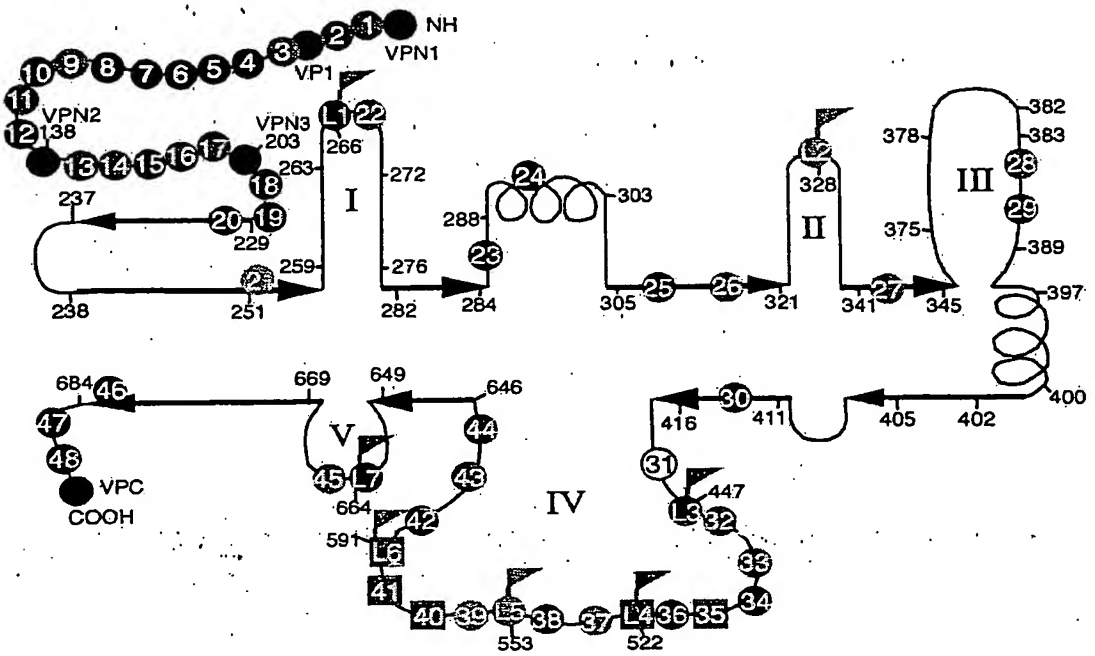

FIG. 1. Distribution of alanine scanning and HA epitope insertion mutants. Positions of the alanine scanning mutants (colored circles or squares) and the HA insertion mutants (flagged circles or squares) are shown on a diagram of the putative secondary structure of the AAV capsid protein adapted from a comparison of parvovirus capsid sequences by Chapman and Rossmann (9). Some important amino acid positions and mutant positions are illustrated by numbers with short lines. Heavy arrows represent putative β sheets, and helices represent putative α helices. The five putative loop regions are numbered I to V. The colors of the circles indicate the phenotypes of the mutants as shown below:

Class	Mutant(s)	Color	Primary phenotype	Defect
1	*mut*1, *mut*2, *mut*3, *mut*9, *mut*11, *mut*13, *mut*14, *mut*16, *mut*17, *mut*29, *mut*32, *mut*38, *mut*43, *mut*44, *mut*45	Red	Wild type	
2a	*mut*4, *mut*5, *mut*6, *mut*7, *mut*8, *mut*10, *mut*12, *mut*15, *mut*18, *mut*30, *mut*34, *mut*36, *mut*48; L1, L3, L7, VPN1, VP1, VPN2	Blue	Partially defective	
2b	*mut*21, *mut*39	Light blue	Partially defective	Unstable capsid
2c	*mut*41, L6	Purple	Partially defective	Heparan binding negative
3a	*mut*26, *mut*27, *mut*28, *mut*33	Green	Temperature sensitive	
3b	*mut*35	Purple	Temperature sensitive	Heparan binding negative
4a	*mut*22, *mut*37; L5, L2	Brown	Noninfectious	
4b	*mut*19, *mut*20, *mut*23, *mut*24, *mut*25, *mut*42, *mut*46, *mut*47; VPN3, VPC	Black	Noninfectious	No capsid made
4c	*mut*31	White	Noninfectious	Empty capsid
4d	*mut*40, L4	Purple	Noninfectious	Heparan binding negative

DNA), we used the quantitative competitive PCR (QC-PCR) assay as described previously (51). The crude rAAV stocks (100 μl) were digested first with DNase I to eliminate contaminating unpackaged DNA in 50 mM Tris-HCl (pH 7.5)–10 mM $MgCl_2$ for 1 h at 37°C and then incubated with proteinase K (Boehringer) in 10 mM Tris HCl (pH 8.0)–10 mM EDTA–1% SDS for 1 h at 37°C. Viral DNA was extracted twice in phenol-chloroform and once with chloroform and then precipitated by ethanol in the presence of glycogen (10%). The DNA was washed with ethanol, dried, and dissolved in 100 μl of H_2O, and 1 μl of the viral DNA was used for QC-PCR. Serial dilutions of the internal standard plasmid DNA with a deletion of GFP were included in the reaction, and the PCR products were separated by 2% agarose gel electrophoresis. The densities of the target and competitor bands in each lane were measured using ZERO-Dscan image analysis system software (version 1.0; Scanalytics) to determine the DNA concentration of the virus stock.

Heparan column binding assay. The ability of mutants to bind to heparan sulfate was tested essentially as previously described (51). Crude rAAV preparations containing wt or mutant capsids were first subjected to iodixanol gradient purification. The 40% layer was then collected and loaded onto a 1-ml preequilibrated heparan column at room temperature (immobilized on cross-linked 4% beaded agarose; Sigma H-6508). The flowthrough fraction, wash (3 column volumes), and 1 M NaCl eluate were collected, and equivalent amounts of each sample were mixed with SDS sample buffer and electrophoresed on SDS-polyacrylamide gels. The yield of capsid proteins in each fraction was monitored with MAb B1 by Western blotting and ECL detection.

EM. Electron microscopy (EM) was done in the ICBR EM lab of the University of Florida. Iodixanol gradient and heparan column-purified wt or mutant GFP-rAAVs were desalted and concentrated by using a Centricon 10 filter (Amicon). About a 5-μl drop of the virus sample was spotted onto carbon-coated grids and left for 1 min at room temperature. Excess fluid was drawn off, and the sample was washed three times with phosphate-buffered saline; 5 μl of 1% uranyl acetate was added for 10 s, and the grid was dried at room temperature for 10 min before viewing under EM.

RESULTS

Generation of AAV capsid mutations. We began our studies by using alanine scanning site-directed mutagenesis in the hope that some of the mutants would be temperature sensitive (11). The mutants were constructed in the noninfectious AAV plasmid, pIM45, which contains all of the AAV DNA sequence except the AAV terminal repeats. There are approximately 60 charged clusters in the AAV capsid gene. Some of the clusters are overlapping; in those cases, only one cluster was chosen. For the initial round of mutagenesis, 48 sites, named *mut*1 to *mut*48, were targeted. These were spaced approximately equally over the capsid gene, with 12 mutants exclusively in VP1, 5 in VP2, and the rest in VP3 (Fig. 1). With the exceptions noted below, in each cluster, all charged amino acids were converted to alanine. The mutations were created so that they also contained a restriction site at the site of mutation to

facilitate confirmation of the mutant sequence and subsequent insertion of foreign epitopes (Table 1). In addition, after sequence comparison of AAV serotypes 1 to 6, several other positions were targeted. *mut*28 and *mut*35 were made at positions where extra amino acids were found in AAV4 by sequence comparison with AAV2. *mut*32 was made by replacing TTT with AAA since TTT was not conserved among other AAV serotypes at aa 454. Finally, in *mut*29 and *mut*31, only one Arg residue was changed to Ala, and in *mut*45 and *mut*48, only one Lys was changed to Ala. The positions of the alanine scanning mutants and the specific amino acid substitutions are summarized in Table 1 and Fig. 1.

Infectious titer assays reveal four general classes of mutants. To determine the effect of each mutation on viral infectivity, we used either wt pIM45 or a mutant pIM45 plasmid to complement the growth of pTRUF5. pTRUF5 is a recombinant AAV plasmid that contains the *gfp* gene under the control of a CMV enhancer-promoter (22). The resulting recombinant TRUF5 virus contained either wt or mutant capsid proteins and could be titered for infectivity by counting green fluorescent cells in the presence of an Ad5 coinfection. We had shown previously that the fluorescent cell assay produced titers within two- to threefold of those obtained with a conventional infectious center assay (51). Initially, each mutant was grown and titered at either 39.5 or 32°C to determine if any of the mutants were temperature sensitive. The experiments were done twice, and there was no significant variation in titer. On the basis of these titers, the mutants could be grouped into four classes (Fig. 2; Table 1). Class 1 contained mutants that have an infectious titer similar to the wt titer (less than 1 log difference; for example, *mut*1 and *mut*2). Class 2 contained partially defective mutants with infectious titers 2 to 3 logs lower than the wt titer (for example, *mut*4 and *mut*5). Class 3 contained temperature-sensitive mutants; three of these (*mut*26, *mut*27, and *mut*33) were heat sensitive, and two (*mut*28 and *mut*35) were cold sensitive. Class 4 consisted of 12 noninfectious mutants, whose titers were more than 5 logs lower than the wt titer.

Noninfectious (class 4) mutants and temperature-sensitive (class 3) mutants were defective in packaging DNA or in forming stable virus particles. To determine the probable causes for the different defective mutants, we focused first on class 3 and 4 mutants. For convenience, we ignored the fact that the temperature-sensitive mutants had low infectivity when grown at the partially restrictive temperature of 37°C (data not shown), and viral preparations for all class 3 and 4 mutants were made at 37°C. To determine if these mutants were able to make capsids, we used the A20 ELISA. The A20 antibody recognizes only intact AAV particles (43) and is useful for determining the physical particle titer irrespective of whether the capsids contain DNA (18). Eight of sixteen mutants that were tested were negative by ELISA reading (Table 2), indicating that they were unable to make capsids or that the capsids were unstable even in crude lysate preparations. All of these were class 4 (noninfectious) mutants and were classified as class 4b (Table 1; Fig. 1).

QC-PCR assays also were performed on most of the class 3 and 4 mutants. The QC-PCR assay measures the titer of AAV particles that contain DNase-resistant rAAV genomes (Fig. 3). We have shown previously that it provides physical particle titers that are equivalent to those obtained by dot blot assay but has better sensitivity at low particle titers (51). As expected, mutants that were negative for the synthesis of AAV particles by A20 ELISA were also negative by QC-PCR assay (Table 2; Fig. 3). Most of the remaining mutants, which were positive for A20 particles, were also positive for packaged viral DNA in the QC-PCR assay (Fig. 3; Table 2). This group of noninfectious mutants (*mut*22 and *mut*37) were called class 4a (Table 1; Fig. 1). Their defect was not in packaging but rather in the binding, internalization, or uncoating steps of the viral entry process. One A20-positive mutant (*mut*31) was an exception in that it was A20 positive but DNA negative by QC-PCR assay. This meant that *mut*31 formed intact virus particles that were empty. To confirm this, *mut*31 was examined by EM (Fig. 4), and it did indeed make empty particles. In contrast, the partially defective class 2 mutant, *mut*4, produced particles similar to wt particles. *mut*31 was assigned to class 4c (Fig. 1; Table 1).

Some mutants are defective for binding the viral receptor. One potential cause for the reduced infectivity of class 2, 3, or 4 mutants might be that they were unable to bind the viral cell surface receptor, the first step of the infectious cycle. Heparan sulfate proteoglycan has been identified as the primary cell surface receptor for AAV (37). To test whether these mutants could bind heparan, we developed a heparan column binding assay (Materials and Methods). Iodixanol-purified wt or mutant rAAVs were passed through a heparan agarose column, and the AAV capsid proteins in the starting material and the bound (eluate) and unbound (flowthrough and wash) fractions were monitored by Western blotting using MAb B1, which recognizes all three capsid proteins (Fig. 5; Table 3). As expected, wt AAV had a high affinity for the heparan column, since little capsid protein was detected in the flowthrough and wash fractions, and most of the capsid protein was detected in the eluate. The same was true of most of the mutants tested (Fig. 5; Table 3). Two mutants, however, *mut*35 and *mut*41, bound poorly to heparan (Fig. 5). A third mutant, *mut*40, which is located about 20 aa away from *mut*41, also bound with reduced affinity (Fig. 5). This suggested that the primary defect in these mutants was their inability to bind to heparan sulfate proteoglycan. We classified *mut*35 as class 3b (temperature sensitive and heparan binding negative), *mut*41 as class 2c (partially defective and heparan binding negative), and *mut*40 as class 4d (noninfectious and heparan binding negative) (Fig. 1; and Table 1).

Three class 4b mutants, *mut*20, *mut*25, and *mut*46, could not be detected by Western analysis (Table 3). This was consistent with the fact that they made no capsid that was detectable with the A20 antibody (Table 2). Additionally, *mut*27, a temperature-sensitive mutant, and two class 2 mutants, *mut*21 and *mut*39, did not give any Western signal with MAb B1 (Fig. 5; Table 3). The heat-sensitive mutant, *mut*27, was presumably unstable at the nonpermissive temperature used for growing this virus. *mut*21 and *mut*39 were partially defective when assayed in crude extracts (Fig. 2). The fact that they could not be detected by capsid antibody after iodixanol centrifugation suggests that these capsids were also unstable during purification. These mutants were assigned to class 2b on the basis of their capsid instability (Table 1; Fig. 1). The rest of the mutants in class 2 that bind to heparan were classified as class 2a, partially defective, and heparan binding positive (Tables 1 and 3; Fig. 1). The nature of their defect was not clear but presumably was due to some step in the infectious process that occurs after viral attachment to the cell surface.

Regions tolerating alanine substitutions do not tolerate other kinds of substitutions. We wanted to determine whether the class 1 mutants defined positions in the capsid genes that were truly nonessential for capsid function. To test this, we constructed a series of mutants in which either the serpin receptor ligand, FVFLI (50), or the FLAG antibody epitope, DY KDDDDKYK, was substituted for capsid sequences at many of the class 1 mutant positions (Table 4). A number of class 2 and class 4 mutants were tried as well. The serpin substitution

TABLE 1. Summary of all mutants

Mutant[a]	Type[b]	Amino acid positions[b]	Class	Phenotype[c]
*mut*1[1]	Ala sub	9-13 DWLED-AWLAA	1	wt
*mut*2[1]	Ala sub	24-28 KLKPG-ALAPG	1	wt
*mut*3[2]	Ala sub	33-37 KPKER-APAAA	1	wt, surface
*mut*4[2]	Ala sub	39-43 KDDSR-AAASA	2a	pd, hep$^+$
*mut*5[3]	Ala sub	63-67 EPVNE-APVNA	2a	pd, hep$^+$
*mut*6[2]	Ala sub	67-71 EADAA-AAAAA	2a	pd, hep$^+$
*mut*7[2]	Ala sub	74-78 EHDKA-AHAAA	2a	pd, hep$^+$
*mut*8[2]	Ala sub	76-80 DKAYD-AAAYA	2a	pd, hep$^+$
*mut*9[1]	Ala sub	84-88 DSGDN-ASGAN	1	wt
*mut*10[2]	Ala sub	95-99 HADAE-AAAAA	2a	pd, hep$^+$
*mut*11[2]	Ala sub	102-107 ERLKED-AALAAA	1	wt
*mut*12[2]	Ala sub	122-126 KKRVL-AAAVL	2a	pd, hep$^+$
*mut*13[2]	Ala sub	142-146 KKRPV-AAAPV	1	wt
*mut*14[1]	Ala sub	152-156 EPDSS-APASS	1	wt
*mut*15[2]	Ala sub	168-172 RKRLN-AAALN	2a	pd, hep$^+$
*mut*16[2]	Ala sub	178-182 GDADS-GAAAS	1	wt
*mut*17[1]	Ala sub	180-184 DSVPD-ASVPA	1	wt
*mut*18[2]	Ala sub	216-220 EGADG-AGAAG	2a	pd, hep$^+$
*mut*19[1]	Ala sub	228-232 WHCDS-WACAS	4b	ni, no capsid
*mut*20[2]	Ala sub	235-239 MGDRV-MGAAV	4b	ni, no capsid
*mut*21[4]	Ala sub	254-258 NHLYK-NALYA	2b	pd, unstable capsid
*mut*22[4]	Ala sub	268-272 NDNHY-NANAY	4a	ni, full particle
*mut*23[4]	Ala sub	285-289 NRFHC-NAFAC	4b	ni, no capsid
*mut*24[2]	Ala sub	291-295 FSPRD-FSPAA	4b	ni, no capsid
*mut*25[2]	Ala sub	307-311 RPKRL-APAAL	4b	ni, no capsid
*mut*26[2]	Ala sub	320-324 VKEVT-VAAVT	3a	hs
*mut*27[1]	Ala sub	344-348 TDSEY-TASAY	3a	hs
*mut*28[2]	Ala ins	384-385 AAA	3a	cs
*mut*29[1]	Ala sub	389 R-A	1	wt
*mut*30[2]	Ala sub	415-419 FEDVP-FAAVP	2a	pd, hep$^+$
*mut*31[4]	Ala sub	432 R-A	4c	ni, empty particle
*mut*32[2]	Ala sub	454-456 TTT-AAA	1	wt
*mut*33[2]	Ala sub	469-472 DIRD-AIAA	3a	hs
*mut*34[2]	Ala sub	490-494 KTSAD-ATSAA	2a	pd, hep$^+$
*mut*35[2]	Ala ins	509 AAAA	3b	cs, hep$^-$, surface
*mut*36[1]	Ala sub	513-517 RDSLV-AASLV	2a	pd, hep$^+$
*mut*37[2]	Ala sub	527-532 KDDEEK-AAAAA	4a	ni, full particle
*mut*38[2]	Ala sub	547-551 SEKTN-SAATN	1	wt
*mut*39[2]	Ala sub	553-557 DIEKV-AIAAV	2b	pd, unstable capsid
*mut*40[2]	Ala sub	561-565 DEEEI-AAAAI	4d	ni, hep$^-$, full particle, surface
*mut*41[2]	Ala sub	585-588 RGNR-AGAA	2c	pd, hep$^-$, surface
*mut*42[2]	Ala sub	607-611 QDRDV-QAAAV	4b	ni, no capsid
*mut*43[2]	Ala sub	624-628 TDGHF-TAGAF	1	wt
*mut*44[1]	Ala sub	637-641 FGLKH-FGLAA	1	wt
*mut*45[2]	Ala sub	665 K-A	1	wt
*mut*46[2]	Ala sub	681-683 EIE-AAA	4b	ni, no capsid
*mut*47[2]	Ala sub	689-693 ENSKR-ASSAA	4b	ni, no capsid
*mut*48[1]	Ala sub	706 K-A	2a	pd, hep$^+$
L1	HA ins	266	2a	pd, A20$^-$, A20 epitope$^-$, surface
L2	HA ins	328	4a	ni, A20$^+$, surface
L3	HA ins	447	2a	pd, hep$^+$, surface
L4	HA ins	522	4d	ni, hep$^-$, surface
L5	HA ins	553	4a	ni, A20$^+$, surface
L6	HA ins	591	2c	pd, hep$^-$, surface
L7	HA ins	664	2a	pd, hep$^+$, surface
VPN1	HA, AU ins	1	2a	pd, hep$^+$, surface
VP1	HA ins, Ser sub	34	2a	pd, hep$^+$, surface
VPN2[d]	HA, Ser ins	138	2a	pd, hep$^+$, surface
VPN3	HA, Ser ins	203	4b	ni, no capsid
VPC	HA, Ser, AU, His ins	735	4b	ni, no capsid
*mut*1subser1	Ser sub	10	4a	ni, A20$^+$
*mut*2subser2	Ser sub	24	4a	ni, A20$^+$
*mut*3subser3	Ser sub	34	2a	pd, hep$^+$
*mut*9subser4	Ser sub	84	4a	ni, A20$^+$
*mut*14subser5	Ser sub	150	4a	ni, A20$^+$
*mut*16subser6	Ser sub	178	4b	ni, no capsid
*mut*19subser7	Ser sub	224	4b	ni, no capsid

Continued on following page

TABLE 1—*Continued*

Mutant[a]	Type[b]	Amino acid positions[b]	Class	Phenotype[c]
*mut*32subser8	Ser sub	454	4b	ni, no capsid
*mut*37subser9	Ser sub	526	4b	ni, no capsid
*mut*39subser10	Ser sub	553	4b	ni, no capsid
*mut*40subser11	Ser sub	562	4b	ni, no capsid
*mut*41subser12	Ser sub	590	4b	ni, no capsid
*mut*44subser13	Ser sub	638	4b	ni, no capsid
*mut*45subser14	Ser sub	664	4b	ni, no capsid
*mut*46subser15	Ser sub	682	4b	ni, no capsid
*mut*4subflg2	FLAG sub	39	4a	ni, A20$^+$
*mut*8subflg3	FLAG sub	76	4a	ni, A20$^+$
*mut*16subflg4	FLAG sub	178	4a	ni, A20$^+$
*mut*32subflg5	FLAG sub	454	4a	ni, A20$^+$
*mut*37subflg6	FLAG sub	526	4a	ni, A20$^+$
*mut*38subflg7	FLAG sub	547	4a	ni, A20$^+$
*mut*40subflg8	FLAG sub	562	4b	ni, no capsid
*mut*44subflg9	FLAG sub	638	4b	ni, no capsid
*mut*45subflg10	FLAG sub	664	4b	ni, no capsid
*mut*46subflg11	FLAG sub	682	4b	ni, no capsid

[a] Superscripts 1 to 4 indicate that a restriction site was introduced as a result of the alanine substitution mutation: 1, *Nhe*I; 2, *Eag*I; 3, *Upn*I; 4, *Mlu*I.

[b] Ala sub, alanine substitution mutant; Ala ins, string of alanine residues inserted after the indicated amino acid; HA, AU, His, or Ser ins, insertion of the HA, AU, His, or Ser epitope immediately after the indicated amino acid of wt cap; Ser or FLAG sub, substitution of the Ser or FLAG epitope for the wt AAV capsid sequence beginning immediately after the indicated AAV amino acid residue. Amino acid tags: HA, YPYDVPDYA; AU, DTYRYI; HIS, HHHHHH; Ser, FVFLI; FLAG, DYKDDDDK.

[c] pd, partially defective for infectivity, between 1 to 3 logs lower than wt; cs and hs, cold sensitive and heat sensitive, respectively; ni, noninfectious, 5 logs lower than wt; hep$^+$ mutant bound to a heparan column; hep$^-$, mutant did not bind to heparan sulfate; no capsid, mutant was A20 ELISA negative and MAb B1 negative; A20$^+$, mutant could be detected with A20 antibody; surface, position was present on the surface of the capsid.

[d] The serpin insertion in VPN2 was KFNKPFVFLI.

(5 aa) was the same size as the largest alanine substitutions. The FLAG epitope is highly charged, as were many of the substituted wt sequences. As expected, substitutions at class 2 (partially defective) or class 4 (nonviable) positions did not produce infectious virus (Table 4). Surprisingly, although many of the class 1 serpin or FLAG substitutions produced some physical particles detectable with the A20 antibody, only one of the substitutions, serpin at aa 34 (the *mut*3 position), produced infectious virus particles in substantial yield (Table 4). Most infectious titers were reduced by 5 logs or more, and particle titers (as judged by A20 ELISA) were reduced or undetectable as well. Thus, although modification of charged residues in class 1 mutants to alanine was permissible, these regions of the capsid were nevertheless essential for capsid formation and were sensitive to other kinds of substitutions.

Putative loop regions and the N-terminal regions of VP1 and VP2 are able to accept insertions of foreign epitopes. We also chose several other sites for insertion of foreign sequences. For

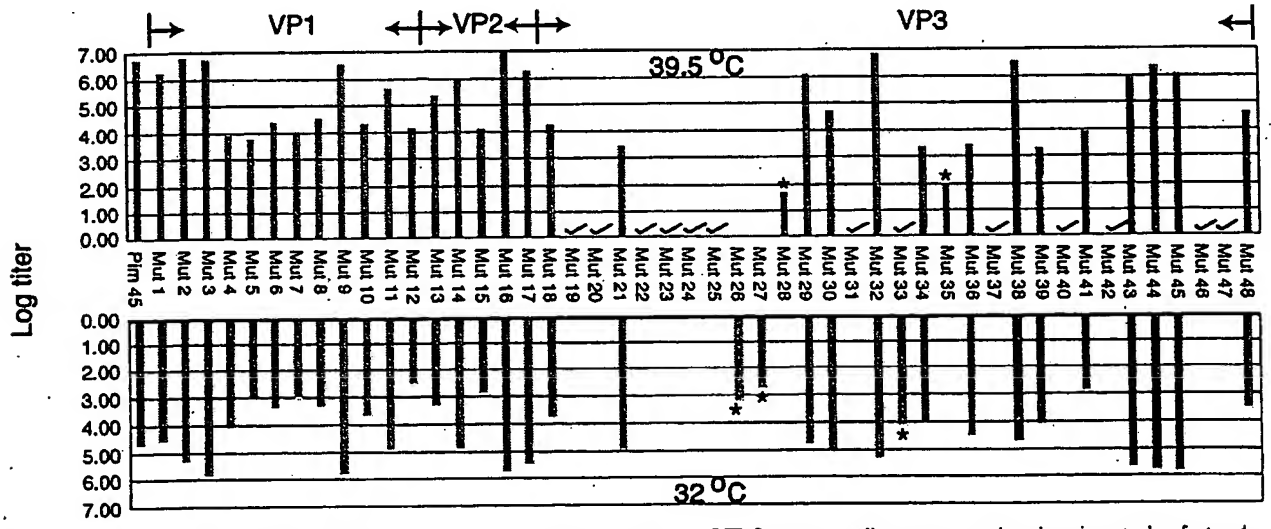

FIG. 2. Infectious titers of virus stocks containing wt and mutant capsid proteins. The GFP fluorescent cell assay was used to titer virus stocks of wt and mutant virus stocks containing the pTRUF5 genome. 293 cells were transfected with wt or mutant pIM45 complementing plasmid in the presence of pTRUF5 and pXX6 at 39.5 and 32°C. Cells were collected 48 h posttransfection and then frozen and thawed three times. The crude lysate was used to infect 293 cells at 39.5 and 32°C with Ad5 (MOI = 10). The log value of the average infectious titer (infectious particles/milliliter) that was obtained from two independent experiments is shown. There was no significant difference between experiments. The distribution of mutants unique to VP1, VP2, or VP3 is shown at the top. Asterisks indicate temperature-sensitive mutants; noninfectious mutants are indicated by check marks.

TABLE 2. Determination of physical particle titer and DNA-containing particle titer of class 2 and 3 mutants

Construct[a]	A20 ELISA[b]	QC-PCR[c]
pIM45 (wt)	+++	+++
*mut*19	−	−
*mut*20	−	−
*mut*22	++	++
*mut*23	−	−
*mut*24	−	−
*mut*25	−	−
*mut*26 (hs)	ND[d]	ND
*mut*27 (hs)	+	ND
*mut*28 (cs)	+	ND
*mut*31	++	−
*mut*33 (hs)	++	+
*mut*35 (cs)	++	++
*mut*37	++	+
*mut*40	++	++
*mut*42	−	−
*mut*46	−	ND
*mut*47	−	ND

[a] hs, heat sensitive; cs, cold sensitive.
[b] +++, $>10^{12}$ particles/ml; ++, $>10^{11}$ particles/ml; +, $>10^{10}$ particles/ml; −, $<10^{8}$ particles/ml, which was the limit of detection by A20 ELISA.
[c] +++, $>10^{11}$ full particles/ml; ++, $>10^{10}$ full particles/ml; +, $>10^{9}$ full particles/ml; −, $<10^{8}$ full particles/ml.
[d] ND, not done.

these mutants, we chose to insert the less charged HA epitope, YPVDVPDYA. The target positions for insertion were the N-terminal regions of the three capsid proteins, VP1, VP2, and VP3, the C terminus of the cap ORF and seven positions (mutants L1 to L7) that were believed to be in loop regions of the capsid protein based on an alignment of the AAV capsid sequence to that of CPV (9). Since these sites were suspected to be on the surface of the capsid, insertions at these sites might not affect capsid assembly or stability (Fig. 1). Mutations in the loop regions had been targeted successfully before by Girod et al. (15), who were able to insert the L14 ligand at aa 587 without significant loss in infectivity.

Insertions at the N termini of VP1 (VPN1) and VP3 (VPN3) and the C terminus of the cap ORF (VPC) were not well tolerated (Table 5). To eliminate the possibility that the defect in these mutants was due to the HA tag, other tags such as AU, His, and Myc were also inserted at the N termini of VP1 and VP3 and the C terminus of cap, and they also were not tolerated at those positions (Table 1 and data not shown). Insertions at three of the putative loop regions were also not viable (Table 5, mutants L2, L4, and L5). Mutants L4 (aa 522) and L5 (aa 553) were interesting in that they produced a significant yield of physical particles that were not infectious.

However, HA insertions were well tolerated at aa 34 within the N-terminal region of VP1, at the N terminus of VP2, and within three of the putative loop regions, loop I (mutant L1), loop IV (mutants L3 and L6), and loop V (mutant L7) (Table 5; Fig. 1).

Some HA insertion positions are on the capsid surface. To determine whether the HA insertion mutants contained the HA sequence exposed on the surface of the capsid, we used batch immunoprecipitation with HA MAb-conjugated beads. In each case virus was purified by iodixanol density centrifugation and heparan column chromatography to remove any soluble capsid protein that might be present in crude viral preparations. As expected, insertion of the HA tag at the N terminus of VP2 (mutant VPN2) produced a slight increase in the molecular weight of VP2 and VP1 compared to wt protein, pIM45 (Fig. 6A, B1 mAb). Western blotting with the HA MAb confirmed that the HA tag was present in both VP1 and VP2 (Fig. 6A, HA mAb). In the case of the VP1 mutant (HA insertion at aa 34 in VP1), only VP1 had a higher molecular weight and only VP1 contained the HA tag (Fig. 6A), as expected. When the viable insertions, VPN2 (HA insertion at the N terminus of VP2) and VP1 (insertion at aa 34), were treated with HA MAb-conjugated beads, substantial amounts of both viruses were precipitated (Fig. 6B, HA mAb). This demonstrated that in both cases the HA epitope was on the surface of the virus particle and accessible to the antibody. Control wt virus particles (Fig. 6B, pIM45), were not precipitated with HA MAb to any significant extent. The amount of virus in the starting material was monitored by Western blotting with B1 or HA MAb.

The putative loop HA insertion mutants, L1 to L7, were also incubated with HA MAb-conjugated beads. Although the insertions in some of these mutants produced noninfectious vi-

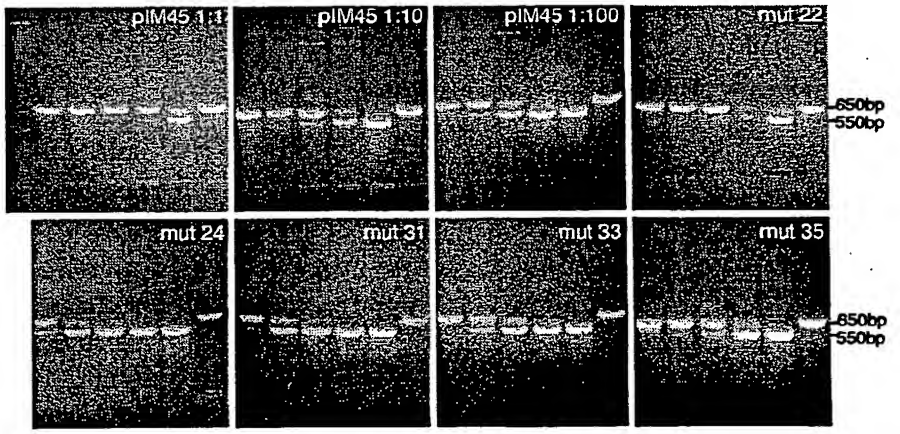

FIG. 3. QC-PCR assay of wt and mutant virus stocks to determine the DNA-containing particle titers. Crude viruses were treated with DNase to digest unpackaged DNA and then treated with proteinase K to release the packaged DNA. The viral DNA was extracted with phenol-chloroform, precipitated with ethanol, and dissolved in water. Equal amounts of viral DNA were incubated with (from left to right in each panel) 100 fg, 1 pg, 10 pg, 100 pg, 1 ng, or none of the pTRUF5 plasmid DNA containing a deletion in the *gfp* gene and amplified by PCR. The PCR products were separated on 2% agarose gels and viewed by ethidium bromide staining. The arrangement of lanes in each panel is the same. Results for wt pIM45 viral DNA at three dilutions (1:1, 1:10, and 1:100) are also shown (top left three panels). Molecular markers were included in the left lane of the top left panel.

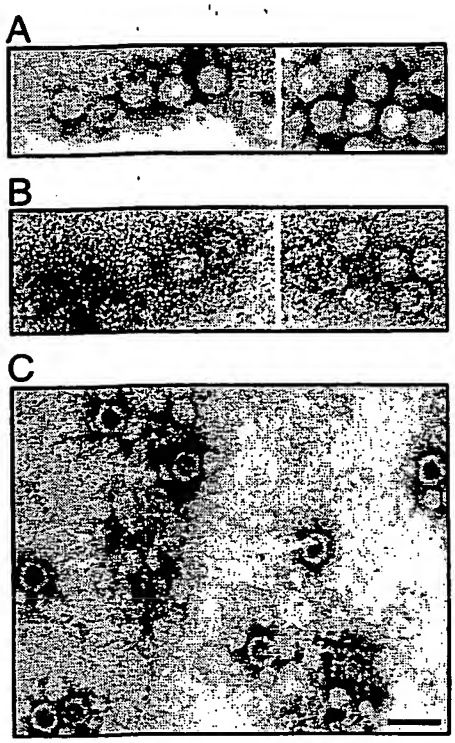

FIG. 4. EM analysis of wt (A) and mutant (*mut*4 [B] and *mut*31 [C]) rAAVs. The viruses were purified by iodixanol step gradient centrifugation and heparan column chromatography as described elsewhere (51), concentrated in a Centricon 10, and negatively stained with 1% uranyl acetate. Bar = 40 nm. Although the iodixanol step gradient might be expected to remove empty particles, these particles apparently accumulate at the 25 to 40% interface, and a significant fraction are recovered during this purification step.

rus, they all produced sufficient A20 antibody-positive virus particles to test for the presence of the HA tag on the surface of the capsid. When this was done, all of the L-series insertions were shown to be in the immunoprecipitate (bound fraction) compared to the wt (pIM45) control (Fig. 7A). This demonstrated that each of these insertions at putative loop sites resulted in the HA epitope being on the surface of the capsid.

We also checked whether these loop insertions affected heparan binding of the mutant capsids. Interestingly, two loop

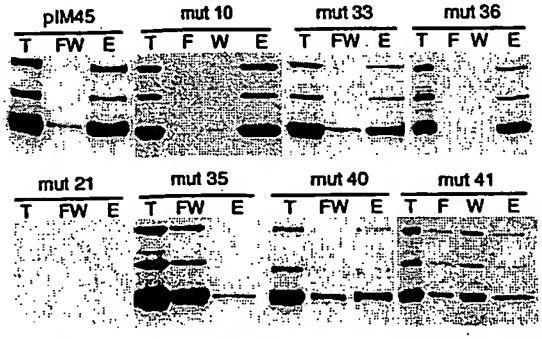

FIG. 5. Heparan binding properties of mutant viruses. Iodixanol gradient-purified virus stocks were loaded onto a heparan column. Equivalent volumes of the starting, 40% iodixanol material (T), flowthrough (F), wash (W), and eluted (E) fractions were separated on SDS–10% acrylamide gels and Western blotted with MAb B1. In some cases, the flowthrough and wash fractions were pooled (FW) and loaded together.

TABLE 3. Heparan column binding properties of class 2, 3, and 4 mutants[a]

Construct	Heparan binding	Construct	Heparan binding
pIM45	+	*mut*27	0
*mut*4	+	*mut*28	+
*mut*5	+	*mut*30	+
*mut*6	+	*mut*31	+
*mut*7	+	*mut*32	+
*mut*8	+	*mut*33	+
*mut*10	+	*mut*34	+
*mut*11	+	*mut*35	−
*mut*12	+	*mut*36	+
*mut*13	+	*mut*37	+
*mut*14	+	*mut*39	0
*mut*15	+	*mut*40	−
*mut*18	+	*mut*41	−
*mut*20	0	*mut*43	+
*mut*21	0	*mut*46	0
*mut*22	+	*mut*48	+
*mut*25	0		

[a] +, mutant virus bound to a heparan column with the same affinity as wt pIM45 virus; −, virus bound with at least a threefold-lower affinity; 0, no protein signal detected by Western blotting.

insertion mutants, L4 and L6, were found to bind heparan columns with reduced affinity (Fig. 7B), which probably accounted for the lower infectivity of these mutants in the standard fluorescent cell assay. The L4 and L6 insertions were near the heparan-binding-negative mutants *mut*35, *mut*40,

TABLE 4. Substitution of serpin or FLAG epitopes at capsid positions that tolerated alanine substitutions

Mutant	Titer[a]	
	Infectious	Physical particle
*mut*1subser1	−	+
*mut*2subser2	−	+
*mut*3subser3	1 log lower	+
*mut*9subser4	−	+
*mut*14subser5	−	+
*mut*16subser6	−	−
*mut*19subser7	−	−
*mut*32subser8	−	−
*mut*37subser9	−	−
*mut*39subser10	−	−
*mut*40subser11	−	−
*mut*41subser12	−	−
*mut*44subser13	−	−
*mut*45subser14	−	−
*mut*46subser15	−	−
*mut*4subflg2	−	+
*mut*8subflg3	−	+
*mut*16subflg4	−	+
*mut*32subflg5	−	+
*mut*37subflg6	−	+
*mut*38subflg7	−	+
*mut*40subflg8	−	−
*mut*44subflg9	−	−
*mut*45subflg10	−	−
*mut*46subflg11	−	−

[a] Either a serpin peptide sequence or the FLAG sequence was substituted for the AAV capsid sequence at the positions used previously for alanine scanning mutagenesis (Fig. 2). Infectious titers were determined by GFP fluorescent cell assay. −, infectious virus could not be detected. Physical particle titers were judged by A20 ELISA. +, particles were detectable; −, particles were not detectable.

TABLE 5. HA insertion mutants

Mutant	Position	Titer	
		Infectious[a]	Physical particle[b]
L1	aa 266	++	+
L2	aa 328	−	+
L3	aa 447	++	++
L4	aa 522	−	++
L5	aa 553	−	++
L6	aa 591	++	++
L7	aa 664	++	++
VPN1	aa 1	+	++
VP1	aa 34	+++	++
VPN2	aa 138	+++	+++
VPN3	aa 203	−	−
VPC	C terminus	−	−

[a] Determined by GFP fluorescence cell assay. +++, 1 log lower than wt; ++, 2 logs lower; +, 3 logs lower; −, at least 5 logs lower.
[b] Determined by A20 ELISA. +, 4 logs lower than wt pIM45; ++, 2 to 3 logs lower; +++, 1 log lower; −, undetectable.

and *mut*41 (Fig. 1). All five of these heparan-binding-negative mutants were located between aa 509 and 591, suggesting that this region within the AAV capsid constitutes the heparan binding domain of the capsid protein.

Changing the tropism of AAV. To determine whether we could change the tropism of rAAV by inserting a novel receptor ligand into the capsid, we constructed two mutant plasmids that contained a serpin receptor ligand. In one case the serpin

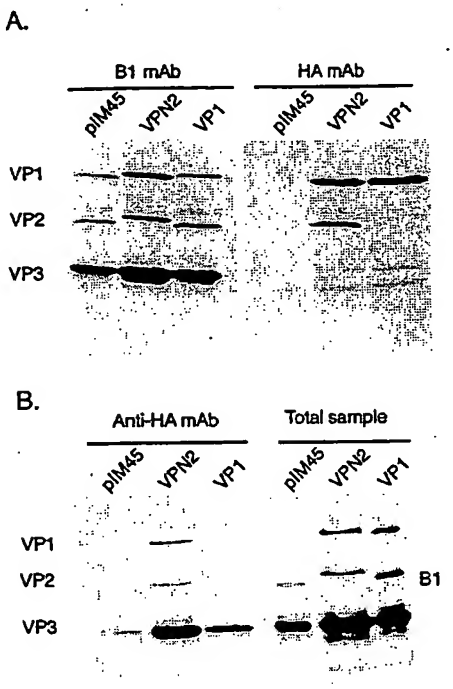

FIG. 6. Immunoprecipitation analysis of VP1 and VPN2 HA insertion mutants to determine the accessibility of the HA epitope. (A) Western blot analysis of iodixanol gradient-purified viruses with either B1 (left) or HA (right) MAb. (B) Iodixanol gradient and heparan column-purified viruses were precipitated with HA antibody coupled to agarose beads. The bound virus (Anti-HA mAb lanes) was eluted with SDS sample buffer and detected by Western blotting using MAb B1. For comparison, virus that had not been treated with HA MAb (Total sample) was also Western blotted with the B1 antibody.

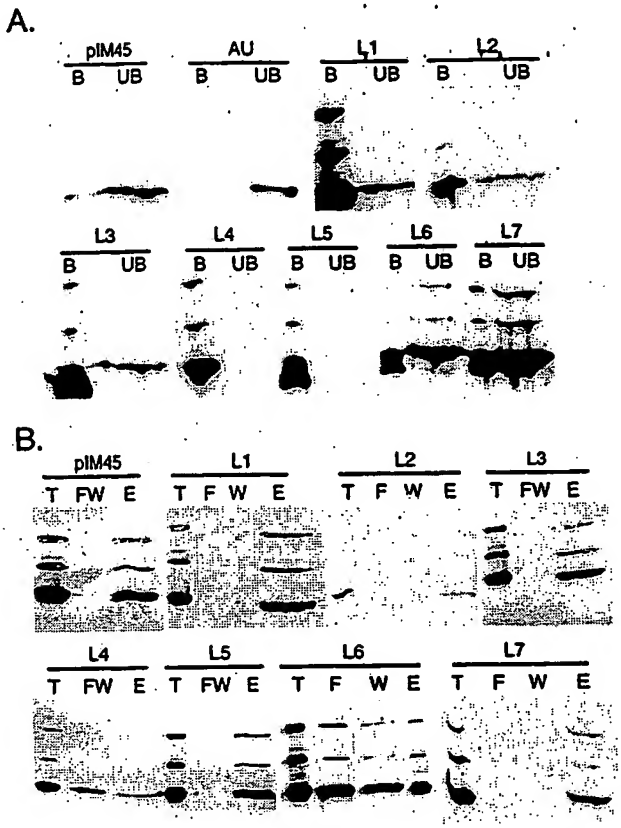

FIG. 7. Properties of HA insertion mutants. (A) Immunoprecipitation of HA loop insertion mutants to determine whether HA is exposed on the capsid surface. Iodixanol gradient and heparan column-purified viruses were incubated with HA MAb beads as described for Fig. 6. The antibody bound (B) and unbound (UB) fractions were separated on SDS–10% gels and detected by Western blotting with MAb B1. As a negative control, AU MAb was used in the panel marked AU. The pIM45 panel contained recombinant virus made with the wt helper plasmid. (B) Heparan binding properties of wt and HA loop insertion mutants. The virus samples were treated as described for Fig. 5. Virus in the starting material (T), flowthrough (F), wash (W), combined flowthrough and wash (FW), or eluate (E) was detected by Western blotting with MAb B1. pIM45 is virus with wt capsid.

ligand FVFLI (50) was substituted for the AAV capsid sequence immediately after aa 34. In the second mutant an expanded serpin receptor ligand, KFNKPFVFLI (50), was inserted at the N terminus of VP2, aa 138 (Table 1). The mutant capsid plasmids were then used to package CBA-AT, an rAAV genome that contained the hAAT gene under the control of a hybrid CMV–β-actin promoter. As seen with the HA insertion mutants described above, the serpin mutants produced rAAV viral titers that were slightly (sixfold) lower in infectivity when titered by the infectious center assay on 293 cells (data not shown). However, when equal amounts of wt or mutant virus (as determined on 293 cells) were infected into IB3 cells, both mutant viruses showed substantially higher infectivity than wt (Fig. 8). The VP2 serpin insertion was 15-fold more infectious, and the VP1 substitution mutant was approximately 62-fold more active. This suggested that IB3 cells, a lung epithelial cell line believed to express the serpin receptor, were a much better target for the serpin-tagged chimeric rAAVs than wt and that the tropism of the mutant rAAVs had been changed. Because both mutants retained the wt heparan binding region, we also infected IB3 cells in the presence of heparan sulfate to see if they continued to use heparan sulfate proteoglycan for viral

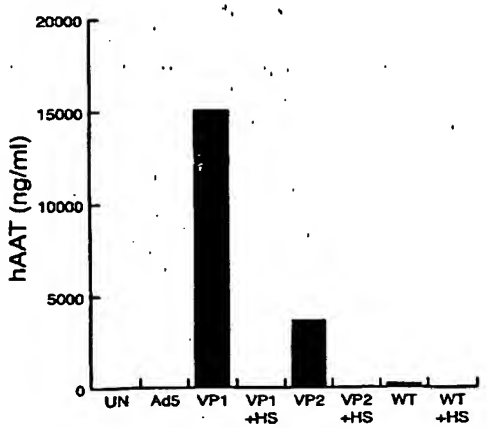

FIG. 8. Infection of IB3 cells with wt and mutant viruses containing a serpin ligand insertion. IB3 cells (1.5×10^5 per 15-mm well) were infected with Ad5 for 60 min at an MOI of 10 and washed twice with medium. The cells then were infected for 60 min at an MOI of 400 with rAAV containing a genome that expressed the hAAT gene under the control of a CMV–β-actin hybrid promoter. Following infection, the cells were washed with medium and incubated at 37°C. At 72 h postinfection, medium samples were taken to determine the AAT concentration by ELISA. All experiments were done in triplicate, and the average for each experiment is shown. WT indicates that rAAV containing a wt AAV capsid (grown by complementation with pIM45) was used. VP1 virus was grown by complementation with a mutant plasmid containing the serpin ligand sequence (FVFLI) substituted for the AAV capsid sequence after aa 34 of the cap ORF. VP2 virus contained a serpin insertion (KFNKPFVFLI) at the N terminus of VP2, aa 138 of the cap ORF. In the +HS samples, rAAV infection was done in the presence of soluble heparan sulfate at a concentration of 2 mg/ml.

entry. When this was done, both wt and mutant infectivity dropped to barely detectable levels (Fig. 8). Taken together, these findings suggested that the serpin-tagged viruses continued to use heparan sulfate proteoglycan as the primary receptor and were using an alternative coreceptor, presumably the serpin receptor.

DISCUSSION

In this study we describe the phenotypes of 93 AAV2 capsid mutants at 59 different positions within the capsid ORF. Several classes of mutants were analyzed, including epitope tag or peptide ligand insertion mutants, alanine scanning mutants, and epitope substitution mutants. From this, we could identify some eight separate phenotypes (Fig. 1; Table 1).

Noninfectious mutants. The bulk of the mutants that were noninfectious either were unable to assemble capsids or the capsids were unstable. These mutants (class 4b) were located predominantly but not exclusively in what are likely to be β-strand structures in the capsid proteins (Fig. 1). Two of these mutants were insertions at the N- and C-terminal residues of VP3, suggesting that both ends of VP3 play a role that is important for capsid assembly or stability. We note that Ruffing et al. (32) have previously characterized deletions of the C terminus of the capsid ORF, and these deletions also were noninfectious.

One noninfectious mutant, *mut*31, produced viable capsids that were empty. This mutant, which consists of a single amino acid substitution (R432A), was apparently defective in packaging viral DNA and is located in putative loop IV (Fig. 1). It is not clear what the mechanism of viral DNA packaging is. Ruffing et al. (33) demonstrated that empty capsids could assemble in the absence of viral DNA. Some studies have suggested that packaging is an active process that requires interaction of Rep proteins with capsid proteins (42) or possibly is coupled with DNA replication (49). Further studies with *mut*31 may be helpful in understanding the mechanism of packaging.

Most of the remaining noninfectious mutants (Fig. 1, class 4a) were capable of assembling capsids and packaging DNA. These are likely to be defective in some aspect of viral entry or uncoating and will require further study to uncover the mechanism of the defect.

Receptor binding mutants. Two of the noninfectious mutants, *mut*40 and L4, were apparently noninfectious because they were unable to bind to heparan sulfate (Fig. 1, class 4d). Heparan sulfate proteoglycan is believed to be the primary cell surface receptor for AAV (37). Three other mutants also were identified as defective for binding heparan sulfate, two partially defective mutants (Fig. 1, class 2c) and one temperature-sensitive mutant (class 3b). Together, the five mutants were distributed into two clusters in loop IV that were separated by 40 aa. The first cluster spanned aa 509 to 520 (*mut*35 and L4); the second was between aa 561 and 591 (*mut*40, *mut*41, and L6). Mutants L4 and L6 consisted of HA epitope insertions into the two heparan binding clusters. These were found to be capable of being immunoprecipitated by HA MAb, confirming that these positions were on the surface of the capsid. We note also that Girod et al. (15) reported that insertion of the L14 epitope at aa 587, the position of our heparan-negative *mut*41 mutant, was capable of targeting the virus to the L14 receptor, thus confirming that this region is on the surface of the capsid. A heparan-negative insertion mutant also was reported by Rabinowitz et al. (30) while this report was in preparation; it fell near the first cluster at aa 522. Taken together, analyses of these mutants suggest that the putative loop IV region contains two blocks of residues that are on the surface of the capsid and involved in heparan sulfate binding.

A heparan binding motif which consists of a negatively charged amino acid cluster of the type XBBBXXBX (where B is a basic amino acid and X is any amino acid) has been identified in several receptors and viruses (19a). Regions containing these clusters also appear to be sensitive to spacing changes. Although no heparan binding consensus motif of this kind was found in our heparan binding mutants, there were basic amino acids near these domains. *mut*35, an insertion at aa 509, was near basic amino acids K507 and H509. Interestingly, K507 is conserved in AAV1, -2, -3, -4, and -6 and in AAV5 is an R. H509 is present only in AAV2 and -3. AAV1, -2, and -3 are known to bind to heparan sulfate, while AAV4 and -5 do not. Additionally, L4, an insertion at aa 520, was near basic amino acids H526 and K527, and L6, an insertion at aa 591, was near R585 and R588. H526 and K527 are conserved except for AAV4 and -5, while R585 and R588 are unique to AAV2. For all of these mutants, the insertions could have disrupted local conformation that hindered normal heparan binding. For *mut*41, R-to-A substitutions at aa 585 and 588 might contribute directly to reduced heparan binding. Finally, *mut*40 did not affect either basic amino acids or spacing within the capsid protein.

Capsid regions that are on the surface of the virus particle. In addition to the heparan binding clusters, several other regions were also present on the capsid surface. These include four of the five putative loop regions (mutants L1 to L7), the N terminus of VP2 (mutant VPN2), and a region within the N terminus of VP1 at amino acid 34 (mutant VP1). HA epitope insertions at these positions were all capable of being immunoprecipitated with anti-HA antibody (Fig. 6 and 7). We note that the L1 insertion mutant at aa 266 had the peculiar phenotype of being partially viable (Table 1) but was not detectable with the A20 MAb, an antibody that recognizes a conformational epitope that is present only in intact viral particles. A

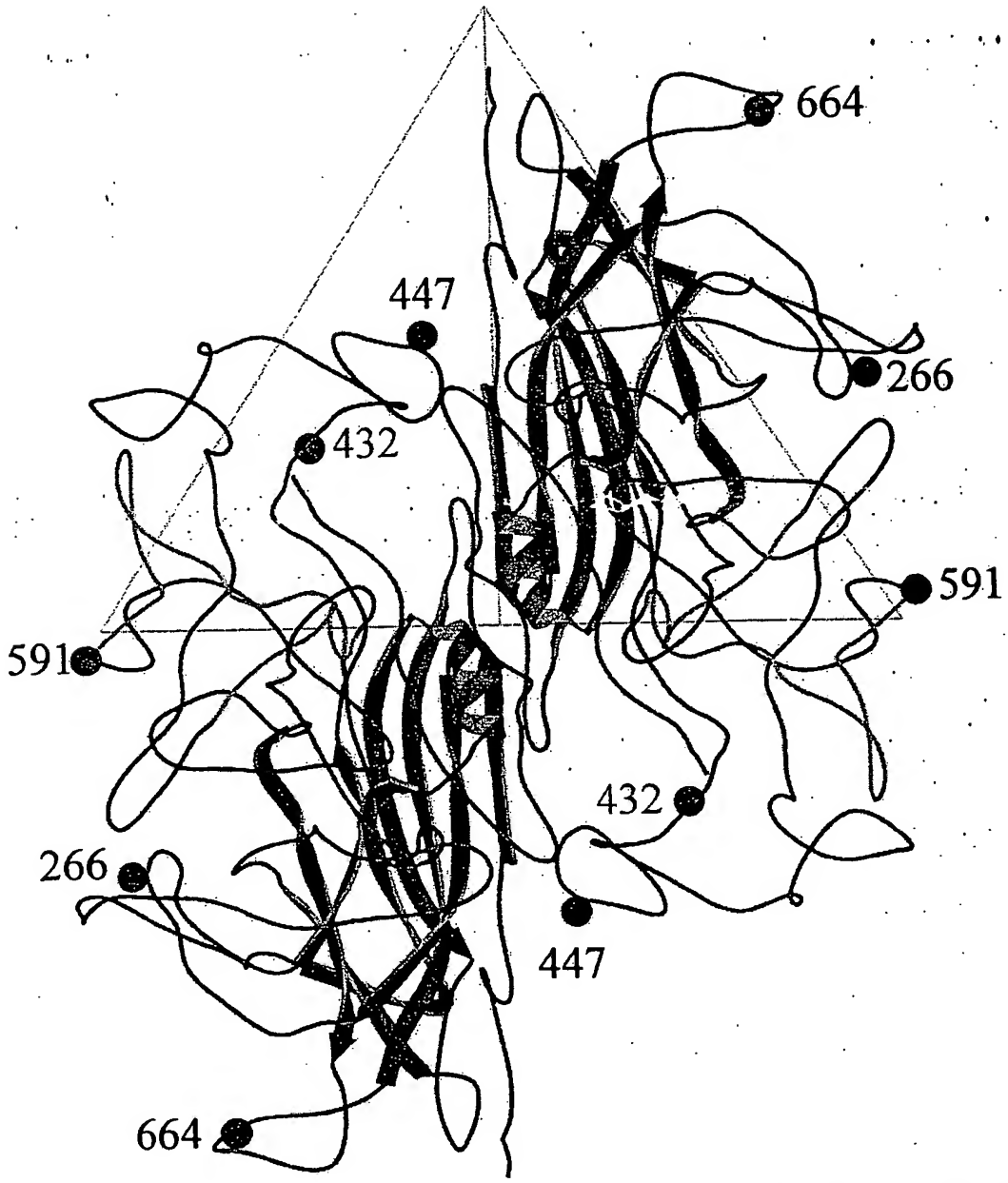

FIG. 9. Ribbon diagrams of a dimer of the AAV VP3 model built based on structural alignments with the VP2 capsid protein of CPV. The view is down an icosahedral twofold axis. The strands of the β-barrel motif are colored blue, and the portion of VP3 in green indicates the heparan binding region. The rest of VP3 is depicted in red. The blue ball identifies the location of residue R432 mutated to an alanine in *mut*31. The gray balls identify the location of residues 266, 477, 591, and 664 (which had HA insertions in mutants L1, L3, L6, and L7, respectively). The large triangle indicates an icosahedral asymmetric unit.

nearby capsid-forming mutant made by Girod et al. (15) at aa 261 was also negative for A20 antibody binding. This suggests that at least part of the epitope for the A20 MAb consists of amino acids between 261 and 266 and confirms that this region is on the surface of the intact particle.

Of the positions identified as being on the surface of the capsid, we found six that potentially are capable of accepting foreign epitope or ligand insertions for retargeting the viral capsid to alternative receptors. These are the N-terminal region of VP1 (near aa 34), the N terminus of VP2 (aa 138), the loop I region (aa 266), the loop IV region (near aa 447 and 591), and the loop V region (aa 664). All of these locations were capable of tolerating an HA (or serpin) insertion and produced recombinant virus titers that were within 1 to 2 logs of the wt value. Furthermore, HA epitope insertions at these positions were capable of being immunoprecipitated with anti-HA antibody (Fig. 6 and 7). Two of these positions, when tested with a serpin ligand insertion or substitution, produced virus that was much more infectious on IB3 cells than wt virus. Curiously, both serpin mutants were still inhibited by soluble heparan sulfate, suggesting that heparan sulfate proteoglycan was still the primary receptor for these mutants and that the serpin receptor was being used as an alternative coreceptor. It is conceivable that one or both of these capsid positions is

involved in binding to one or both of the proteins that normally act as coreceptors for wt virus, fibroblast growth factor (28), or integrin $\alpha_v\beta_5$ (36). This would explain their partial defect on 293 cells and the recovery of infectivity on IB3 cells. Further studies will be needed to test this possibility.

Mutants with unstable capsids and temperature-sensitive phenotypes. Three mutants, *mut*21, *mut*27, and *mut*39, were found to have capsids that were unstable when purified through an iodixanol gradient. Iodixanol is an iso-osmotic gradient purification method that appears to be gentler than CsCl centrifugation (51). Thus, these mutants appear to be particularly sensitive to capsid denaturation. *mut*21 and *mut*27 are in putative β sheets, and *mut*39 is in loop IV. It is worth noting that Rabinowitz et al. (30) also isolated an unstable capsid mutant at aa 247 that is near the *mut*21 position, aa 254. *mut*27 is also one of five temperature-sensitive mutants isolated during this study. The temperature-sensitive mutants and the unstable capsid mutants should prove useful in future studies for identifying steps in the capsid assembly or the infection process.

Viable and partially defective mutants. The two largest classes of mutants isolated were either wt (class 1) or partially defective (class 2a) with no identifiable defect (Fig. 1). Both class 1 and class 2a mutants were distributed either in the VP1 and VP2 unique regions or in the predicted loop regions of the capsid protein. We naively assumed that class 1 mutant positions, which produced viable capsids after substitution of two to five alanine residues, were regions that were nonessential for capsid assembly or stability and therefore should accommodate other kinds of substitutions. However, when serpin or FLAG epitopes were substituted at many of these sites, most of the mutants were nonviable, with the exception of aa 34 in VP1. Indeed, many of these viruses were negative for capsid assembly and should also be useful for identifying possible intermediates in capsid assembly.

Ruffing et al. (33) showed previously that VP1 and VP2 but not VP3 contained nuclear localization signals (NLS), and three putative NLS are located in the VP1/VP2 region at aa 121 to 125, 141 to 145, and 167 to 171. Hoque et al. (19b) have shown that aa 167 to 172 were sufficient to target VP2 to the nucleus, although their experiments did not rule out possible redundancy with the other two putative NLS sequences. All three of these putative signals were targeted with alanine scanning mutants (*mut*12, *mut*13, and *mut*15) in our study. Two of these mutants, *mut*12 and *mut*15, were partially defective, and the inactivation of an NLS may be the reason for their phenotype (19b, 33). We note that *mut*15 should have eliminated the NLS identified by Hoque and colleagues. The fact that *mut*15 was only partially defective suggests that there may be an alternative, redundant NLS sequences that are used by the capsid proteins. The third mutant (*mut*13) was classified as viable, but it also showed a lower than wt titer (Fig. 1).

Molecular computer graphics construction of an AAV model and structural localization of mutant residues. Because the AAV crystal structure is not available, the atomic coordinates of CPV VP2 (PDB accession no. 4DPV) were interactively mutated using the program O (20) to generate a homology-based model of the AAV capsid, using modifications of the alignments of the AAV major capsid protein (VP3) with the VP2 capsid protein of CPV (9, 15). The mutations were followed by refinement constrained with standard geometry in the O database. The model provided a means for preliminary structural identification of the heparan receptor attachment sites in the surface depression (dimple) near the twofold icosahedral axes of the capsid, surface loop regions which can tolerate foreign peptide sequence insertions, and a possible explanation for the phenotype of *mut*31 (Fig. 9).

The topographic location of the putative heparan binding region is consistent with regions that have been suggested as being involved in host cellular factor(s) recognition and implicated in tissue tropism and *in vivo* pathogenicity for other parvoviruses (3, 4, 24, 39). It is of interest that the putative heparan binding site is adjacent to a region of the AAV capsid that contains a peptide insert when the AAV VP3 sequence is compared to that of CPV VP2 and the VP2 of most of the other autonomous parvovirus sequences (9). Also a similar insertion of peptide sequences compared to CPV (although not in a homologous region of the VP2 to that observed in AAV) is present in the capsid of Aleutian mink disease parvovirus and minute virus of mice, proximal to residues in the dimple depression which are implicated in tissue tropism (24). Thus, these insertions may be capsid surface adaptations that enable the capsids to recognize different receptors during infection. In the case of AAV, its dimple peptide insertion, which is absent in the other parvoviruses, may enable it to recognize heparan sulfate, which has not been implicated in cellular infectivity by any other parvovirus.

The model also clearly shows that regions of the capsid which tolerated the insertions of the HA epitope (i.e., at residues 266, 447, 591, and 664) are on the surface loops present between the β strands of the β-barrel motif (Fig. 9). The β-barrel motif forms the core contiguous shell of parvovirus capsids, while the surface loops make up the surface decorations, dictating the strain-specific biological properties of the members. The observation that these surface regions can tolerate foreign peptide insertion is an indication that they are not involved in the interactions that govern capsid assembly.

Finally, the model provides a possible explanation for the observation that *mut*31 (R432A) is able to form only empty particles. In the unassembled VP3 monomer, the side chain of R432, points toward the interior of the capsid and would most likely be in contact with DNA. If recognition and encapsidation of AAV DNA precede final capsid assembly and involve oligomeric intermediates, then R432 contacts with DNA may be essential for initiating capsid assembly around a nascent DNA strand.

In summary, we have reported a preliminary analysis of mutants at 59 positions within the AAV2 capsid ORF. We have identified regions in the capsid proteins that affect infectivity, capsid formation, capsid stability, DNA packaging, and receptor binding. These mutants should be valuable for defining the functional domains of AAV capsid proteins and for dissecting the molecular mechanism of viral entry. Additionally, we have defined a number of regions in the capsid gene at which foreign ligands can be inserted and have demonstrated that insertion of a foreign receptor ligand at some of these positions can change the tropism of the virus. This is the first step in the development of the next generation of AAV vectors, which can be targeted to specific cellular receptors or tissues.

ACKNOWLEDGMENTS

We thank J. Kleinschmidt for kindly providing MAbs A20 and B1. We also thank R. J. Samulski for providing plasmid pXX6. We acknowledge the Vector Core Laboratory at the Powell Gene Therapy Center, University of Florida Medical School, for technical assistance on rAAV production. We thank Corrine Abernathy, Daniel Lackner, and Eric Kolbrener for help on this project.

This work was supported by grants PO1 HL59412, PO1 HL51811, and PO1 NS36302 from the National Institutes of Health.

REFERENCES

1. Agbandje, M., S. Kajigaya, R. McKenna, N. S. Young, and M. G. Rossmann. 1994. The structure of human parvovirus B19 at 8 Å resolution. Virology 203: 106–115.

2. Agbandje, M., R. McKenna, M. G. Rossmann, M. L. Strassheim, and C. R. Parrish. 1993. Structure determination of feline panleukopenia virus empty particles. Proteins 16:155–171.
3. Agbandje-McKenna, M., A. L. Llamás-Saiz, F. Wang, P. Tattersall, and M. G. Rossmann. 1998. Functional implications of the structure of the murine parvovirus, minute virus of mice. Structure 6:1369–1381.
4. Barbis, D. P., S. F. Chang, and C. R. Parrish. 1992. Mutations adjacent to the dimple of the canine parvovirus capsid structure affect sialic acid binding. Virology 191:301–308.
5. Berns, K. I., and R. A. Bohenzky. 1987. Adeno-associated viruses: an update. Adv. Virus Res. 32:243–306.
6. Berns, K. I., and C. Giraud. 1995. Adenovirus and adeno-associated virus as vectors for gene therapy. Ann. N. Y. Acad. Sci. 772:95–104.
7. Buller, R. M., J. E. Janik, E. D. Sebring, and J. A. Rose. 1981. Herpes simplex virus types 1 and 2 completely help adenovirus-associated virus replication. J. Virol. 40:241–247.
8. Casto, B. C., J. A. Armstrong, R. W. Atchison, and W. M. Hammon. 1967. Studies on the relationship between adeno-associated virus type 1 (AAV-1) and adenoviruses. II. Inhibition of adenovirus plaques by AAV; its nature and specificity. Virology 33:452–458.
9. Chapman, M. S., and M. G. Rossmann. 1993. Structure, sequence, and function correlations among parvoviruses. Virology 194:491–508.
10. Chiorini, J. A., L. Yang, Y. Liu, B. Safer, and R. M. Kotin. 1997. Cloning of adeno-associated virus type 4 (AAV4) and generation of recombinant AAV4 particles. J. Virol. 71:6823–6833.
11. Cunningham, B. C., and J. A. Wells. 1989. High resolution epitope mapping of hGH-receptor interactions by alanine-scanning mutagenesis. Science 244: 1081–1085.
12. Fisher, K. J., G. P. Gao, M. D. Weitzman, R. DeMatteo, J. F. Burda, and J. M. Wilson. 1996. Transduction with recombinant adeno-associated virus for gene therapy is limited by leading-strand synthesis. J. Virol. 70:520–532.
13. Fisher-Adams, G., K. K. Wong, Jr., G. Podsakoff, S. J. Forman, and S. Chatterjee. 1996. Integration of adeno-associated virus vectors in CD34+ human hematopoietic progenitor cells after transduction. Blood 88:492–504.
14. Flotte, T. R., S. A. Afione, C. Conrad, S. A. McGrath, R. Solow, H. Oka, P. L. Zeitlin, W. B. Guggino, and B. J. Carter. 1993. Stable in vivo expression of the cystic fibrosis transmembrane conductance regulator with an adeno-associated virus vector. Proc. Natl. Acad. Sci. USA 90:10613–10617.
15. Girod, A., M. Ried, C. Wobus, H. Lahm, K. Leike, J. Kleinschmidt, G. Deleage, and M. Hallek. 1999. Genetic capsid modifications allow efficient re-targeting of adeno-associated virus type 2. Nat. Med. 5:1438.
16. Gnatenko, D., T. E. Arnold, S. Zolotukhin, G. J. Nuovo, N. Muzyczka, and W. F. Bahou. 1997. Characterization of recombinant adeno-associated virus-2 as a vehicle for gene delivery and expression into vascular cells. J. Investig. Med. 45:87–98.
17. Graham, F. L., J. Smiley, W. C. Russell, and R. Nairn. 1977. Characteristics of a human cell line transformed by DNA from human adenovirus type 5. J. Gen. Virol. 36:59–74.
18. Grimm, D., A. Kern, M. Pawlita, F. Ferrari, R. Samulski, and J. Kleinschmidt. 1999. Titration of AAV-2 particles via a novel capsid ELISA: packaging of genomes can limit production of recombinant AAV-2. Gene Ther. 6:1322–1330.
19. Hermonat, P. L., M. A. Labow, R. Wright, K. I. Berns, and N. Muzyczka. 1984. Genetics of adeno-associated virus: isolation and preliminary characterization of adeno-associated virus type 2 mutants. J. Virol. 51:329–339.
19a. Hileman, R. E., J. R. Fromm, J. M. Weiler, and R. J. Linhardt. 1998. Glycosaminoglycan-protein interactions: definition of consensus sites in glycosaminoglycan binding proteins. Bioessays 2:156–167.
19b. Hoque, M., K. Ishizu, A. Matsumoto, S. I. Han, F. Arisaka, M. Takayama, K. Suzuki, K. Kato, T. Kanda, H. Watanabe, and H. Handa. 1999. Nuclear transport of the major capsid protein is essential for adeno-associated virus capsid formation. J. Virol. 73:7912–7915.
20. Jones, T. A., J. Y. Zou, S. W. Cowan, and Kjeldgaard. 1991. Improved methods for binding protein models in electron density maps and the location of errors in these models. Acta Crystallogr. A 47:110–119.
21. Kaplitt, M. G., P. Leone, R. J. Samulski, X. Xiao, D. W. Pfaff, K. L. O'Malley, and M. J. During. 1994. Long-term gene expression and phenotypic correction using adeno-associated virus vectors in the mammalian brain. Nat. Genet. 8:148–154.
22. Klein, R. L., E. M. Meyer, A. L. Peel, S. Zolotukhin, C. Meyers, N. Muzyczka, and M. A. King. 1998. Neuron-specific transduction in the rat septohippocampal or nigrostriatal pathway by recombinant adeno-associated virus vectors. Exp. Neurol. 150(2):183–194.
23. McCarty, D. M., M. Christensen, and N. Muzyczka. 1991. Sequences required for coordinate induction of adeno-associated virus p19 and p40 promoters by Rep protein. J. Virol. 65:2936–2945.
24. McKenna, R., N. H. Olson, P. R. Chipman, T. S. Baker, T. F. Booth, J. Christensen, B. Aasted, J. M. Fox, M. E. Bloom, J. B. Wolfinbarger, and M. Agbandje-McKenna. 1999. Three-dimensional structure of Aleutian mink disease parvovirus: implications for disease pathogenicity. J. Virol. 73:6882–6891.
25. Muralidhar, S., S. P. Becerra, and J. A. Rose. 1994. Site-directed mutagenesis of adeno-associated virus type 2 structural protein initiation codons: effects on regulation of synthesis and biological activity. J. Virol. 68:170–176.
26. Muzyczka, N. 1992. Use of adeno-associated virus as a general transduction vector for mammalian cells. Curr. Top. Microbiol. Immunol. 158:97–129.
27. Ponnazhagan, S., P. Mukherjee, X. S. Wang, K. Qing, D. M. Kube, C. Mah, C. Kurpad, M. C. Yoder, E. F. Srour, and A. Srivastava. 1997. Adeno-associated virus type 2-mediated transduction in primary human bone marrow-derived CD34+ hematopoietic progenitor cells: donor variation and correlation of transgene expression with cellular differentiation. J. Virol. 71:8262–8267.
28. Qing, K., C. Mah, J. Hansen, S. Zhou, V. Dwarki, and A. Srivastava. 1999. Human fibroblast growth factor receptor 1 is a co-receptor for infection by adeno-associated virus 2. Nat. Med. 5:71–77.
29. Rabinowitz, J. E., and J. Samulski. 1998. Adeno-associated virus expression systems for gene transfer. Curr. Opin. Biotechnol. 9:470–475.
30. Rabinowitz, J. E., W. Xiao, and R. J. Samulski. 1999. Insertional mutagenesis of AAV2 capsid and the production of recombinant virus. Virology 265: 274–285.
31. Rossmann, M. G. 1989. The canyon hypothesis. Hiding the host cell receptor attachment site on a viral surface from immune surveillance. J. Biol. Chem. 264:14587–14590.
32. Ruffing, M., H. Heid, and J. A. Kleinschmidt. 1994. Mutations in the carboxy terminus of adeno-associated virus 2 capsid proteins affect viral infectivity: lack of an RGD integrin-binding motif. J. Gen. Virol. 75:3385–3392.
33. Ruffing, M., H. Zentgraf, and J. A. Kleinschmidt. 1992. Assembly of viruslike particles by recombinant structural proteins of adeno-associated virus type 2 in insect cells. J. Virol. 66:6922–6930.
34. Song, S., M. Morgan, T. Ellis, A. Poirier, K. Chesnut, J. Wang, M. Brantly, N. Muzyczka, B. J. Byrne, M. Atkinson, and T. R. Flotte. 1998. Sustained secretion of human alpha-1-antitrypsin from murine muscle transduced with adeno-associated virus vectors. Proc. Natl. Acad. Sci. USA 95:14384–14388.
35. Srivastava, A., E. W. Lusby, and K. I. Berns. 1983. Nucleotide sequence and organization of the adeno-associated virus 2 genome. J. Virol. 45:555–564.
36. Summerford, C., J. S. Bartlett, and R. J. Samulski. 1999. AlphaVbeta5 integrin: a co-receptor for adeno-associated virus type 2 infection. Nat. Med. 5:78–82.
37. Summerford, C., and R. J. Samulski. 1998. Membrane-associated heparan sulfate proteoglycan is a receptor for adeno-associated virus type 2 virions. J. Virol. 72:1438–1445.
38. Tratschin, J. D., I. L. Miller, and B. J. Carter. 1984. Genetic analysis of adeno-associated virus: properties of deletion mutants constructed in vitro and evidence for an adeno-associated virus replication function. J. Virol. 51:611–619.
39. Tresnan, D. B., L. Southard, W. Weichert, J. Y. Sgro, and C. R. Parrish. 1995. Analysis of the cell and erythrocyte binding activities of the dimple and canyon regions of the canine parvovirus capsid. Virology 211:123–132.
40. Tsao, J., M. S. Chapman, M. Agbandje, W. Keller, K. Smith, H. Wu, M. Luo, T. J. Smith, M. G. Rossmann, R. W. Compans, et al. 1991. The three-dimensional structure of canine parvovirus and its functional implications. Science 251:1456–1464.
41. Tsao, J., M. S. Chapman, H. Wu, M. Agbandje, W. Keller, and M. G. Rossmann. 1992. Structure determination of monoclinic canine parvovirus. Acta Crystallogr. B 48:75–88.
42. Weger, S., M. Wendland, J. A. Kleinschmidt, and R. Heilbronn. 1999. The adeno-associated virus type 2 regulatory proteins Rep78 and Rep68 interact with the transcriptional coactivator PC4. J. Virol. 73:260–269.
43. Wistuba, A., A. Kern, S. Weger, D. Grimm, and J. A. Kleinschmidt. 1997. Subcellular compartmentalization of adeno-associated virus type 2 assembly. J. Virol. 71:1341–1352.
44. Wistuba, A., S. Weger, A. Kern, and J. A. Kleinschmidt. 1995. Intermediates of adeno-associated virus type 2 assembly: identification of soluble complexes containing Rep and Cap proteins. J. Virol. 69:5311–5319.
45. Xiao, X., J. Li, and R. J. Samulski. 1996. Efficient long-term gene transfer into muscle tissue of immunocompetent mice by adeno-associated virus vector. J. Virol. 70:8098–8108.
46. Xiao, X., J. Li, and R. J. Samulski. 1998. Production of high-titer recombinant adeno-associated virus vectors in the absence of helper adenovirus. J. Virol. 72:2224–2232.
47. Yang, Q., M. Mamounas, G. Yu, S. Kennedy, B. Leaker, J. Merson, F. Wong-Staal, M. Yu, and J. R. Barber. 1998. Development of novel cell surface CD34-targeted recombinant adeno-associated virus vectors for gene therapy. Hum. Gene Ther. 9:1929–1937.
48. Zhou, S. Z., S. Cooper, L. Y. Kang, L. Ruggieri, S. Heimfeld, A. Srivastava, and H. E. Broxmeyer. 1994. Adeno-associated virus 2-mediated high efficiency gene transfer into immature and mature subsets of hematopoietic progenitor cells in human umbilical cord blood. J. Exp. Med. 179:1867–1875.
49. Zhou, X., and N. Muzyczka. 1998. In vitro packaging of adeno-associated virus DNA. J. Virol. 72:3241–3247.
50. Ziady, A. G., J. C. Perales, T. Ferkol, T. Gerken, H. Beegen, D. H. Perlmutter, and P. B. Davis. 1997. Gene transfer into hepatoma cell lines via the serpin enzyme complex receptor. Am. J. Physiol. 273(2 Pt. 1):G545–G552.
51. Zolotukhin, S., B. J. Byrne, E. Mason, I. Zolotukhin, M. Potter, K. Chesnut, C. Summerford, R. J. Samulski, and N. Muzyczka. 1999. Recombinant adeno-associated virus purification using novel methods improves infectious titer and yield. Gene Ther. 6:973–985.

doi:10.1016/S1525-0016(03)00042-X

RGD Inclusion in VP3 Provides Adeno-Associated Virus Type 2 (AAV2)-Based Vectors with a Heparan Sulfate-Independent Cell Entry Mechanism

Wenfang Shi[3] and Jeffrey S. Bartlett[1,2,3,*]

[1]Gene Therapy Center, Columbus Children's Research Institute, Children's Hospital, Columbus, OH
[2]Department of Molecular Virology, Immunology, and Medical Genetics, College of Medicine and Public Health, The Ohio State University, Columbus, OH
[3]Division of Molecular Medicine, Department of Pediatrics, College of Medicine and Public Health, The Ohio State University, Columbus, OH

*To whom correspondence and reprint requests should be addressed. Children's Research Institute, Room W531, 700 Children's Drive, Columbus, OH 43205. Phone: (614) 722-2683/2876. Fax: (614) 722-3273. E-mail: Bartlaf@pediatrics.ohio-state.edu.

Recombinant adeno-associated virus (AAV) has become an attractive vector system for a number of gene therapy paradigms. However, the utility of AAV vectors is often limited by the absence of heparan sulfate proteoglycan (HSPG), the virus's primary attachment receptor, on the desired target cell population. In order to achieve HSPG-independent gene delivery, several groups have shown that the endogenous tropism of AAV can be expand by genetically altering the viral capsid. However, the parameters of this developing technology have yet to be defined and it has not yet been determined if these modified vectors actually infect cells via these engineered interactions. Previously we constructed a series of insertion mutants spanning the AAV capsid protein gene and identified specific sites that can tolerate the insertion of small exogenous peptides. Here we describe a number of sites within the AAV capsid gene that can be used for the insertion of integrin-targeting peptide epitopes. Incorporation of an Arg-Gly-Asp (RGD)-containing peptide at these sites enables AAV to infect integrin-expressing cells independent of HSPG. Mutant AAV vectors displaying these peptide ligands can be produced to wild-type titer and have been shown to specifically interact with the targeted integrin receptors and mediate infection via this interaction. We report significant increases in gene transfer to Raji, K562, and SKOV-3 cell lines that express integrin, but little HSPG, suggesting that rAAV vectors displaying RGD peptides may be of great utility for treatment of neoplasms characterized by the deficiency of HSPG expression. We have also demonstrated that due to their expanded tropism, these novel vectors are capable of efficient transduction of AAV2-resistant tumors *in vivo* suggesting that they may offer significant therapeutic advantages.

Key Words: AAV, vector targeting, RGD peptide, integrin, gene therapy

Introduction

Gene transfer vectors based on adeno-associated virus type-2 (AAV2) have shown great promise for human gene therapy due to the stability of AAV2-mediated gene expression, lack of significant toxicity or immune response, and the efficiency of gene transfer *in vivo*. However, while AAV2 vectors can effectively transfer genes to a number of different cell types, including muscle, brain, and liver [1], there appear to be conditions which limit transduction of other cell types [2–6]. One such condition is related to the requirement for heparan sulfate proteoglycan (HSPG) [3,7], the primary attachment receptor for AAV2-based vectors, in order to achieve significant levels of gene transfer. In this regard, targeting virus to alternative cell-surface receptors may significantly improve the utility of the present generation of AAV2 vectors for gene therapy.

The initial steps of AAV infection require interaction of specific protein components of the virus capsid with HSPG [7]. This is followed by the internalization of the virus within a clathrin-coated endosome [3] which is thought to be mediated by the interaction of another region of the AAV capsid with $\alpha_v\beta_5$ integrin [8]. Once internalized, the virus escapes from the endosome by triggering its acidification, translocates to the nuclear pore complex, and enters the cell nucleus where subsequent steps of viral uncoating and replication take place [3].

As the capsid protein is the sole mediator of cell entry

1525-0016/03 $30.00

and intracellular trafficking, targeting of recombinant AAV vectors to alternative cellular receptors can be achieved by genetic modification of the capsid [9–13]. We have recently determined that a number of regions within the AAV capsid protein can be altered by the incorporation of small peptides. It has then been hypothesized that if these peptides possess receptor-binding specificities, the virus should be able to attach to and infect cells via these novel interactions [9]. Previously, we have re-directed vector tropism to cells expressing luteinizing hormone receptors by incorporating a small peptide epitope derived from luteinizing hormone into the AAV capsid [9]. Similarly, other groups have investigated the targeting of AAV-based vectors to cell-surface integrin receptors [11,12], serpin receptors [10], and endothelial cell-specific receptors [13]. In each of these cases, AAV-mediated gene transduction was either enhanced or the tropism of the vector was expanded to a previously non-permissive cell type. These accomplishments represent a significant advancement in the filed of AAV-mediated gene transfer. However there remain a number of issues that must be resolved before this technology can be embraced for widespread gene transfer applications.

Importantly, it has not been convincingly demonstrated that infection actually proceeds via the engineered interaction, completely independent of the virus's endogenous receptor. In fact, in one instance transduction of targeted cells with a modified AAV2 vector was inhibited by competition with soluble heparin sulfate [10]. In another instance, gene transduction was maintained in the presence of heparin sulfate, but the role played by the targeted receptor in mediating infection was not determined [13]. The ability to convincingly "re-target" AAV vectors to alternative cellular attachment receptors and alternative pathways of cellular entry has yet to be established. The second issue that must be resolved is a better understanding of the optimum sites within the AAV capsid for insertion of targeting peptide ligands. In each of the previous reports only a small number of sites were investigated. Furthermore, the use of different peptide insertions in these different sites has made if difficult to determine which sites might be best for any one particular peptide ligand.

Previously, we investigated 25 unique sites within the AAV2 capsid protein and determined which could be altered by peptide insertion without significantly affecting vector titer [9]. Capitalizing on this previous work, and the published reports of other groups [10,11], we have compared the best of these sites for their ability to support efficient assembly and packaging of recombinant AAV genomes and for display of a prototypical targeting peptide on the surface of the virus particles. We have chosen the RGD motif as a targeting peptide due to its proven *in vivo* targeting capabilities [14–16] and report the construction of 14 different AAV vectors comprised of capsids containing RGD peptide insertions at 7 different sites within the capsid protein monomers. Furthermore, we show that incorporation of this motif into the AAV VP3 monomer allowed the virus to specifically use the RGD-integrin interaction as an alternative infection pathway, thereby dramatically improving the ability of the virus to transduce several cell types, which are normally poorly infected by this virus. Importantly we show that RGD-modified AAV2 vectors physically interact with the targeted integrin receptors, both in solid-phase binding assays and on the cell surface, and that this interaction is sufficient and required for targeted gene transduction.

Finally, in order to provide a practical means of overcoming limitations imparted by the endogenous viral tropism, targeted AAV vectors must be able to be produced to comparable levels as unmodified vector. In earlier reports there have been large discrepancies in the ability to maintain wild-type titer in targeted AAV vector preparations. Here we show that in addition to promoting efficient display of targeting peptide ligands, the identified sites also allow the maintenance wild-type titer and vector production capabilities.

Results

Generation of AAV Capsid Mutants

It has previously been shown that AAV can tolerate the insertion of exogenous peptide sequences into each of the 3 viral capsid proteins [9]. Importantly, it has been shown that the inserted peptides can be displayed on the surface of AAV particles and can promote the interaction of these viral particles with alternate cell surface receptors [9,11]. To utilize these findings for the purpose of retargeting AAV infection, we introduced a 4C-RGD peptide, CDCRGDCFC, which is known to bind with high affinities to several integrins present on the surfaces of mammalian cells, into each of the AAV capsid protein monomers. This effort was undertaken in an attempt to generate an AAV vector that would bind to cells utilizing a capsid-RGD-integrin interaction as has previously been reported by Girod *et al.* [11] and allow us to define the important parameters of this technology. Based on our previous work [9] and the published work of others [10–12], we selected seven sites within the AAV capsid gene into which to insert RGD-encoding oligonucleotides (Table 1). One site was within the VP1 unique region of the AAV2 capsid protein gene, 3 were within the VP1/VP2 unique region, and the remaining 3 sites were located within the VP3 region of the capsid ORF (Table 1). The mutants were constructed in the non-infectious AAV plasmid, pACG2, by PCR-based site-directed mutagenesis and all were created so that they contained a restriction site at the location of insertion to facilitate confirmation of the mutant sequence and subsequent insertion or swapping of foreign epitopes. A total of 14 different mutants were generated. The 4C-RGD peptide epitope was either inserted alone, or flanked by one of two different 5 amino acid connecting

doi:10.1016/S1525-0016(03)00042-X

TABLE 1: Characteristics of mutant AAV vectors

Virus	Upstream linker	Inserted peptide epitope (4C-RGD)	Downstream linker	Particle titer (ELISA)
A46-RGD4C	TG	CDCRGDCFC	—	8.5×10^7
A46-RGD4CGLS	TG	CDCRGDCFC	GLS	4.5×10^6
A115-RGD4C	TG	CDCRGDCFC	—	4.5×10^6
A115-RGD4CGLS	TG	CDCRGDCFC	GLS	6.0×10^7
A139-RGD4C	TG	CDCRGDCFC	—	8.5×10^7
A139-RGD4CGLS	TG	CDCRGDCFC	GLS	9.0×10^7
A161-RGD4C	TG	CDCRGDCFC	—	4.5×10^6
A161-RGD4CALS	TG	CDCRGDCFC	ALS	5.0×10^6
A459-RGD4C	TG	CDCRGDCFC	—	4.5×10^6
A459-RGD4CGLS	TG	CDCRGDCFC	GLS	4.5×10^6
A584-RGD4C	TG	CDCRGDCFC	—	8.5×10^7
A584-RGD4CALS	TG	CDCRGDCFC	ALS	9.0×10^7
A588-RGD4C	TG	CDCRGDCFC	—	9.0×10^7
A588-RGD4CGLS	TG	CDCRGDCFC	GLS	9.0×10^7
Wild-type	—	—	—	7.5×10^7

peptide linkers [9], at each of the 7 different positions within the AAV capsid protein (Table 1).

These additional sequences were included in an attempt to maintain flexibility and promote efficient display of the engineered RGD epitope on the surface of the AAV particles. We have previously shown that incorporation of these sequences can significantly enhance particle assembly and infectious titer [9].

All of the mutant capsid proteins were able to effectively assemble and package AAV vector genomes (Table 1). Furthermore, all of the resulting AAV vectors were infectious, although there were significant differences in the efficiencies of the different mutant AAV capsids to mediate gene transduction (Figure 1). These differences were related to both the site of peptide insertion and the presence, or absence, of linker sequences flanking the inserted 4C-RGD peptide. Insertion of the RGD epitope following AAV VP1 amino acid 46, 115, 161, or 459 severely diminished infectious titer. However, insertions following amino acids 139, 584, or 588 were well tolerated and did not affect titer appreciably. In all cases, inclusion of linker/scaffolding sequences resulted in

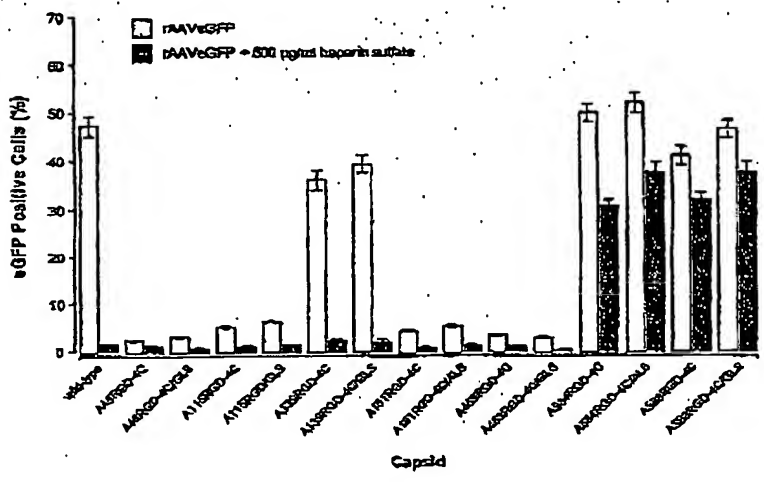

FIG. 1. Gene transduction mediated by mutant AAV vectors. AAV vectors containing 4C-RGD epitope insertions at various sites within the capsid protein were assayed for their ability to direct eGFP gene transduction in the presence and absence of heparin sulfate. Adenovirus-infected HeLa C12 cells (3 hu/cell) were exposed for 2 h at 4°C to RGD-mutant rAAVeGFP vectors or standard AAVeGFP vector (wild-type) at an MOI of 100 pp/cell. Unbound virus was then removed, fresh medium was added, and the cells were analyzed by FACS for eGFP expression after 48 h. Where indicated, the viruses were bound to the cells in the presence of 500 μg/ml heparin sulfate. Data represents the percent of the cell population that expressed the eGFP transgene and is shown as the mean of triplicate samples. Bars indicate the standard error of the mean (SEM).

doi:10.1016/S1525-0016(03)00042-X

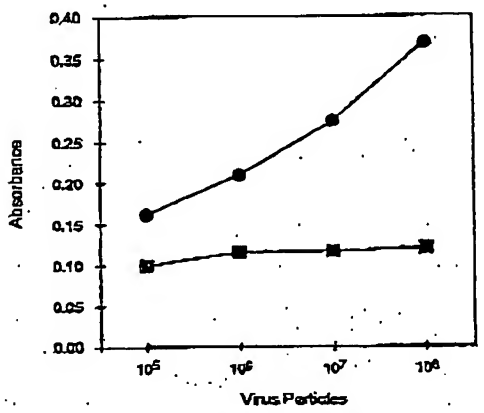

FIG. 2. Solid-phase binding of RGD mutant AAV vector to purified $\alpha_v\beta_3$ integrin. Iodixanol purified AAV vector with either wild-type capsid or A5884C-RGD capsid was bound to assay plates via immobilized heparin sulfate and then incubated with affinity-purified $\alpha_v\beta_3$ integrin. Integrin bound to AAV was detected with anti-α subunit monoclonal antibody, VNR139. ●, A5884C-RGD capsid; ■, wild-type capsid. Assay was performed in triplicate.

slightly more efficient infection and maintenance of titer (Figure 1). We assume that the increases we observed in infection were a direct result of enhanced particle stability, as exemplified by the increased particle titer (Table 1), and supported by our previous work [9]. In an attempt to determine if the inserted 4C-RGD motif had provided the mutant vectors with a HSPG-independent cell entry mechanism, gene transduction assays were also performed in the presence of soluble heparin sulfate [9]. Whereas vectors containing unmodified capsids were unable to transduce cells in the presence of heparin sulfate, mutants containing the 4C-RGD epitope following amino acids 584 or 588 were still able to transduce cells in the presence of heparin sulfate. These results strongly suggested that the mutant vector particles might be directing infection via an alternative cellular receptor.

AAV-RGD Particles Efficiently Interact with Integrins via the RGD Tripeptide

In order to assess the ability of the AAV-RGD particles to bind integrin receptors we employed a solid-phase ELISA assay using purified $\alpha_v\beta_3$ integrin. This analysis clearly showed efficient binding of integrin to immobilized particles of A5884C-RGD AAV, while binding of $\alpha_v\beta_3$ integrin to a control virus was at the background level at all concentrations of virus used (Figure 2). Based on these results, we hypothesized that A5884C-RGD AAV particles are able to interact with other RGD-binding integrins and that this interaction might be responsible for the HSPG-independent gene transfer we observed (Figure 1).

Mutant AAV Vectors Containing RGD Peptide Insertions Have an Expanded Cellular Tropism

Our next goal was to examine whether introduction of the RGD motif in the AAV capsid protein of AAVeGFP resulted in any changes with respect to the ability of the virus to infect different cell types. In order to investigate the entry pathway utilized by A5884C-RGD vectors, we assessed gene transfer to cell lines expressing various levels of HSPG as well as integrins $\alpha_v\beta_3$ and $\alpha_v\beta_5$. The panel of cell lines we used included human HeLa cells; K562, human chronic myelogenous leukemia cells; Raji, human lymphoblast-like cells; and SKOV-3, human ovarian adenocarcinoma cells. While HeLa cells readily support AAV infection, K562, Raji, and SKOV-3 cells are poorly transduced by rAAV vectors [2,22]. Our flow cytometry assay showed that HeLa cells express high levels of HSPG and $\alpha_v\beta_5$ integrins, whereas $\alpha_v\beta_3$ integrins are poorly expressed (Figure 3). K562 cells demonstrated low levels of HSPG expression, no expression of $\alpha_v\beta_3$ integrins, but high expression of $\alpha_v\beta_5$ integrins (Figure 3). Whereas, Raji and SKOV-3 cells expressed little to no HSPG, but expressed high levels of both $\alpha_v\beta_3$ and $\alpha_v\beta_5$ integrins. Therefore, for our subsequent gene transfer experiments we established a set of cell lines covering a range of HSPG expression profiles and with moderate to high levels of $\alpha_v\beta_3$ and $\alpha_v\beta_5$ integrins present on their cell membranes.

Although K562, Raji, and SKOV-3 cells were poorly transduced by AAVeGFP vectors containing wild-type AAV capsid protein, they were efficiently transduced by the same vector packaged into A5884C-RGD capsids (Figure 4). The efficiency of eGFP gene transfer in these cells mediated by the A5884C-RGD capsid approached that observed in the HeLa cells mediated by the wild-type capsid (Figure 4). Furthermore, our experiments revealed striking differences between the transduction profiles demonstrated by these two viruses (Figure 4). Gene transfer mediated by the RGD-containing particles was 40-fold higher on the K562 cells, 13-fold higher on the Raji cells, and 6-fold higher on the SKOV-3 cells, than gene transfer mediated by particles with wild-type capsids. These experiments clearly showed that incorporation of the 4C-RGD epitope into the VP3 monomer of AAV2 vectors resulted in dramatic changes in the initial steps of virus-cell interaction, presumably by creating an alternative cell attachment and entry pathway.

AAV-RGD Vectors Demonstrate Increased Efficiencies of Cell Binding Due to Utilization of RGD-Integrin Interaction

Having established that A5884C-RGD capsids and wild-type AAV capsids demonstrate different efficiencies of gene delivery as well as different profiles of HS-mediated inhibition of transduction, our next task was to compare the cell binding profiles of these two viruses. To address this issue, we blocked virus binding to HSPG with soluble heparin sulfate, and then detected surface-bound AAV

doi:10.1016/S1525-0016(03)00042-X

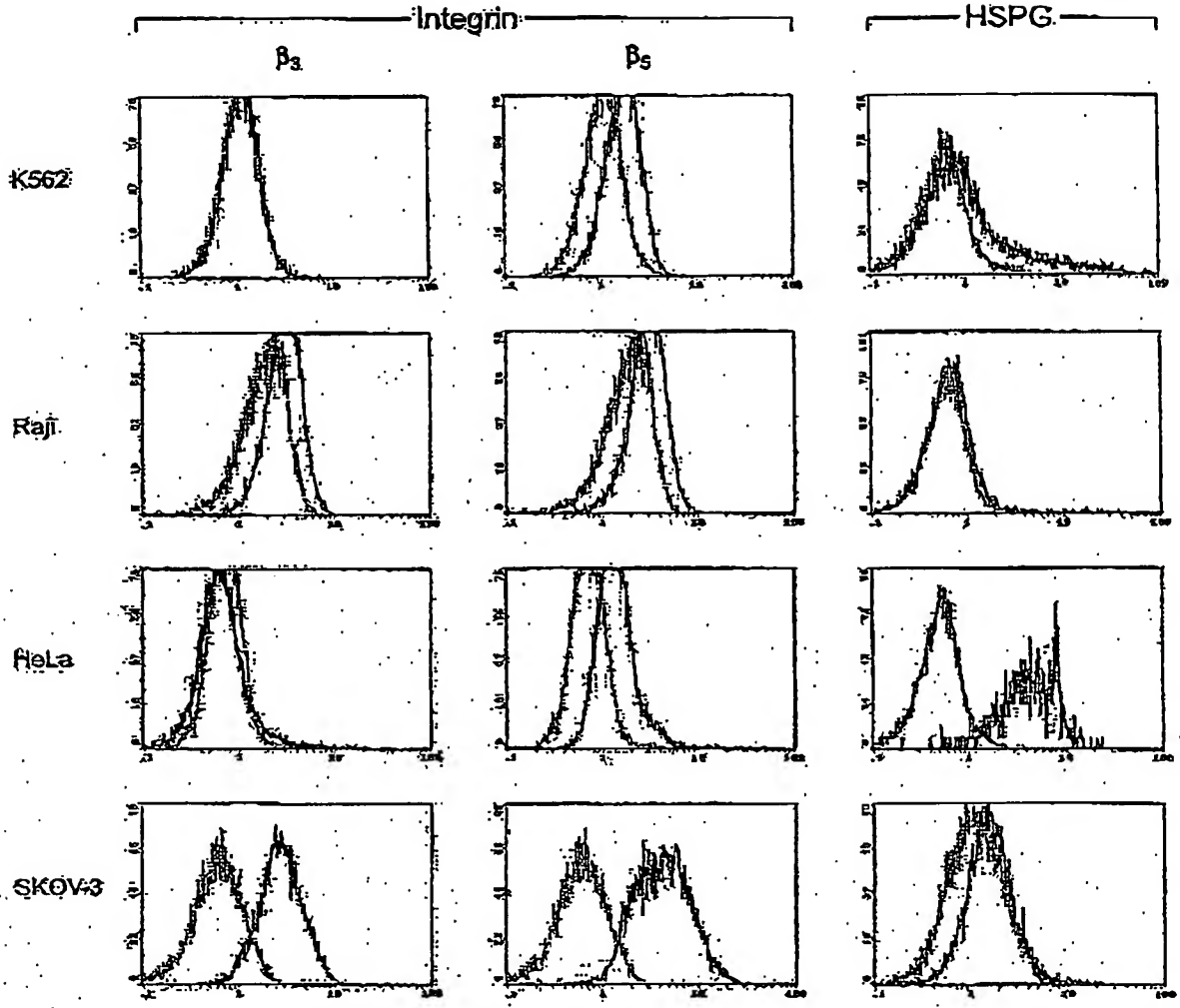

FIG. 3. Integrin and heparan sulfate proteoglycan (HSPG) expression on K562, Raji, HeLa, and SKOV-3 cell lines. Expression of $\alpha_v\beta_3$ integrin was determined using LM609 antibody, whereas $\alpha_v\beta_5$ expression was determined using P1F6 antibody. HSPG expression was determined using HepSS-1 monoclonal antibody. In all cases, secondary FITC-labeled anti-mouse antibody was used and detected by FACS analysis (dark line). The light line shows the results for negative controls. Representative histograms are shown.

using the anti-AAV mAb, A20, and FACS analysis. As shown in Figure 5, AAV comprised of wild-type capsid monomers is not able to bind HeLa cells in the presence of heparin sulfate. However, particles containing A5884C-RGD capsid proteins were still able to bind HeLa cells in the presence of heparin, and it was not until these cells were also treated with synthetic RGD peptide that binding could be completely inhibited. Since the RGD peptides could efficiently block binding, these data further suggest that A5884C-RGD capsids are able to use cellular integrins as alternative receptors during the cell attachment process.

AAV-RGD Vectors are Capable of Mediating Gene Delivery via Integrin Receptors

Having established that A5884C-RGD vectors were able to specifically bind integrins in both solid phase and cell-binding assays, we next utilized these vectors for an assay based on competitive inhibition of AAV-mediated gene delivery by soluble heparin sulfate, known to efficiently block virus binding to cell surface HSPG. Furthermore, we utilized a synthetic RGD peptide and anti-integrin antibody to see if they could also inhibit infection in the presence of soluble heparin sulfate. As shown in Figure 6, eGFP expression in HeLa cells mediated by control virus,

FIG. 4. Gene transduction mediated by A5884C-RGD mutant AAV vector. Vectors displaying the 4C-RGD motif have an increased ability to mediate gene transfer to K562, Raji, and SKOV-3 cells. Cells were exposed for 2 h at 4°C to either RGD-mutant (AAV-A5884C-RGD-eGFP) or standard AAVeGFP vector (wild-type capsid) at an MOI of 100 pp/cell. Unbound virus was then removed, fresh medium was added, and the cells were analyzed by FACS after 48 h. Data represents the percent of the cell population that expressed the eGFP transgene and is shown as the means and standard deviations of triplicate experiments.

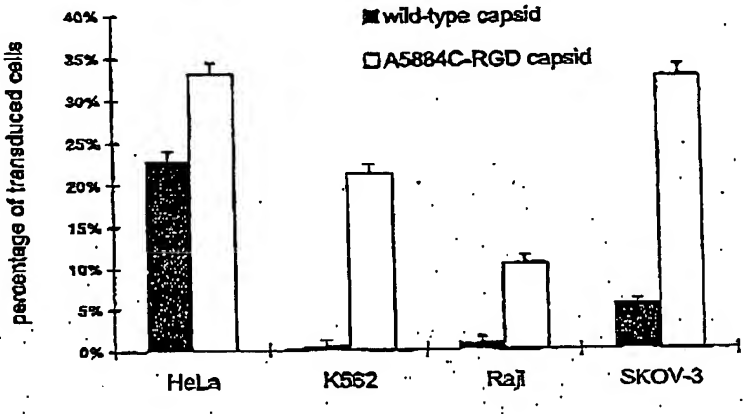

AAVeGFP with a wild-type capsid, was efficiently blocked by soluble heparin sulfate. In marked contrast, the same concentration of heparin sulfate was able to block only about 20% of A5884C-RGD capsid-mediated eGFP expression in HeLa cells, thereby indicating that in addition to the well-characterized capsid-HSPG interaction utilized

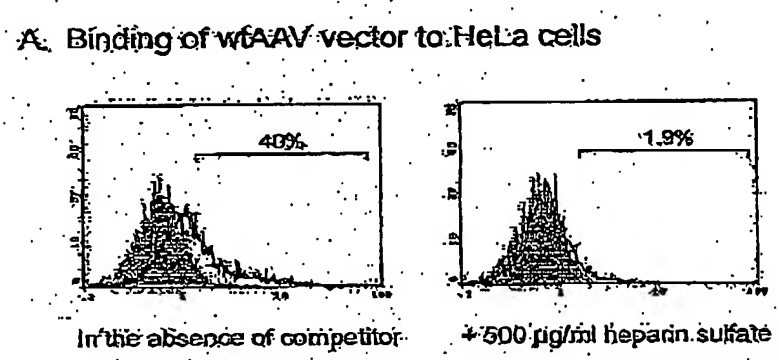

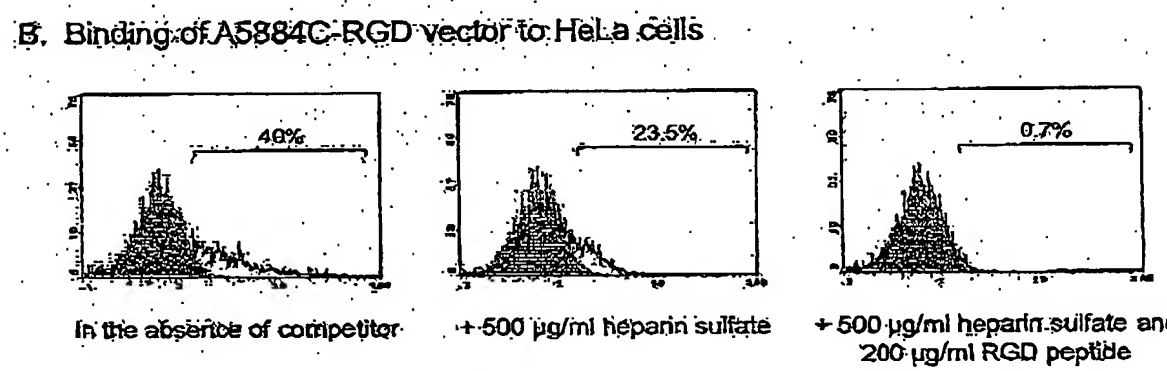

FIG. 5. HSPG-independent binding of A5884C-RGD vector to HeLa cells is mediated by the inserted 4C-RGD motif. Vector particles bound to HeLa cells were detected by staining with anti-AAV A20 mAb and FACS analysis. Histograms from representative experiments are shown. (A) Binding of wild-type AAV (wtAAV) particles to the cell-surface is inhibited in the presence of soluble heparin sulfate (500 µg/ml), whereas, (B) binding of A5884C-RGD particles is only partially inhibited in the presence of heparin sulfate and not completely inhibited until both heparin sulfate and RGD peptide (200 g/ml) are used. The percentage of cells with bound AAV particles is indicated above the histograms.

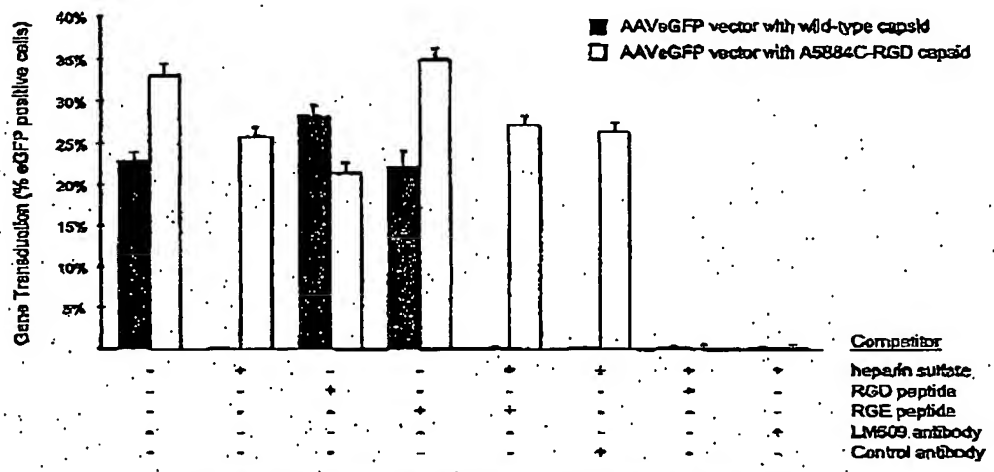

FIG. 6. RGD mutant vectors can use a HS-independent pathway for infection of HeLa cells and are specifically targeted to integrin receptors. HeLa cells were exposed for 2 h at 4°C to either RGD-mutant (AAV-A5884C-RGD-eGFP) or standard AAVeGFP vector (wild-type capsid) at an MOI of 100 pp/cell. Unbound virus was then removed, fresh medium was added, and the cells were analyzed for αGFP gene transduction by FACS after 48 h. For the competition experiments, the viruses were bound to the cells for 2 h at 4°C in the presence of 500 μg/ml heparin sulfate, 200 μg/ml RGD-peptide, 200 μg/ml RGE-peptide, and/or 1:200 dilution of anti-integrin or isotype-matched control antibody. Data represents the means and standard deviations of triplicate experiments.

by wild-type AAV, A5884C-RGD capsids are capable of using an alternative, HSPG-independent cell entry pathway. We assume that the partial reduction in gene transduction observed in the presence of HS is due to loss of the HSPG-dependent cell entry pathway. The contribution of the alternative pathway of cell entry was quite significant accounting for entry of approximately 80% of total transducing vector particles. To assess the specificity of this new interaction infections were performed in the presence of either excess free RGD peptide or anti-integrin antibody in conjunction with soluble heparin sulfate. Both of these competitors were able to completely abolish A5884C-RGD-mediated gene expression when utilized in conjunction with heparin sulfate, while no inhibition was observed with control RGE peptide or isotype-matched control antibody. These data demonstrate the specificity of the engineered interaction for RGD-binding integrins expressed on the cell surface (Figure 6).

Mutant AAV Vectors Containing RGD Peptide Insertions Mediate Enhanced *In Vivo* Gene Delivery to SVOV-3 Adenocarcinomas

Having established that A5884C-RGD vectors were able to target infection via cell-surface integrin receptors and mediate efficient gene transfer to SKOV-3 cells and other cell types that were poorly transduced by unmodified AAV2 vectors, we next utilized these vectors for *in vivo* gene transfer to a murine model of ovarian cancer. As shown in Figure 7, eGFP expression in peritoneal SVOV-3 tumors mediated by control virus, AAV2eGFP with a wild-type capsid, was inefficient when assessed 15 days after vector administration. In marked contrast, the same dose of AAV2eGFP vector with an A5884C-RGD capsid was much more efficient, and transgene product could be detected in essentially all tumor cells by 35 days post vector administration. These experiments clearly show that incorporation of the 4C-RGD epitope into the VP3 monomer of AAV2 vectors results in dramatic changes in the *in vivo* gene transduction potential of these vectors and greatly increases their utility for treatment of neoplasms characterized by the deficiency of HSPG expression.

Discussion

AAV vectors efficiently transduce a wide variety of cells. However, it has recently been established that low levels of HSPG-mediated vector binding limits AAV transduction of several important gene therapy target cells [2,22–24]. It is also likely that other, yet uncharacterized, cell types may likewise lack sufficient levels of HSPG to permit efficient gene transduction. The significant increases in transduction of cells lacking HSPG shown here demonstrates that genetically modified, targeted AAV vectors can be successfully used to expand the range of tissues amenable to efficient AAV-mediated gene therapy.

In this study we describe the generation and characterization of a panel of recombinant AAV vectors containing 4C-RGD epitope insertions within their capsids. These vectors were constructed in an effort to reconcile previous reports of the generation of targeted AAV vectors, identify optimal sites for peptide insertion, define the receptor-

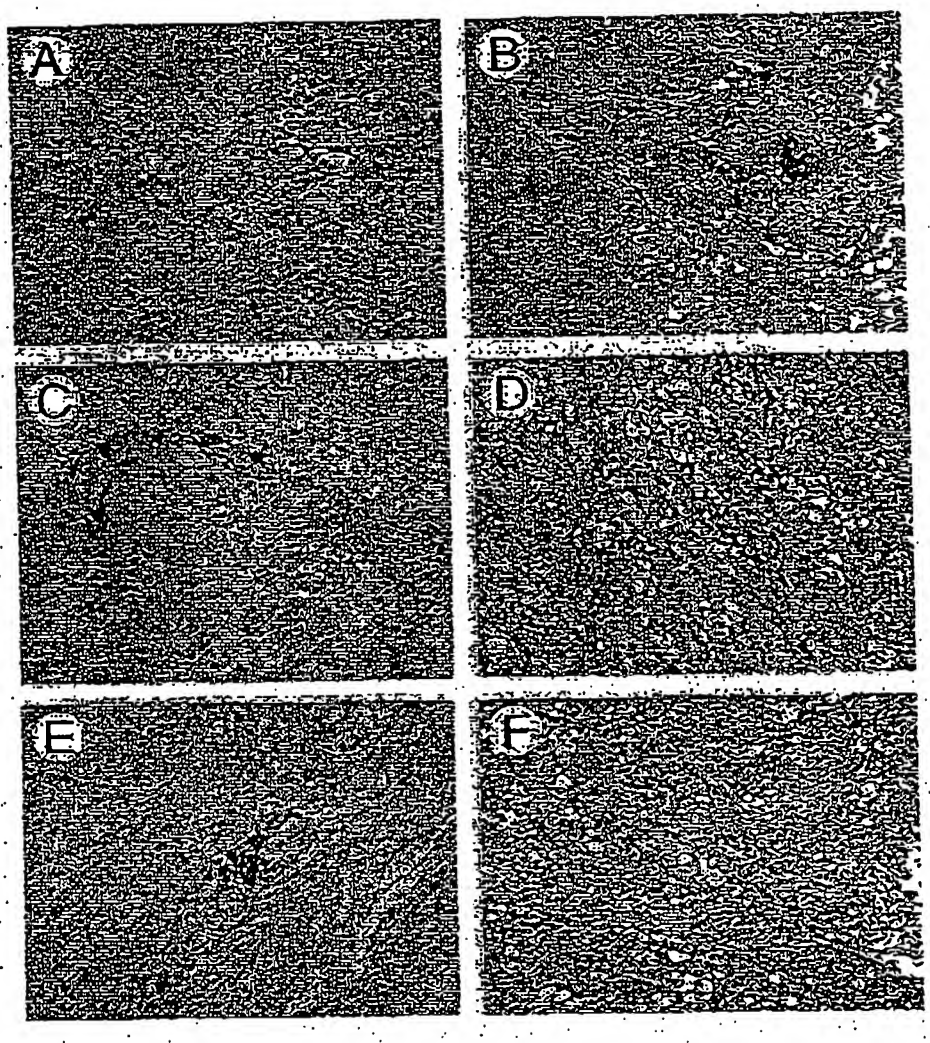

FIG. 7. Gene transfer to an orthotopic murine model of peritoneal ovarian cancer mediated by AS884C-RGD mutant AAV vector. Tumors were established by i.p. injection of 1×10^7 SKOV-3 cells. Five days later 1×10^{10} DRP of either AAV2-eGFP (panels A, C, and E), or AAV-AS884C-RGD-eGFP (panels B, D, and F) was administered i.p. To determine the efficiency of AAV vector-mediated eGFP expression in the tumors, mice were sacrificed on days 15 (A and B), 25 (C and D) and 40 (E and F) after vector administration. Tumor nodules were dissected and immunostaining for eGFP was performed on 4-μm paraffin sections counterstained with hematoxylin. Vectors displaying the 4C-RGD motif were considerably more efficient in mediating gene transfer to these tumors *in vivo*.

binding specificities of these vectors, and further demonstrate the utility of peptide insertions for targeting AAV vectors to ligand-specific receptors. We took advantage of the well-characterized interaction between cellular integrins and various proteins containing RGD tripeptides. This interaction plays an important role in a variety of fundamental biological processes, including cell adhesion and viral infection. Furthermore, integrin expression is activated in a wide variety of tumors [25–29] and targeting AAV to these receptors might allow the specific delivery of a gene while avoiding delivery to surrounding healthy tissue. Girod *et al.* [11] reported that genetic incorporation of RGD-containing sequences into AAV2 capsid protein expanded tropism to previously non-permissive cell types. Similarly, recent studies have shown that incorporation of RGD-peptides into human adenovirus fiber proteins permits specific interaction of these viral particles with cellular integrins and infection of target cells via this interaction [14,16].

We constructed 14 different RGD-capsid insertion mutants and showed that these mutant capsid proteins could still assemble into AAV particles and efficiently package recombinant AAV vector genomes. The crystal structure of AAV2 has recently been reported [30]. The core structure is a β-barrel motif, consisting of anti-parallel β-sheets with interspersed looped-out domains. The largest of these loops is located between β-sheets G and H (GH loop) and contains the majority of sites that have been shown to be amenable to manipulation [9]. The optimum sites for epitope insertion appear to define a subdomain within this loop on the basis of surface exposure and local structural flexibility. By using an ELISA-based binding assay,

we were then able to show direct interaction of RGD-modified viral particles with purified integrin $\alpha_v\beta_3$. Furthermore, we were able to show that these modified AAV particles were able to bind integrin receptors on the surface of appropriate target cells and utilize this interaction for cell entry, thereby supporting the concept of augmented efficiency of transgene expression as a result of more-efficient primary interaction between the virus and the target cell and specific targeting via an alternative cellular receptor.

The modified RGD-containing AAV vectors display a significantly different profile of gene transfer compared to AAV2 vectors with unmodified capsid. This difference was especially dramatic when HSPG-negative cell lines were utilized for gene delivery experiments. Targeting gene delivery via the RGD-integrin interaction also demonstrates that attachment via HSPG is not required for efficient transduction of cells by AAV. A previous attempt to target AAV vectors via peptic insertion of a serpin receptor ligand showed a continued dependence on HSPG [10], which was not observed in this study. Transduction of receptor-blocked HeLa cells using soluble heparin sulfate and RGD-targeted AAV vector was nearly as efficient as transduction with un-modified vector in the absence of competitor. Therefore, in the absence of HSPG-mediated binding, the transducing activity of an AAV particle is not compromised by attachment via an alternative receptor. Although several cell types may lack HSPG expression, a number of tissues are known to express the AAV receptor. Therefore, the efficient targeting and restriction of transduction to a particular cell type or tissue will necessitate AAV vectors that lack HSPG-binding activity. It will be important to determine the levels of HSPG expression in tissues targeted for AAV-mediated gene therapy. If the levels of HSPG expression are low, using AAV vectors that have been engineered to interact with an alternative receptor is likely to increase the efficiency and specificity of gene transfer.

Finally, we have used an RGD-targeted AAV vector to assess gene transfer to a stringent orthotopic murine model of peritoneal ovarian cancer and show significant improvement in gene transfer efficiency. These results suggest that AAV vectors packaged into capsids containing VP3 4C-RGD epitope insertions could be effective agents for the treatment of ovarian cancer and other cancers characterized by low HSPG and moderate RGD-binding integrin expression.

Materials and Methods

Cells and tissues. Low passage number (passage number 20–40) HEK 293 cells [17], HeLa cells, and HeLa C12 cells [18] were grown in Dulbecco's modified Eagle's medium (DMEM) supplemented with 10% heat-inactivated fetal bovine serum (FBS), penicillin (100 U/ml) and streptomycin (100 U/ml), at 37°C and 5% CO_2. Raji, a human lymphoblast-like cell line, and K562, a human chronic myelogenous leukemia cell line, were obtained from the American Type Culture Collection (ATCC, Rockville, MD) and grown in RPMI 1640 containing 10% FBS. SKOV-3, a human adenocarcinoma cell line, was also obtained from ATCC and grown in DMEM containing 10% FBS.

Enzymes. Restriction endonucleases, T4 DNA ligase, Platinum *pfx* DNA polymerase, benzonase and proteinase K were purchased from Life Technologies (Gaithersburg, MD).

Monoclonal antibodies. Anti-$\alpha_v\beta_3$ integrin monoclonal antibody LM609 and anti-$\alpha_v\beta_5$ integrin monoclonal antibody P1F6 were purchased from Chemicon International, Inc. (Temecula, Calif). Anti-bacterial β-galactosidase monoclonal antibody was used as an isotype-matched (IgG_1) control and was also purchased from Chemicon. Anti-human α_v integrin monoclonal antibody VNR139 was purchased from Life Technologies (Gaithersburg, MD). Anti-heparan sulfate, HepSS-1, purified mouse IgM antibody was purchased from Seikagaku America (Falmouth, MA) and FITC-labeled secondary goat anti-mouse IgG (H + L) antibody was obtained from either Chemicon or Vector Laboratories (Burlingame, CA). Anti-AAV2 monoclonal antibody A20 was obtained from American Research Products, Inc. (Belmont, MA).

ELISA. Solid-phase binding assays were performed by the following method. Neutravidin-coated plates (Pierce) were incubated with 1 μg/well of biotinylated heparin in PBST (0.05% Tween 20, 0.2% bovine serum albumin (BSA)) overnight at 4°C. The wells were then washed five times with wash buffer (PBS containing 0.05% Tween-20 and 0.1% BSA) and AAV particles were bound at room temperature (RT) for 2 h with gentle shaking. The plate was then washed five times with wash buffer and purified integrin $\alpha_v\beta_3$ (Chemicon) in binding buffer (20 mM Tris-HCl, 150 mM NaCl, 2 mM $CaCl_2$, 1 mM $MgCl_2$, 1 mM $MnCl_2$, and 0.1% BSA, pH 7.5) was added to each well at a concentration of 1 μg/ml. The plates were incubated over night at 4°C, washed three times with wash buffer and incubated with VNR139 mAb (GIBCO-BRL; anti-α_v subunit, 1:2000 dilution) in binding buffer for 2 h at RT. The plates were then washed five times and incubated with secondary antibody (HRP-conjugated anti-mouse IgG) for 1 h at RT. Following a final wash the ELISA plate was developed with ABTS substrate solution and VECTASTAIN kit (Vector Laboratories) as recommended by the manufacturer. Color development was stopped by the addition of 1N H_2SO_4, and plates were read in a plate reader set at 405 nm.

Construction of recombinant AAV packaging plasmids. Recombinant AAV constructs encoding capsid proteins with inserted 4C-RGD peptide epitopes were generated as described previously [9]. Briefly, DNA primers were designed encoding the peptide sequence and used to direct PCR-based mutagenesis of plasmid pACG2 [19]. This plasmid contains the AAV genome, less the two viral ITRs, and an ATG-to-ACG mutation of the *Rep78/68* start codon which has been shown to increase rAAV vector yield by attenuating Rep78/68 synthesis [20]. In some instances additional non-homologous flanking sequences were included in the PCR primers. These sequences encoded linker/scaffolding sequences on either side of the RGD epitope insertion. The PCR products were digested with *DpnI* endonuclease to eliminate the parental plasmid template and were propagated in DH-5α bacteria (Life Technologies). Mini-prep DNAs were extracted from ampicillin resistant colonies and were screened by restriction endonuclease digestion.

Viruses. Recombinant AAV vector, AAVeGFP, containing the enhanced green fluorescent protein gene (eGFP) driven by the human CMV IE promoter/enhancer region packaged into wild-type AAV2 capsids was produced by triple-transfection as previously described [9]. To produce rAAV with RGD-containing capsid proteins, 293 cells were transfected with mutant pACG2 plasmids, constructed as described above, in place of normal pACG2 plasmid. Transfections were carried out at 37°C using the calcium phosphate transfection system (Life Technologies) according to the manufacturer's specifications. Forty eight hours after transfection, cells were harvested by centrifugation at 500 × g for 10 min, resuspended in PBS, and recombinant virus was released by freezing and thawing three times. The crude lysate was clarified by centrifugation at 500 × g for 10 min and treated with benzonase at 250 U/ml final concentration at 37°C

doi:10.1016/S1525-0016(03)00042-X

for 30 min. Virus was further purified by iodixanol step gradient and heparin sulfate affinity chromatography [21] and stored at −20°C in PBS containing 20% glycerol. Particle titers were determined by ELISA and DNA dot blot as previously described [9], and infectious titers were determined by gene transduction assay on HeLa C12 cells in the presence of adenovirus type-5 (Ad5) at 2 hi/cell as described below.

Flow cytometry. For analysis of integrin expression, adherent cells were released from culture flasks by the addition of EDTA and resuspended in SM buffer (HEPES-buffered saline containing 1% BSA) at 2×10^6 cell/ml as described by Dmitriev *et al.* [16]. Cells were incubated briefly at 37°C to allow regeneration of surface integrin, then incubated with FITC-labeled LM609 antibody, or FITC-labeled P1F6 antibody (1:200 dilution) for 2 h at 4°C, washed five times with SM buffer and analyzed by flow cytometry at the Children's Research Institute Cell Morphology Core Facility. For analysis of HSPG expression, 2×10^5 cells were incubated with anti-HSPG monoclonal antibody, HepSS-1, at a dilution of 1:200 for 2 h at 4°C. The cells were then washed five times with SM buffer and incubated with FITC-labeled goat anti-mouse IgM serum (1:800) for 1 h at 4°C. The cells were then washed with SM buffer and analyzed by flow cytometry.

Gene transduction assays. Briefly, HeLa C12, Raji, K562, or SKOV-3 cells were seeded in 24-well plates the day before infection so that they would reach about 75% confluence or about 5×10^5 cells/ml the next day. Serial dilutions of wild-type AAVeGFP and RGD-mutant AAVeGFP preps were added to the cells which were then infected with Ad5 at an MOI of 3 hi/cell. The cells and viruses were incubated at 37°C for 48 h, after which time the media was removed and the cells were washed twice with PBS, fixed, and analyzed for GFP gene transduction by FACS. Data has been presented as the percentage of transduced cells in the cell population infected at the indicated particle multiplicity. Transduction assays were also carried out in the absence of adenovirus with no differences in the relative titers of mutants.

For determination of HSPG-independent gene transduction, AAV vectors were first incubated with 1500 μg/ml heparin sulfate for 2 h at 37°C, then incubated with target cells at 4°C in the presence 500 μg/ml heparin sulfate for another 2 h. The cells were then washed three times with fresh medium to remove unbound vector and incubated for 48 h at 37°C prior to determination of gene transduction. For determination of RGD-dependent gene transduction, rAAV vectors were incubated with either RGD-peptide (RGDS, Sigma: 200 μg/ml), RGE-peptide (RGES, Sigma: 200 μg/ml), anti-integrin monoclonal antibody (LM609), or isotype-matched control antibody, in addition to heparin sulfate at 4°C as described above.

Cell-surface binding assays. Cells were resuspended in binding buffer containing 5% FBS at concentration of 2×10^6 per ml. AAV vectors (±heparin sulfate, 500 μg/ml) were added and incubated with the cells for 2 h at 4°C, the cells were then washed three times and fixed with 4% paraformaldehyde for 15 min at room temperature. The cells were then blocked with 10% horse serum and 0.05% Tween-20 in PBS and incubated with A20 anti-AAV mAb for 4 h at 4°C, and then with FITC-labeled secondary antibody in PBS containing 0.05% Tween-20 and 0.2% BSA for 1h at RT. After a final wash, the cells were analyzed by flow cytometry.

Ovarian carcinoma model, immunostaining and histopathology. CB17 SCID mice (n = 12 mice/group) were injected with 1×10^7 SKOV-3 cells intraperitoneal (i.p.) on day 0. On day 5, mice were injected i.p. with 1×10^{10} DNase-resistant particles (DRP) of AAV2-eGFP, RGD-mutant AAVeGFP (AS884C-RGD AAVeGFP), or no virus. To determine the efficiency of AAV vector-mediated eGFP expression in the tumors, twelve mice (four per group) were sacrificed on days 15, 25 and 40 after vector administration. Immunostaining for eGFP was performed on 4-μm paraffin sections. Following deparaffinization and blocking of endogenous peroxidases, slides were heated for 1 h at 65°C, 190 kpa, in citrate buffer to recover antigen. Sections were then blocked with 10% dry milk and incubated with rabbit anti-GFP antibody (Research Diagnostics, Inc., Flanders, NJ) for 12–18 h in a humidified chamber. An equivalent concentration of rabbit IgG was used as a reagent negative control on matching sections. Biotinylated secondary antibody (Goat anti-rabbit, Vector Laboratories) was applied to the slides for 1 h at room temperature. Sections were incubated with avidin-peroxidase complex (Vector Rabbit Elite ABC kit) following the manufacturer's instructions. Either diaminobenzedine (DAB) or 3-amino-9-ethylcarbazole (AEC) were used as chromagens and counterstained with hematoxylin (Vector Laboratories). Slides were dehydrated with xylene and mounted (Permount) before examination on a Nikon E600 microscope. Representative images were collected using a color video camera.

Acknowledgments

We would like to acknowledge the Vector Core Laboratory at Columbus Children's Research Institute, Children's Hospital, Columbus and Dr. K. R. Clark for technical assistance on AAV vector production and titering. This work was supported by grants from the National Institutes of Health (R21 DK55557), and Columbus Children's Research Institute.

RECEIVED FOR PUBLICATION SEPTEMBER 30, 2002; ACCEPTED JANUARY 30, 2003.

References

1. Samulski, R. J., Sally, M., and Muzyczka, N. (1999). Adeno-associated viral vectors. In *The Development of Human Gene Therapy* (T. Friedmann, Ed.), pp. 131–172, Cold Spring Harbor Laboratory Press, Cold Spring Harbor.
2. Bartlett, J. S., Kleinschmidt, J., Boucher, R. C., and Samulski, R. J. (1999). Targeted adeno-associated virus vector transduction of nonpermissive cells mediated by a bispecific F(ab')$_2$ antibody. *Nat. Biotechnol.* 17: 181–186 [published erratum appears in *Nat. Biotechnol.* 1999 Apr;17(4):393].
3. Bartlett, J. S., Wilcher, R., and Samulski, R. J. (1999). Infectious entry pathway of adeno-associated virus and adeno-associated virus vectors. *J. Virol.* 74: 2777–2785.
4. Terashima, S., *et al.* (1998). Factors influencing adeno-associated virus-mediated gene transfer to human cystic fibrosis airway epithelial cells: a comparison with adenovirus vectors. *J. Virol.* 44: 8904–8912.
5. Qing, K., *et al.* (1999). Adeno-associated virus type 2-mediated gene transfer: correlation of tyrosine phosphorylation of the cellular single-stranded D sequence-binding protein with transgene expression in human cells in vitro and murine tissues in vivo. *J. Virol.* 73: 1593–1599.
6. Halbert, C. L., Alexander, I. A., Wolgamot, G. M., and Miller, A. D. (1995). Adeno-associated virus vectors transduce primary cells much less efficiently than immortalized cells. *J. Virol.* 69: 1473–1479.
7. Summerford, C., and Samulski, R. J. (1998). Membrane-associated heparan sulfate proteoglycan is a receptor for adeno-associated virus type 2 virions. *J. Virol.* 72: 1438–1445.
8. Summerford, C., Bartlett, J. S., and Samulski, R. J. (1999). $\alpha v\beta_5$ integrin: a co-receptor for adeno-associated virus type 2 infection. *Nat. Med.* 5: 78–82.
9. Shi, W., Arnold, G. S., and Bartlett, J. S. (2001). Insertional mutagenesis of the adeno-associated virus type 2 (AAV2) capsid gene and generation of AAV2 vectors targeted to alternative cell-surface receptors. *Hum. Gene Ther.* 12: 1697–1711.
10. Wu, P., *et al.* (2000). Mutational analysis of the adeno-associated virus type 2 (AAV2) capsid gene and construction of AAV2 vectors with altered tropism. *J. Virol.* 74: 8635–8647.
11. Girod, A., *et al.* (1999). Genetic capsid modifications allow efficient re-targeting of adeno-associated virus type 2 [published erratum appears in *Nat. Med.* 1999 Dec;5(12): 1438]. *Nat. Med.* 5: 1052–1056.
12. Grifman, M., *et al.* (2001). Incorporation of tumor-targeting peptides into recombinant adeno-associated virus capsids. *Mol. Ther.* 3: 964–975.
13. Nicklin, S. A., *et al.* (2001). Efficient and selective AAV2-mediated gene transfer directed to human vascular endothelial cells. *Mol. Ther.* 4: 174–181.
14. Wickham, T. J., *et al.* (1997). Increased in vitro and in vivo gene transfer by adenovirus vectors containing chimeric fiber proteins. *J. Virol.* 71: 8221–8229.
15. Nishio, K., *et al.* (1999). CAR-dependent and CAR-independent pathways of adenovirus vector-mediated gene transfer and expression in human fibroblasts. *J. Clin. Invest.* 103: 579–587.
16. Dmitriev, I., *et al.* (1998). An adenovirus vector with genetically modified fibers demonstrates expanded tropism via utilization of a coxsackievirus and adenovirus receptor-independent cell entry mechanism. *J. Virol.* 72: 9706–9713.
17. Graham, F. L., Smiley, J., Russell, W. C., and Nairn, R. (1977). Characteristics of a human cell line transformed by DNA from human adenovirus type 5. *J. Gen. Virol.* 36: 59–74.
18. Clark, K., Vouligaropoulou, F., and Johnson, P. (1996). A stable cell line carrying adenovirus-inducible rep and cap genes allows for infectivity titration of adeno-associated virus vectors. *Gene Ther.* 3: 1124–1132.
19. Xiao, X., Li, J., and Samulski, R. (1998). Production of high-titer recombinant adeno-associated virus vectors in the absence of helper adenovirus. *J. Virol.* 72: 2224–2232.
20. Li, J., Samulski, R. J., and Xiao, X. (1997). Role for highly regulated rep gene expression in adeno-associated virus vector production. *J. Virol.* 71: 5236–5243.

21. Zolotukhin, S. (1999). Recombinant adeno-associated virus purification using novel methods improves infectious titer and yield. *Gene Therapy* 6: 973–985.
22. Qing, K., *et al.* (1999). Human fibroblast growth factor receptor 1 is a co-receptor for infection by adeno-associated virus 2. *Nat. Med.* 5: 71–77.
23. Ponnazhagan, S., *et al.* (1997). Adeno-associated virus type 2-mediated transduction in primary human bone marrow-derived CD34+ hematopoietic progenitor cells: donor variation and correlation of transgene expression with cellular differentiation. *J. Virol.* 71: 8263–8267.
24. Bals, R., *et al.* (1999). Transduction of well-differentiated airway epithelium by recombinant adeno-associated virus is limited by vector entry. *J. Virol.* 73: 6085–6088.
25. Albelda, S. M., *et al.* (1990). Integrin distribution in malignant melanoma: association of the beta 3 subunit with tumor progression. *Cancer Res.* 50: 6757–6764.
26. Damjanovich, L., Albelda, S. M., Mette, S. A., and Buck, C. A. (1992). Distribution of integrin cell adhesion receptors in normal and malignant lung tissue. *Am. J. Respir. Cell Mol. Biol.* 6: 197–206.
27. Lessey, B. A., *et al.* (1995). Distribution of integrin cell adhesion molecules in endometrial cancer. *Am. J. Pathol.* 146: 717–726.
28. Smythe, W. R., LeBel, E., Bavaria, J. E., Kaiser, L. R., and Albelda, S. M. (1995). Integrin expression in non-small cell carcinoma of the lung. *Cancer Metastasis Rev.* 14: 225–239.
29. Gladson, C. L., and Cheresh, D. A. (1991). Glioblastoma expression of vitronectin and the alpha v beta 3 integrin. Adhesion mechanism for transformed glial cells. *J. Clin. Invest.* 88: 1924–1932.
30. Xie, Q., *et al.* (2002). The atomic structure of adeno-associated virus (AAV-2), a vector for human gene therapy. *Proc. Natl. Acad. Sci. U S A* 99: 10405–10410.

HUMAN GENE THERAPY 12:1697–1711 (September 20, 2001)
Mary Ann Liebert, Inc.

Insertional Mutagenesis of the Adeno-Associated Virus Type 2 (AAV2) Capsid Gene and Generation of AAV2 Vectors Targeted to Alternative Cell-Surface Receptors

WENFANG SHI,[3] GREGORY S. ARNOLD,[1] and JEFFREY S. BARTLETT[1–3]

ABSTRACT

Recombinant adeno-associated virus (AAV) vectors are of interest in the context of gene therapy because of their ability to mediate efficient transfer and stable expression of therapeutic genes in a wide variety of tissues. However, AAV-mediated gene delivery to specific cell populations is often precluded by the widespread distribution of heparan sulfate proteoglycan (HSPG), the primary cellular receptor for the virus. Conversely, an increasing number of cell types are being identified that do not express HSPG and are therefore poor targets for AAV-mediated gene transfer. To address these issues, we have developed strategies to physically modify AAV vectors and allow efficient, HSPG-independent, receptor-targeted infection. We began by generating a series of 38 virus capsid mutants containing peptide insertions at 25 unique sites within the AAV capsid protein. The mutant viruses were characterized on the basis of their phenotypes and grouped into three classes: class I mutants (4 of 38) did not assemble particles; class II mutants (14 of 38) assembled noninfectious particles; and class III mutants (20 of 38) assembled fully infectious particles. We examined the HSPG-binding characteristics of the class II mutants and showed that a defect in receptor binding was a common reason for their lack of infectivity. The display of foreign peptide epitopes on the surface of the mutant AAV particles was found to be highly dependent on the inclusion of appropriate scaffolding sequences. Optimal scaffolding sequences and five preferred sites for the insertion of targeting peptide epitopes were identified. These sites are located within each of the three AAV capsid proteins, and thus display inserted epitopes 3, 6, or 60 times per vector particle. Modified AAV vectors displaying a 15-amino acid peptide, which binds to the human luteinizing hormone receptor (LH-R), were generated and assessed for their ability to target gene delivery to receptor-bearing cell lines. Titers of these mutant vectors were essentially the same as wild-type vector. The LH-R-targeted vector was able to transduce ovarian cancer cells (OVCAR-3) in an HSPG-independent manner. Furthermore, transduction was shown to proceed via the LH-R and therefore treatment of OVCAR-3 cells with progesterone, to increase LH-R expression, accordingly increased LH mutant-mediated gene transfer. This technology may have a significant impact on the use of AAV vectors for human gene therapy.

OVERVIEW SUMMARY

Previous attempts to retarget AAV vectors by genetic modification of the capsid have met with limited success and have been plagued by low titers and poor targeting efficiencies. Here we demonstrate that the AAV capsid can tolerate the insertion of heterologous peptide ligands at several sites. Importantly, the inserted epitopes are displayed on the surface of the AAV particle and the mutant vectors can be produced to high titer. Furthermore, we demonstrate, for the first time, heparin-independent targeted gene delivery mediated by these vectors.

[1]Children's Research Institute, Children's Hospital, Columbus, OH 43205.
[2]Department of Molecular Virology, Immunology, and Medical Genetics, College of Medicine and Public Health, Ohio State University, Columbus, OH 43210.
[3]Division of Molecular Medicine, Department of Pediatrics, College of Medicine and Public Health, Ohio State University, Columbus, OH 43210.

INTRODUCTION

Adeno-associated virus (AAV) vectors are being used in a growing number of clinical trials for monogenic hereditary disorders and have been proposed as useful agents for the treatment of acquired diseases such as cancer. Ideally, these vectors should deliver and express their transgene only in the desired target cells *in vivo*. However, a number of barriers exist that limit their efficacy in this regard. First, widespread distribution of the virus receptors makes it difficult to restrict infection to particular cells. Second, some therapeutic targets express only low levels of receptors, meaning that high vector doses are required, thereby reducing efficacy and favoring vector spread. Third, many therapeutic targets do not express virus receptors. Finally, neutralizing antibodies specific to the AAV capsid protein can prevent readministration of vector *in vivo*. For example, intratumoral administration of recombinant AAV in a murine model of glioma has been associated with vector dissemination and transduction of normal tissue (Okada *et al.*, 1996). Clinical data have also established the presence of recombinant virus in body fluids of patients intramuscularly injected with even low doses of AAV vectors (Kay *et al.*, 2000). Furthermore, an increasing number of therapeutic targets are being identified that do not express sufficient levels of virus receptors (Bartlett *et al.*, 1998; Duan *et al.*, 1998). Taken together, these data emphasize the need to adapt the vector tropism to particular cells in order to enhance infection while reducing transduction of nontarget tissues, vector dissemination, and shedding.

Virus cell attachment, the initial step that dictates viral tropism, proceeds through high-affinity binding of the AAV2 capsid to cell surface heparan sulfate proteoglycan (Summerford and Samulski, 1998; Bartlett *et al.*, 1999b). Accordingly, targeting strategies have focused on the capsid-mediated attachment step. For example, incubation of recombinant virus with an anti-capsid antibody chemically conjugated to a cell-specific ligand (e.g., a second antibody) has been shown to enhance the transduction of cells displaying the appropriate receptors (Bartlett *et al.*, 1999a). Additional strategies are also being investigated, including the direct chemical conjugation of targeting ligands to the capsid surface (Bartlett, 1999), peptidic insertion (Girod *et al.*, 1999; Wu *et al.*, 2000), and N-terminal extension of the VP2 capsid protein (Yang *et al.*, 1998). Although these approaches are not examples of true retargeting, since the native tropism is maintained, they have each expanded the tropism of AAV vectors by giving the virus the ability to deliver and express genes in novel cell types. For example, insertion of a serpin receptor peptide ligand at the N terminus of the VP2 capsid protein increased transduction of cells believed to express the serpin receptor. However, this mutant vector retained the native heparan sulfate proteoglycan (HSPG)-binding capability and infection could be inhibited by soluble heparin sulfate. Therefore, this vector probably used the serpin receptor only as an alternative coreceptor and primary cellular attachment was still mediated by HSPG.

The AAV capsid is composed of three structural proteins designated VP1, VP2, and VP3. These are encoded in the same open reading frame (ORF) and are expressed from the same viral p40 promoter. The amino acid sequence of the major capsid protein VP3 is contained within the two larger and less abundant capsid proteins VP1 and VP2 (Janik *et al.*, 1984). VP2 is synthesized from the same mRNA as VP3, using an upstream ACG start codon. Mutants with alterations within the VP3 region make little capsid protein (Hermonat *et al.*, 1984) and produce only small amounts of progeny single-stranded viral DNA (Tratschin *et al.*, 1984). Therefore it seems likely that in the absence of capsid protein, or procapsid assembly, nascently synthesized viral DNA is rapidly degraded (Hermonat *et al.*, 1984; Tratschin *et al.*, 1984). Mutations within the VP1 N-terminal region suggest that VP1 is important at some later stage of capsid processing (Hermonat *et al.*, 1984; Tratschin *et al.*, 1984). VP1 is synthesized from an alternatively spliced p40 transcript. Mutants lacking VP1 produce low yields of infectious viral particles but are viable for viral DNA synthesis, which suggests that these mutants are making procapsid and packaging single-stranded viral DNA but are defective in a later stage of capsid assembly than that reliant on VP3 expression. It is not clear whether noninfectious or unstable viral particles can be made in the absence of VP1. Two mutagenesis studies of AAV capsid proteins have revealed that mutations within the capsid gene can dramatically affect particle assembly and virus infection (Rabinowitz *et al.*, 1999; Wu *et al.*, 2000). Since the crystal structure of AAV is not known, the functional domains of the AAV capsid have been largely predicted on the basis of information derived from other related parvoviruses, including canine parvovirus (CPV), feline panleukopenia virus (FPV), minute virus of mice (MVM), Aleutian mink disease parvovirus (ADV), and the human parvovirus B19, whose structures are available (Tsao *et al.*, 1991; Agbandje *et al.*, 1994; Agbandje-McKenna *et al.*, 1998; McKenna *et al.*, 1999). Sequence comparison of AAV with these viruses has revealed a few conserved functional domains (Chapman and Rossmann, 1993; Chiorini *et al.*, 1997), but the true nature of these domains is not clear. Genetic engineering of the AAV capsid has proven tricky: insertions as small as four residues can prevent the generation of infectious virus (Rabinowitz *et al.*, 1999) and even single-residue substitutions can drastically impair virus growth (Wu *et al.*, 2000).

In this study, we used site-directed mutagenesis to mutate the capsid ORF in a search for regions that could tolerate insertions for the purpose of retargeting AAV vectors. Thirty-eight insertion mutants were made, in which 2 to 15 amino acids were inserted in the AAV capsid ORF. By analyzing these mutants we obtained a preliminary functional map of the AAV capsid protein. Our results identified critical regions within the capsid that were potentially responsible for receptor binding, DNA packaging, capsid formation, and infectivity. Importantly, we identified sites that were suitable for epitope insertions that might be useful for targeted gene delivery. We tested this paradigm by inserting a targeting peptide ligand into the AAV capsid protein and have shown that we can redirect vector infection to receptor-bearing cell lines independent of the endogenous AAV tropism.

MATERIALS AND METHODS

Cell culture

Low passage number (passage number 20–40) HEK 293 cells (Graham *et al.*, 1977), HeLa cells, and HeLa C12 cells (Clark

et al., 1996) were grown in Dulbecco's modified Eagle's medium (DMEM) supplemented with 10% fetal bovine serum, penicillin (100 U/ml), and streptomycin (100 U/ml), at 37°C and 5% CO_2. NIH:OVCAR-3 (human ovarian adenocarcinoma, HTB-161) cells were grown in RPMI 1640 medium with 2 m*M* L-glutamine adjusted to contain sodium bicarbonate (1.5 g/liter), glucose (4.5 g/liter), 10 m*M* HEPES, and 1.0 m*M* sodium pyruvate and supplemented with bovine insulin (0.01 mg/ml) and 20% fetal bovine serum.

Construction of AAV capsid mutant plasmids

The plasmid pACG2 (Xiao *et al.*, 1998) was used as the template for all mutant constructions. This plasmid contains the AAV genome, less the two viral inverted terminal repeats (ITRs), and an ATG-to-ACG mutation of the Rep78/68 start codon, which has been shown to increase recombinant AAV (rAAV) vector yield by attenuating Rep78/68 synthesis (Li *et al.*, 1997). Sites for mutagenesis were chosen on the basis of a computer-generated model of AAV structure. The secondary structure of the AAV2 VP1 capsid protein was first modeled solely on the basis of its primary amino acid sequence, using three different computer algorithms (Garnier *et al.*, 1996; Chou and Fasman, 1978; and Deleage and Roux, 1987). This analysis yielded a predictability assessment for each amino acid based on the likelihood of that residue being within a β barrel, α helix, etc. This structural probability matrix was then interactively fit to a common secondary structure prediction derived from a comparison of the five solved parvovirus structures (CPV, FPV, MVM, B19, and ADV). The resulting AAV2 model provided the means for the preliminary structural identification of surface loop regions that were envisioned as possibly tolerating foreign peptide sequence insertions. Mutagenesis was achieved by using the ExCite polymerase chain reaction (PCR)-based site-directed mutagenesis kit according to the supplier manual (Stratagene, La Jolla, CA) except that Platinum *Pfx* DNA polymerase (Life Technologies, Rockville, MD) was often substituted for the polymerase blend used in the kit. For each mutant, two PCR primers were designed that contained the sequence of the desired insertion plus a unique endonuclease restriction site (either *AgeI* or *NgoMIV*) flanked by 15 to 20 homologous base pairs on each side of the insertion. The restriction site was included to facilitate the identification of mutant plasmids and for the potential later swapping of foreign epitopes. In some instances additional nonhomologous flanking sequences were included in the PCR primers. These sequences encoded linker/scaffolding sequences on either side of the desired insertion. The PCR products were digested with *DpnI* endonuclease to eliminate the parental plasmid template and were propagated in DH-5α bacteria (Life Technologies). Minipreparation DNAs were extracted from ampicillin-resistant colonies and were screened by restriction endonuclease digestion.

Production of recombinant AAV particles with modified capsids

To produce rAAV with mutant capsid proteins, we transfected 293 cells with three plasmids. The three plasmids used were as follows: either (1) pAB-11, which contains the *Escherichia coli* β-galactosidase gene (*lacZ*) driven by the cytomegalovirus (CMV) promoter and flanked by the AAV terminal repeats (TRs) (Goodman *et al.*, 1994) or pTR-UF5, which contains the enhanced green fluorescent protein (eGFP) gene also driven by the CMV promoter and flanked by the AAV terminal repeats; (2) the pXX6 plasmid, which contains the Ad helper genes (Xiao *et al.*, 1998); and (3) the modified pACG plasmid, which supplies the mutant capsid proteins. As a control, rAAV was also prepared with unmodified pACG plasmid. The plasmids were mixed at a 1:1:1 molar ratio. Plasmid DNAs used for transfection were purified with a Qiagen (Valencia, CA) Maxi-prep kit according to the supplier manual.

Transfections were carried out as follows. 293 cells were split 48 hr before transfection so that they could reach 75% confluency at the time of transfection. Four 10-cm plates were transfected at 37°C, using the calcium phosphate transfection system (Life Technologies) according to the manufacturer specifications, and incubated at 37°C. Forty-eight hours after transfection, cells were harvested by centrifugation at 500 × *g* for 10 min, resuspended in phosphate-buffered saline (PBS) and virus was released by freezing and thawing three times. The crude lysate was clarified by centrifugation at 500 × *g* for 10 min and treated with Benzonase (Sigma, St. Louis, MO) at 50-U/ml final concentration at 37°C for 30 min. Virus was further purified by iodixanol step gradient (Zolotukhin, 1999), and in some instances by heparin sulfate affinity chromatography (Zolotukhin, 1999).

To determine whether mutants were temperature sensitive, some transfections were repeated as duplicates in 10-cm plates/dishes at 30 and 32°C. Recombinant AAV stocks were titered immediately and then aliquoted and stored at −20°C for further analysis.

Virus titers

Physical titers of the mutant rAAV preparations were determined with an A20 enzyme-linked immunosorbent assay (ELISA) kit (American Research Bioproducts, Belmont, MA). Crude, or purified, rAAV stocks were serially diluted and incubated with the A20 kit plate. The readings that fell into the linear range were taken, and the titers were read off the standard according to the manufacturer instructions. The A20 monoclonal antibody detects both full and empty AAV particles (Wistuba *et al.*, 1995).

Titers of DNA-containing rAAV particles were determined by DNA dot-blot assay. Briefly, 5 μl of the purified rAAV stock was diluted 1:40 in digestion buffer (50 m*M* Tris-HCl [pH 7.5], 1 m*M* $MgCl_2$, and 1 m*M* $CaCl_2$) containing RNase A (10 μg/ml) and DNase I (10 μg/ml) and incubated at 37°C for 30 min. Sarcosine was then added to 0.5% final concentration, EDTA and EGTA were added to final concentrations of 10 m*M*, and the sample was heated to 70°C for 10 min and then cooled to 37°C. Proteinase K was added to a final concentration of 1 mg/ml and the samples were incubated at 37°C for 2 hr. Viral DNA was denatured by adding NaOH and EDTA to final concentrations of 400 and 20 m*M*, respectively. DNA samples were applied to Nylon membranes (Hybond-N+; Amersham Pharmacia Biotech, Piscataway, NJ) and probed with a digoxigenin-labeled DNA fragment from the human CMV (hCMV) promoter found in the vector genomes. AAV vector genomes were visualized by enzyme immunoassay, using the chemiluminescence substrate CSPD (Roche, Nutley, NJ) as suggested by the manufacturer. Dot intensities were quantitated from densitometrically

canned films with NIH Image software. Alternatively, titers of DNA-containing rAAV particles were determined by real-time PCR using a PE-Applied Biosystems (Foster City, CA) Prism 7770 sequence detector as previously described (Clark *et al.*, 1999).

Infectious titers of rAAV containing wild-type or mutant capsids were determined by gene transduction assay. Briefly, HeLa S12 cells were seeded in 24-well plates the day before infection so that they would reach about 75% confluence the next day. Serial dilutions of wild-type and mutant rAAVlacZ preparations were added to the cells in the presence of Ad5 at a multiplicity of infection (MOI) of 3. The cells and viruses were incubated at 37°C for 48 hr, after which time the medium was removed and the cells were washed twice with PBS and then fixed in 2% formaldehyde and 0.2% glutaraldehyde for 15 min at 20°C. Cells expressing vector-encoded β-galactosidase were detected by histochemical staining as previously described (Sanes *et al.*, 1986). Titers were determined by counting the number of positively stained cells with an inverted tissue culture microscope. Cells expressing eGFP transgenes were detected by fluorescence-activated cell sorting (FACS) analysis. Infectious titers were also determined in the absence of adenovirus with no differences in the relative titers of mutants.

Gel electrophoresis and immunoblotting

Purified rAAV and mutant rAAV samples were analyzed by 10% sodium dodecyl sulfate-polyacrylamide gel electrophoresis (SDS-PAGE). The samples were mixed with sample buffer and boiled for 5 min before loading. For immunoblotting, the proteins were transferred to Hybond-P membranes (Amersham Pharmacia Biotech) and the membranes were probed with either polyclonal guinea pig anti-AAV2 serum (Serotec, Raleigh, NC), or with monoclonal antibody B1 (MAb B1) directed against the AAV2 VP3 capsid protein (Wistuba *et al.*, 1995). The capsid bands were visualized with biotinylated anti-mouse IgG secondary antibodies (Vector Laboratories, Burlingame, CA) using enhanced chemiluminescence detection (ECL) as suggested by the supplier (Amersham Pharmacia Biotech).

Epitope display

Surface display of the bovine papillomavirus (BPV) peptide epitope was assessed by immunoprecipitation with anti-BPV antibody. Purified rAAV samples were diluted in 50 volumes of PBS-MK buffer (PBS containing 1 m*M* $MgCl_2$ and 2.5 m*M* KCl) and incubated for 2 hr at 4°C in the presence of monoclonal antibody to the BPV epitope (MAb BPV, clone AU5). Fifty microliters of protein G–Sepharose beads (Amersham Pharmacia Biotech) was then added and the sample was incubated for another 2 hr at 4°C. For negative controls, an unrelated primary antibody or no primary antibody was used. After incubation the samples were centrifuged for 1 min at 16,000 × *g* at 4°C. The beads were washed three times with 1 ml of PBS-MK for 10 min at room temperature and resuspended in proteinloading buffer. The samples were then boiled and analyzed by Western blotting with MAb B1 as described above.

Heparin-binding assay

The ability of mutants to bind heparin sulfate was assessed by precipitation with heparin sulfate affinity resin (POROS). Briefly, crude rAAV preparations containing wild-type or mutant capsids were first subjected to iodixanol gradient purification. The 40% iodixanol layer was collected (approximately 0.7-ml total volume) and 10 μl of this material was diluted in 250 μl of PBS-MK containing 50 μl of heparin sulfate affinity-resin. The mixture was incubated for 2 hr with gently mixing at 4°C and then centrifuged at 16,000 × *g* for 2 min at 4°C to collect the resin and bound virus. The resin was washed three times with 1 ml of PBS-MK for 10 min at room temperature and resuspended in loading buffer. The samples were then boiled and analyzed by Western blotting with MAb B1 as described above. Controls included precipitation of vectors with wild-type capsids and precipitation of vectors with unconjugated resin.

Heparin-independent targeted transduction of OVCAR-3 cells

Targeted AAV-mediated transduction experiments were performed in triplicate. Luteinizing hormone receptor-positive (LH-R$^+$) OVCAR-3 cells or HeLa cells were grown overnight in appropriate medium at a count of 1×10^4 cells/well in 24-well plates. In some instances, LH-R expression was further stimulated by growth of OVCAR-3 cells in the presence of progesterone (50 μg/ml; Sigma) (Hamilton *et al.*, 1984; Abrahamsson *et al.*, 1997; Ji *et al.*, 1997; Konishi *et al.*, 1999). Mutant AAV vectors, AAV-A139LH-lacZ or AAV-A139BPV-lacZ, were incubated in medium (RPMI 1640 without FBS) in the presence or absence of heparin sulfate (500 μg/ml; Sigma) or LH (200 μg/ml) for 1 hr at 4°C. The cells were washed with PBS and incubated with the vector ± heparin sulfate ± LH (100 physical particles [PP]/cell) for 2 hr at 4°C. The cells were then washed twice with fresh medium and incubated at 37°C for 24 hr. The cells were then infected with Ad5 at an MOI of 10 IU/cell and incubated for another 24 hr at 37°C. Cells expressing the vector-encoded *lacZ* transgene were identified by histochemical staining as described above. The experiments were repeated three times.

RESULTS

Generation of AAV capsid mutants

Previous attempts to retarget AAV vectors by inserting foreign peptide ligands into the capsid have met with limited success (Girod *et al.*, 1999; Rabinowitz *et al.*, 1999; Wu *et al.*, 2000). Random mutagenesis strategies have led to poor vector titers and have been inefficient in generating functional mutants capable of supporting foreign peptide insertion (Rabinowitz *et al.*, 1999; Wu *et al.*, 2000). Since the crystal structure of AAV is unavailable, an earlier site-specific mutagenesis strategy (Girod *et al.*, 1999) relied on the comparison of AAV and canine parvovirus (CPV) capsid protein amino acid sequences, and then chose regions for peptide insertion that were thought to be on the AAV capsid surface on the basis of this alignment. Using that approach, six mutants were constructed. However, only one of these mutants proved capable of packaging vector DNA and targeting infection to receptor-bearing cell lines. Furthermore, infectivity of the mutant was reduced by three orders of magnitude compared with vector with wild-type capsid. It is clear that a more detailed prediction of AAV capsid structure

and construction and analysis of a much larger number of capsid mutants are needed to generate vectors able to efficiently display foreign epitopes and redirect vector infection to alternative cell surface receptors.

We began by developing a structural model of the AAV2 capsid by fitting a computer-generated prediction of the capsid secondary structure to a conserved tertiary model of parvovirus capsids derived from the defined structures of five different viruses. On the basis of this prediction we then chose specific sites for epitope insertion, using three different criteria: (1) predicted accessibility to the capsid surface, (2) predicted flexibility of the surrounding amino acids, and (3) scarcity of charged or hydrophobic amino acids. Twenty-five sites were chosen; 4 sites were within the VP1 unique region of the AAV2 capsid protein, 2 were within the VP1/VP2 unique region, and the remaining 19 sites were located within the VP3 region of the capsid ORF (Table 1). The mutants were constructed in the noninfectious AAV plasmid, pACG2, by PCR-based site-directed mutagenesis. All of the mutations were created so that they also contained a restriction site at the location of insertion to facilitate confirmation of the mutant sequence and subsequent insertion or swapping of foreign epitopes. A total of 38 different mutants was generated. The length of the inserted sequences ranged from 2 to 15 amino acids. The smaller insertions contained only the restriction endonuclease sites (*Age*I or *Ngo*MIV), whereas the larger insertions encoded foreign peptide epitopes. Three different foreign epitopes were used. The first was a 6-amino acid peptide (TPFYLK) derived from bovine papillomavirus (BPV); the second was a cyclic RGD-containing peptide specific to α_v integrins (CDCRGDCFC); and the last was a 10-amino acid peptide (HCSTCYYHKS) derived from human luteinizing hormone (LH) and known to bind the luteinizing hormone receptor (LH-R). The foreign peptide epitopes were each flanked by 5 amino acids connecting peptide linkers of three different sequences (Table 1).

TABLE 1. SUMMARY OF ALL MUTANTS

Mutant plasmid designation[a]	*Location*	*Insertion (epitope)*
pACG-A26	VP1	TG (*Age*I)
pACG-A46	VP1	TG (*Age*I)
pACG-A115-4C-RGD/GLS	VP1	TGCDCRGDCFCGLS (4C-RGD)
pACG-A120	VP1	TG (*Age*I)
pACG-A139	VP2	TG (*Age*I)
pACG-A139BPV/GLS	VP2	TGTPFYLKGLS (BPV)
pACG-A139LH/GLS	VP2	TGHCSTCYYHKSGLS (LH)
pACG-A161BPV/ALS	VP2	TGTPFYLKALS (BPV)
pACG-A161BPV/LLA	VP2	TGTPFYLKLLA (BPV)
pACG-A161BPV/GLS	VP2	TGTPFYLKGLS (BPV)
pACG-A161LH/GLS	VP2	TGHCSTCYYHKSGLS (LH)
pACG-A312	VP3	TG (*Age*I)
pACG-N319	VP3	AG (*Ngo*MIV)
pACG-A323-4C-RGD/GLS	VP3	TGCDCRGDCFCGLS (4C-RGD)
pACG-A339BPV	VP3	TGTPFYLK (BPV)
pACG-A375BPV	VP3	TGTPFYLK (BPV)
pACG-A441	VP3	TG (*Age*I)
pACG-A459	VP3	TG (*Age*I)
pACG-A459BPV/GLS	VP3	TGTPFYLKGLS (BPV)
pACG-A459LH/GLS	VP3	TGHCSTCYYHKSGLS (LH)
pACG-A466	VP3	TG (*Age*I)
pACG-N472	VP3	AG (*Ngo*MIV)
pACG-A480-4C-RGD/GLS	VP3	TGCDCRGDCFCGLS (4C-RGD)
pACG-N496	VP3	AG (*Ngo*MIV)
pACG-A520LH/GLS	VP3	TGHCSTCYYHKSGLS (LH)
pACG-A520BPV/GLS	VP3	TGTPFYLKGLS (BPV)
pACG-A540	VP3	TG (*Age*I)
pACG-N549	VP3	AG (*Ngo*MIV)
pACG-N584	VP3	AG (*Ngo*MIV)
pACG-A584BPV/ALS	VP3	TGTPFYLKALS (BPV)
pACG-A584BPV/LLA	VP3	TGTPFYLKLLA (BPV)
pACG-A584BPV/GLS	VP3	TGTPFYLKGLS (BPV)
pACG-A587BPV/ALS	VP3	TGTPFYLKALS (BPV)
pACG-A587BPV/LLA	VP3	TGTPFYLKLLA (BPV)
pACG-A587BPV/GLS	VP3	TGTPFYLKGLS (BPV)
pACG-A595-4C-RGD/GLS	VP3	TGCDCRGDCFCGLS (4C-RGD)
pACG-A597-4C-RGD/GLS	VP3	TGCDCRGDCFCGLS (4C-RGD)
pACG-A657	VP3	TG (*Age*I)

[a]Insertions were made into the wild type AAV2 capsid sequence, beginning immediately after the indicated AAV residue.

Particle and infectious titer assays reveal three classes of mutants

To determine the effect of each mutation on particle assembly and infectivity we used either wild-type pACG2 or a mutant pACG2 plasmid to complement the growth of the recombinant AAV construct, pAB-11, which contains the *lacZ* gene under the control of a CMV promoter (Goodman *et al.*, 1994). The resulting recombinant AAVlacZ vectors contained either wild-type or mutant capsid proteins. To determine the relative efficiencies of particle assembly among mutant and wild-type vectors, we used the A20 ELISA. The A20 antibody recognizes only intact particles (Wistuba *et al.*, 1995), and is therefore useful for determining the physical particle titer of vector preparations irrespective of whether the capsids contain DNA (Grimm *et al.*, 1999). Eight of the 38 mutants that were tested were negative by this ELISA (Table 2), indicating that they were unable to assemble capsids, or that the capsids were unstable, or that the A20 epitope had been disrupted in the mutants.

DNA dot-blot assays were also performed on all of the mutant vector preparations. The dot-blot assay measures the titer of AAV particles that contain DNase-resistant recombinant AAV genomes. Fifteen of the 38 mutants tested negative by the dot-blot assay. Interestingly, several mutants that were positive for the synthesis of AAV particles by A20 ELISA were nega-

TABLE 2. DETERMINATION OF TITERS AND CLASSIFICATION OF MUTANT AAV VECTORS

Mutant vector designation[a]	*Particle titer (PP/ml)*		*Infectious titer (IU/ml)*	*Mutant type*
	Dot blot	*A20 ELISA*		
AAV-A26	(+)[b]	7.5×10^7	—	II
AAV-A46	9.2×10^7	8.0×10^7	1.2×10^3	III
AAV-A115-4C-RGD/GLS	5.6×10^7	7.5×10^7	1.2×10^2	III
AAV-A120	3.4×10^7	8.0×10^7	1.0×10^3	III
AAV-A139	2.0×10^7	9.0×10^7	5.0×10^5	III
AAV-A139BPV/GLS	1.4×10^8	9.0×10^7	6.8×10^5	III
AAV-A139LH/GLS	1.2×10^8	8.0×10^7	3.3×10^5	III
AAV-A161BPV/ALS	4.0×10^7	8.0×10^7	1.2×10^5	III
AAV-A161BPV/LLA	1.4×10^6	7.5×10^5	5.9×10^2	III
AAV-A161BPV/GLS	1.2×10^7	7.5×10^6	8.7×10^4	III
AAV-A161LH/GLS	4.0×10^6	8.0×10^7	3.4×10^4	III
AAV-A312	1.8×10^6	—	5.3×10^2	III
AAV-N319	2.4×10^7	4.5×10^5	0.6×10^3	III
AAV-A323-4C-RGD/GLS	(+)	—	—	II
AAV-A339BPV	(+)	—	—	II
AAV-A375BPV	—	—	—	I
AAV-A441	—	—	—	I
AAV-A459	7.2×10^6	8.0×10^7	6.5×10^4	III
AAV-A459BPV/GLS	5.6×10^7	4.5×10^6	2.2×10^5	III
AAV-A459LH/GLS	3.2×10^6	4.5×10^5	—	II
AAV-A466	(+)	7.5×10^7	—	II
AAV-N472	—	—	—	I
AAV-A480-4C-RGD/GLS	—	—	—	I
AAV-N496	2.2×10^6	—	1.1×10^2	III
AAV-A520LH/GLS	(+)	7.5×10^7	—	II
AAV-A520BPV/GLS	(+)	7.5×10^7	—	II
AAV-A540	(+)	8.0×10^7	—	II
AAV-N549	(+)	4.5×10^6	—	II
AAV-N584	1.1×10^8	8.0×10^7	4.0×10^5	III
AAV-A584BPV/ALS	3.0×10^7	8.0×10^7	6.5×10^2	III
AAV-A584BPV/LLA	1.3×10^7	9.0×10^6	—	II
AAV-A584BPV/GLS	(+)	7.5×10^5	—	II
AAV-A587BPV/ALS	1.8×10^7	8.0×10^6	5.0×10^1	III
AAV-A587BPV/LLA	7.2×10^5	9.0×10^5	—	II
AAV-A587BPV/GLS	3.5×10^7	9.0×10^7	2.7×10^2	III
AAV-A595-4C-RGD/GLS	—	2.5×10^4	—	II
AAV-A597-4C-RGD/GLS	—	2.5×10^4	—	II
AAV-A657	1.8×10^7	7.5×10^7	5.2×10^4	III
AAV (wild type)	4.8×10^7	9.0×10^7	6.2×10^5	N/A

[a]All insertions contained a restriction site (*Age*I or *Ngo*MIV), designated A or N. BPV, LH, and 4C-RGD indicate the insertion of these epitopes immediately after the indicated amino acid of the wild-type AAV2 capsid sequence. The inserted peptides are as follows: A, TG; N, AG; BPV, TPFYLK; LH, HCSTCYYHKS; 4C-RGD, CDCRGDCFC.

[b]Particle titer: (+), below the sensitivity of the DNA dot-blot assay, but detected by PCR assay.

tive by the DNA dot-blot assay, indicating that either the sensitivity of the dot-blot assay was not sufficient to detect low numbers of packaged AAV genomes, that the mutant capsids were unstable and no longer protected the packaged genomes from DNase digestion as efficiently, or that several of the mutants produced empty viral particles. To address the issue of assay sensitivity, titers of DNA-containing rAAV particles were also determined by quantitative real-time PCR. This assay has previously been shown to have a sensitivity of less than 100 vector genomes (Clark *et al.*, 1999) and we have determined that it is approximately 40-fold more sensitive that the nonradioactive DNA dot-blot assay (data not shown). By combining the A20 ELISA and real-time PCR assays we were able to determine that only four mutants were truly defective in particle formation (Table 2). These were classified as class I mutants. To ensure that spurious second-site mutations had not been introduced into these packaging constructs, we Western blotted from the packaging cells as well as assayed Rep function. Each of the class I mutants produced all three of the viral capsid proteins and the packaging cell lysates were positive for AAV genome replication (data not shown). Therefore, these mutants simply did not assemble functional viral particles. Two mutants, A595-4C-RGD/GLS and A597-4C-RGD/GLS, produced empty particles, and nine mutants (A26, A323-4C-RGD/GLS, A339BPV, A466, A520LH/GLS, A520BPV/GLS, A540, N549, and A584BPV/GLS) had low particle titers that could be detected only by the real-time PCR assay. Presumably this low titer was caused by a general destabilization of the viral particle, resulting in an increased susceptibility to DNase digestion. The remaining mutants, which were positive for A20 particles, were positive for packaged viral DNA by the dot-blot assay.

For infectivity assays, special mutants were initially grown

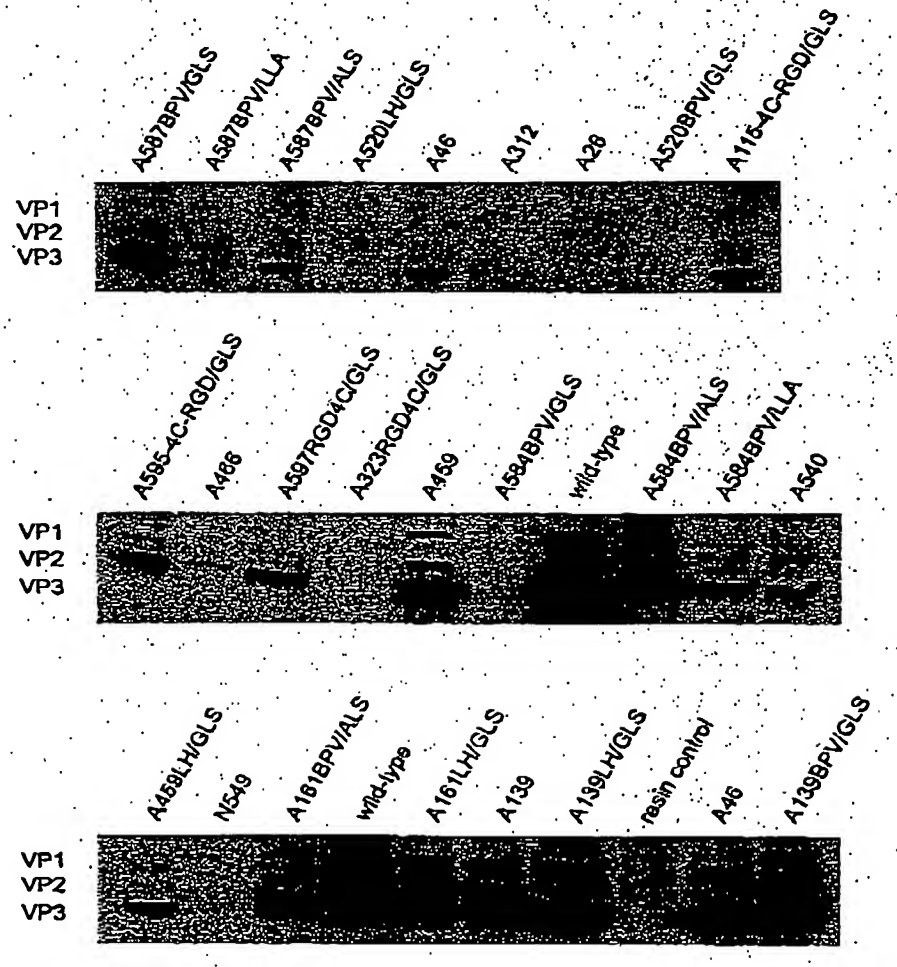

FIG. 1. Heparin sulfate (HS)-binding characteristics of epitope insertion mutants. Iodixanol gradient-purified virus particles were bound to HS resin for 2 hr at 4°C. After extensive washing, the resin was resuspended in loading buffer and the fractions were separated on SDS–10% acrylamide gels and analyzed by Western blotting, using the anti-AAV B1 monoclonal antibody. The positions of VP1, VP2, and VP3 are indicated. Wild-type, precipitation of vectors containing unmodified capsids; resin control, precipitation of vector particles with unconjugated resin.

and titered at both 37 and 32°C to determine whether any of the mutants were temperature sensitive. These experiments were done at least twice, and there was no significant variation in titer value. No temperature-sensitive mutants were identified (data not shown). On the basis of the infectious titers the mutants were further grouped into two more classes (Table 2). Class II contained mutants that produced viral particles, but were noninfectious (e.g., A459LH/GLS and A466), whereas class III contained mutants that were fully infectious. The majority of mutants generated fell into the class III designation.

Some noninfectious (class II) mutants were defective for binding the viral receptor

We were able to show, as described above, that a number of class II mutants were defective in packaging DNA or in forming stable virus particles. Another potential cause for lack of infectivity of these class II mutants might be that they were unable to bind the viral cell surface receptor, the first step of the infectious entry pathway (Bartlett *et al.*, 1999b). Heparan sulfate proteoglycan has been identified as the primary cell surface receptor for AAV (Summerford and Samulski, 1998). Therfore, we developed a small-scale heparin-binding assay to test whether these mutants could bind heparin, the native AAV receptor (see Materials and Methods). Aliquots of iodixanol-purified wild-type or mutant AAV vectors were precipitated with heparin sulfate (HS) affinity resin and the bound material was visualized by Western blotting with the B1 antibody that recognizes each of the AAV capsid proteins (Fig. 1 and Table 3). As expected, most of the mutant AAV vectors were precipitated easily by the heparin resin, and capsid protein could be detected on the Western blot (Fig. 1 and Table 3). However, several of the class II mutants bound poorly to heparin (Fig. 1) and some did not bind to the HS resin at all. This suggested that a potential defect in these mutants was their inability to bind to heparan sulfate proteoglycan. The other class II mutants were clearly defective at a subsequent point in the cell entry pathway.

Display of foreign peptide epitopes on the surface of mutant AAV particles

To determine whether the BPV insertion mutants contained the BPV sequence exposed on the surface of the capsid, we used batch immunoprecipitation with BPV monoclonal antibody and protein G-conjugated beads. In each case virus was purified by iodixanol density gradient centrifugation to remove any soluble capsid protein that might be present in crude viral preparations. In most cases, when the viable BPV insertion mutants were treated with BPV monoclonal antibody and protein G-conjugated beads, substantial amounts of vector were precipitated (Table 4 and Fig. 2). Control wild-type virus particles were not precipitated with anti-BPV antibody. This demonstrated that in most cases the BPV epitope was efficiently displayed on the surface of the virus particle and accessible to the antibody. These results also demonstrate the effectiveness of our site-specific mutagenesis technique and modeling of AAV2 structure in that all sites predicted to be on the surface of the viral particles and chosen for BPV epitope insertion were capable of displaying the inserted epitope in such a manner that it could be bound by antibody and precipitated from solution with the protein G beads. Interestingly, the two BPV insertion mutants that did not efficiently display the BPV epitope were also noninfectious and in one case, A584BPV/GLS, did not bind heparin sulfate.

Influence of linker/scaffolding sequence on titer and receptor binding

It was predicted that the inserted peptide epitopes might destabilize the local AAV capsid structure near the site of insertion. To address this issue, three different linker sequences were designed and used in the context of the BPV epitope insertions. These sequences consisted of small, flexible amino acids that were designed to lessen the conformational stress imposed on the vector virion by the insertion. It was immediately clear that mutants with insertions at identical sites, but with different linker sequences, had different properties (Table 5). In all cases, the BPV insertion mutants with the ALS linker sequence were infectious. However, this linker was not the best for every site. In one case (mutants N584BPV/ALS and N584BPV/GLS), a single amino acid change within the linker sequence (A → G) decreased the titer from wild-type levels to essentially nothing. At the other sites (following AAV2 capsid protein amino acid 161 or amino acid 587) changing linker se-

TABLE 3. HEPARIN-BINDING PROPERTIES OF SELECTED CLASS II AND CLASS III MUTANTS

Mutant vector designation	*HSPG binding*[a]
AAV-A26	—
AAV-A46	++
AAV-A115-4C-RGD/GLS	++
AAV-A139	++
AAV-A139BPV/GLS	++
AAV-A139LH/GLS	++
AAV-A161BPV/ALS	++
AAV-A161LH/GLS	++
AAV-A312	—
AAV-A323-4C-RGD/GLS	—
AAV-A459	++
AAV-A459LH/GLS	++
AAV-A466	+
AAV-A520LH/GLS	—
AAV-A520BPV/GLS	—
AAV-A540	++
AAV-N549	—
AAV-A584BPV/ALS	++
AAV-A584BPV/LLA	++
AAV-A584BPV/GLS	—
AAV-A587BPV/ALS	++
AAV-A587BPV/LLA	+
AAV-A587BPV/GLS	++
AAV-A595-4C-RGD/GLS	++
AAV-A597-4C-RGD/GLS	++
AAV (wild type)	++

[a] ++, Greater than 90% of the mutant virus particles bound to the heparin sulfate affinity resin and the precipitated capsid proteins were readily detected by Western blotting; +, less than 90% of the mutant virus particles bound to the heparin sulfate affinity resin, but precipitated capsid proteins could still be detected by Western blotting; —, no protein signal detected by Western blotting.

TABLE 4. DISPLAY OF FOREIGN EPITOPES ON THE SURFACE OF MUTANT AAV PARTICLES[a]

Mutant vector designation	*Epitope display*
AAV-A139BPV/GLS	++
AAV-A161BPV/ALS	++
AAV-A161BPV/LLA	++
AAV-A161BPV/GLS	++
AAV-A339BPV	—
AAV-A459BPV/GLS	++
AAV-A520BPV/GLS	—
AAV-A584BPV/ALS	++
AAV-A584BPV/LLA	+
AAV-A584BPV/GLS	—
AAV-A587BPV/ALS	++
AAV-A587BPV/LLA	—
AAV-A587BPV/GLS	++

[a] ++, >90% of the mutant virus was immunoprecipitated with anti-BPV MAb and the precipitated capsid proteins were readily detected by Western blotting; +, less than 90% of the mutant virus particles were immunoprecipitated, but precipitated capsid proteins could still be detected by Western blotting; —, no protein signal was detected by Western blotting.

quences also influenced particle and infectious titers over several orders of magnitude. Appropriate linker sequences had similar effects on heparin binding and epitope display (Table 5).

Vector-mediated gene transfer to human ovarian cancer cell lines via genetically modified AAV

To determine whether we could change the tropism of AAV vectors by inserting a novel receptor ligand into the capsid, several of the mutants we constructed contained either an LH receptor ligand or an integrin receptor ligand (4C-RGD). The LH ligand was inserted into the AAV capsid sequence at four different positions (following amino acids 139, 161, 459, and 520) (Table 1). The 4C-RGD ligand was inserted at five different positions (following amino acids 115, 323, 480, 595, and 597) (Table 1). The A139LH/GLS, A161LH/GLS, and A115-4C-RGD/GLS mutants were each infectious. The LH mutant A139LH/GLS produced recombinant AAV titers indistinguishable from those of wild-type vector on 293 cells (Table 2) and was used to assess LH-R-directed infection of OVCAR-3 cells. A second mutant, A139BPV/GLS, containing the BPV peptide epitope, produced a titer on 293 cells identical to that of wild-type vector and was used as a control also in these experiments to assess the specificity of vector targeting. When equal amounts of A139BPV/GLS or A139LH/GLS mutant virus (as determined by particle titer) were used to infect OVCAR-3 cells, the LH mutant showed a slightly higher infectivity than the BPV mutant (Fig. 3A). However, when the OVCAR-3 cells were pretreated with progesterone to increase expression of the targeted receptor (Hamilton *et al.*, 1984; Abrahamsson *et al.*, 1997; Ji *et al.*, 1997; Konishi *et al.*, 1999), LH mutant-mediated transduction increased substantially whereas transduction mediated by the nontargeted BPV mutant did not change (Fig. 3A). Because both mutants retained wild-type heparin-binding activity, we also infected OVCAR-3 and HeLa cells in the presence of heparin sulfate to determine whether the mutants could infect cells independent of this endogenous interaction. The BPV mutant vector was unable to transduce either cell line in the presence of heparin sulfate (Fig. 3B). Transduction of HeLa cells, which do not express measurable LH-R (data not shown), with the LH mutant vector was similarly lacking (Fig. 3B). However, when OVCAR-3 cells were infected with the LH mutant vector, significant gene transduction was maintained even in the presence of heparin sulfate and this could be further augmented by pretreating the cells with progesterone to increase expression of the targeted receptor. To demonstrate specificity for the targeted LH receptor we infected OVCAR-3 cells and HeLa cells in the presence of both heparin sulfate and luteinizing hormone. The combination of these soluble competitors was able to completely inhibit gene transduction to OVCAR-3 cells. Taken together, these data suggest that the LH-tagged vectors can independently use either heparan sulfate proteoglycan or the LH receptor as a primary cellular attachment receptor and demonstrate efficient retargeting of AAV vectors to an alternative cell surface receptor.

DISCUSSION

This study demonstrates that the site-directed insertion of heterologous ligands into the AAV2 capsid permits retargeting of AAV2-based vectors to alternative cell-surface receptors and targeted gene delivery to receptor-bearing cell lines. Importantly, the results show that it is possible to alter the tropism of

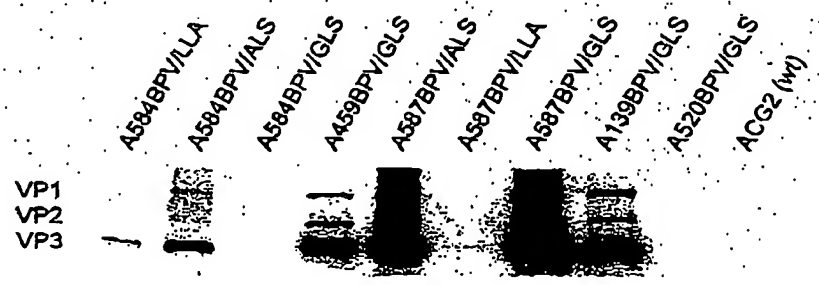

FIG. 2. Immunoprecipitation and Western blot analysis of BPV epitope insertion mutants. Iodixanol gradient-purified virus was precipitated with anti-BPV MAb, using protein G–Sepharose. The bound virus was eluted with SDS sample buffer and subjected to Western analysis with anti-AAV B1 antibody.

TABLE 5. DEPENDENCE OF LINKER/SCAFFOLDING SEQUENCES ON MUTANT TITER, EPITOPE DISPLAY, AND RECEPTOR BINDING

Mutant vector designation	*Linker sequence*	*Particle titer*	*Infectious titer*	*HSPG binding*	*Epitope display*	*Type*
AAV-A161BPV/ALS	TG–ALS	4.0×10^7	1.2×10^5	++	++	III
AAV-A161BPV/LLA	TG–LLA	1.4×10^6	5.9×10^2	++	++	III
AAV-A161BPV/GLS	TG–GLS	1.2×10^7	8.7×10^4	++	++	III
AAV-A584BPV/ALS	TG–ALS	3.0×10^7	6.5×10^2	++	++	III
AAV-A584BPV/LLA	TG–LLA	1.3×10^7	—	++	+	II
AAV-A584BPV/GLS	TG–GLS	$<10^2$	—	—	—	II
AAV-A587BPV/ALS	TG–ALS	1.8×10^7	5.0×10^1	++	++	III
AAV-A587BPV/LLA	TG–LLA	7.2×10^5	—	+	—	II
AAV-A587BPV/GLS	TG–GLS	3.5×10^7	2.7×10^2	++	++	III

AAV2 without disrupting any of the essential functions of the AAV viral capsid proteins, since the mutant vectors can be efficiently produced and retain their ability to direct transgene delivery to the nucleus of target cells. Furthermore, we demonstrate heparan-independent targeted transduction of cells by AAV2-based vectors.

Generation of AAV vectors with mutant capsids

We constructed 38 mutants by insertion of small peptide epitopes at 25 unique sites within the AAV2 capsid. Some mutants contained small, two-amino acid insertions, whereas others contained larger insertions that could be used to assess epitope display or could bind alternative cell surface receptors and possibly redirect vector tropism to receptor-bearing cells. The mutants were grouped into three classes based on their phenotypes (Table 2).

Most of the mutants that were noninfectious were either unable to assemble capsids or assembled capsids that were not stable. These mutants (classes I and II) showed no regional specificity with regard to the location of the insertions within the predicted AAV2 structure (Fig. 4). In fact, the sites of peptide insertion of several of these mutants were the same as many infectious mutants (class III), the only difference being the primary amino acid sequence of the inserted motifs. This suggests that a major determinant in maintaining infectivity is the maintenance of capsid assembly or stability by inclusion of appropriate linker/scaffolding sequences.

Four noninfectious mutants failed to produce capsids, suggesting that capsid assembly was sensitive to peptide insertion. The fact that two of these mutants had small insertions, that is, two amino acids, highlights this point. The remaining noninfectious mutants produced viable capsids; however, these mutants were uniformly defective in their ability to package vector genomes that were resistant to DNase digestion. The two most likely explanations for this observation are that these mutants are defective in DNA packaging or produced unstable particles. It seems reasonable that insertion of additional residues may result in the assembly of a defective particle that fails to protect its genome as effectively from nuclease digestion. The finding that different insertions into the same site can have different phenotypes is supportive of this hypothesis. For instance, mutant A584BPV/GLS is a class II mutant that packages few DNase-resistant genomes. However, mutant A584BPV/ALS, which is essentially the same as A585BPV/GLS except for a G→A substitution in the linker sequence, is fully infectious and packages wild-type levels of DNase-resistant vector genomes. Here, it appears that the different linker sequence causes a localized destabilization of the capsid structure, which is not as effective at protecting the genome from nuclease digestion. On the other hand, two noninfectious mutants (A595-4C-RGD/GLS and A597-4C-RGD/GLS) produced viable capsids that were empty. These mutants are apparently defective in packaging viral DNA and are located in putative loop IV (Fig. 4). It is not clear what the mechanism of viral DNA packaging is. Ruffing *et al.* (1992) demonstrated that empty capsids could assemble in the absence of viral DNA. Some studies have suggested that packaging is an active process that requires interaction of AAV Rep proteins with capsid proteins or is coupled with DNA replication (Zhou and Muzyczka, 1998). A DNA-packaging mutant was also reported by Wu *et al.* (2000), and it falls within the same putative loop region of the AAV2 capsid at residue 432. Further studies with these mutants may be helpful in understanding the mechanism of packaging.

Since the pAB-11 *lacZ* AAV genome is slightly larger than wild-type size (106%) we were concerned that it might be packaged less efficiently by some mutant capsids. However, we have not noted any differences in packaging efficiency in comparing

FIG. 3. LH mutant vectors can use an HS-independent pathway for infection of OVCAR-3 cells and are specifically targeted to the LH receptor. (A) OVCAR-3 cells treated without (*left*) or with (*right*) progesterone (50 μg/ml) were subsequently exposed for 2 hr at 4°C to either LH-mutant (AAV-A139LH-LacZ) or BPV-mutant (AAV-A139BPV-LacZ) vectors at an MOI of 100 pp/cell. Unbound virus was then removed, fresh medium was added, and the cells were stained with X-Gal after 48 hr. (B and C) Same as for (A), except that HeLa and OVCAR-3 cells were used and the mutant viruses were bound to the cells for 2 hr at 4°C either in the presence (solid columns), or absence (open columns), of heparin sulfate (500 μg/ml). In (C) vector binding was also blocked with luteinizing hormone (LH, 200 μg/ml). Data represent the means and standard deviations of triplicate experiments. ***$p < 0.005$.

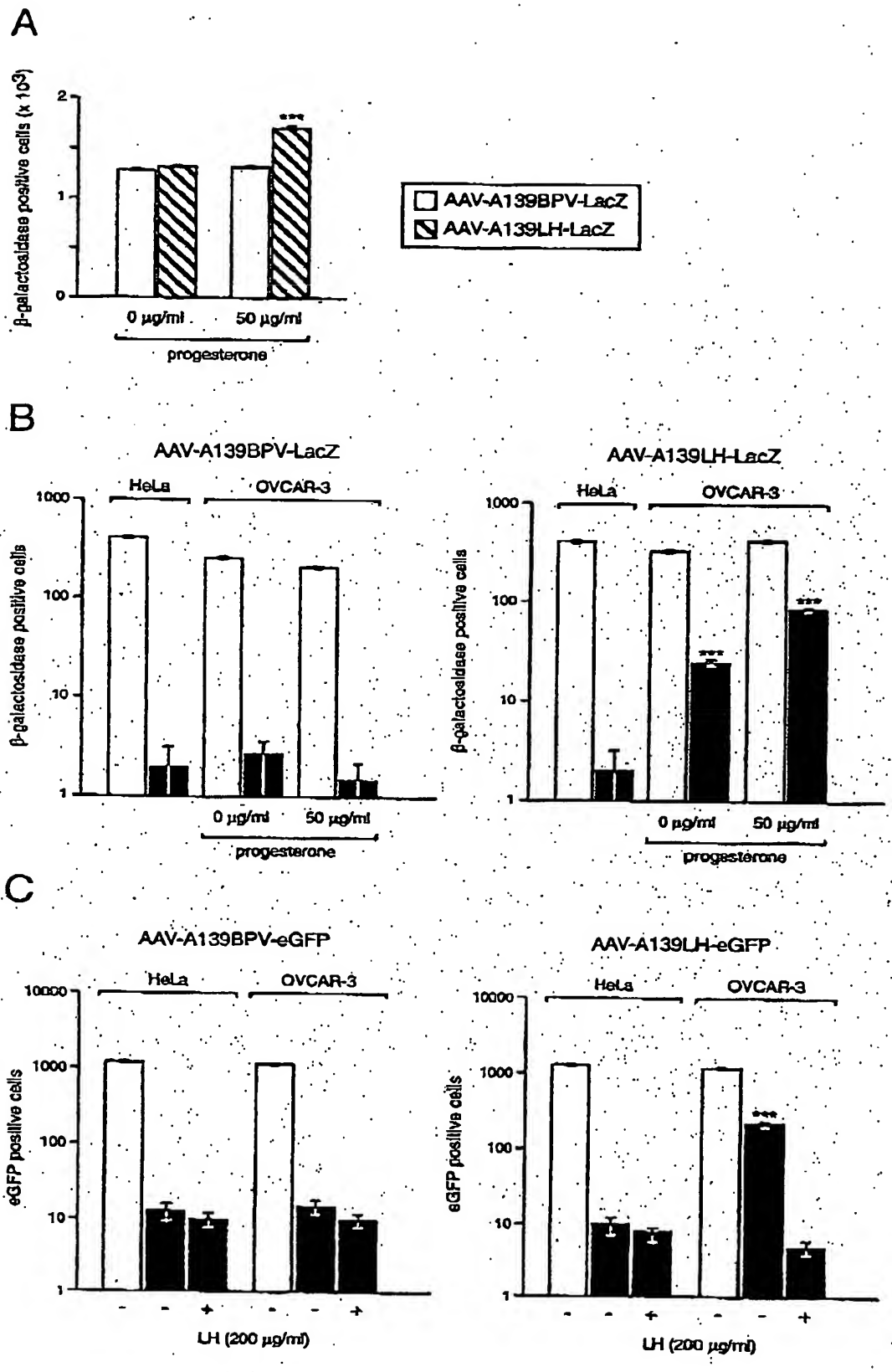
A
β-galactosidase positive cells (x 10³)
2
1
0
***
0 μg/ml
50 μg/ml
progesterone
AAV-A139BPV-LacZ
AAV-A139LH-LacZ
B
AAV-A139BPV-LacZ
AAV-A139LH-LacZ
β-galactosidase positive cells
1000
100
10
1
HeLa
OVCAR-3
***
0 μg/ml
50 μg/ml
progesterone
C
AAV-A139BPV-eGFP
AAV-A139LH-eGFP
eGFP positive cells
10000
1000
100
10
1
HeLa
OVCAR-3
***
- - + - - +
LH (200 μg/ml)

the pAB-11 *lacZ* genome with the pTR-UF5 eGFP genome, which is only 72% of wild-type size.

The majority of the noninfectious mutants are inefficient at packaging DNase-resistant genomes. However, since most of them are still capable of assembling some complete particles, they must be secondarily defective in an aspect of the viral entry pathway. Approximately half of these (class II) mutants are unable to bind to heparin sulfate (HS) (Table 3 and Fig. 1). Heparin sulfate has been shown to be the primary cell surface receptor for AAV2 (Summerford and Samulski, 1998). However, since all of the mutants shown to be defective in HS binding were also poor at protecting viral genomes from DNase digestion, it seems possible that the defect in HS binding was due to a general destabilization of the particle, altering either the display or structure of the HS-binding epitope, rather than a specific mutation within this epitope. These findings are significant in light of reports that suggest the existence of two blocks of residues on the surface of AAV capsids involved in HS binding (Wu *et al.*, 2000). Several of the HS-binding mutants identified here fall within these two clusters (e.g., mutants A520LH/GLS and A584BPV/GLS). Interestingly, HS binding can be rescued in these mutants by changing the linker sequences used to display the foreign ligands. For example the HS-binding negative mutant A584BPV/GLS can be rescued by changing the linker sequence from GLS to ALS (Table 5). This single-residue change is also associated with a three orders of magnitude increase in DNA particle titer. Therefore, although this location within the AAV capsid protein can obviously impact heparin binding, there is no evidence that this region is directly involved in receptor binding. As such, the reported heparin-binding motifs must be viewed with skepticism and it is more likely that mutations within these regions have strained the local three-dimensional structure of the capsid resulting in a secondary loss of heparin binding rather than a primary disruption of the HS-binding epitope. Interestingly, one HS-binding mutant we identified retained infectivity (A312; Tables 2 and 3 and Fig. 1). Although the infectious titer of this mutant is reduced by several orders of magnitude, further studies with this mutant may be helpful in understanding secondary mechanisms of infection.

Display of foreign ligands on the surface of AAV vectors

As shown by immunoprecipitation with an antibody against the BPV epitope, nearly all of the BPV insertion mutants reacted with this antibody (Table 3 and Fig. 2), suggesting that the BPV epitope was present on the surface of the capsid. Differences in capsid protein band intensity (Fig. 2) are a combined result of different efficiencies of virus assembly and varying accessibility of the BPV sequence for the anti-BPV antibody, which seems to be dependent on the site of insertion and the linker sequences used to display the epitope (Table 3 and Fig. 2). In all cases where stable, high-titer particles were produced, the epitope was efficiently displayed on the capsid surface (A139BPV/GLS, A161BPV/GLS, A161BPV/ALS, A161BPV/LLA, A459BPV/GLS, A584BPV/ALS, A584BPV/LLA, A587BPV/ALS, and A587BPV/GLS). Mutants that were unable to assemble particles efficiently, or produced less stable particles, did not efficiently display the BPV epitope (A339BPV and A520BPV/GLS). Furthermore, those mutants with inappropriate linker sequences flanking the BPV epitope were also not efficiently precipitated with the anti-BPV antibody (Table 4 and Fig. 2). It seems likely that this difference is due to a reduced accessibility of the BPV sequence for the anti-BPV antibody since particle titers of these mutants, although lower than wild type, were still well above the level of detection by Western blot if the immunoprecipitation step was omitted (data not shown).

In one case the type of inserted ligand had a dramatic effect on infectious titer. Mutants A459BPV/GLS and A459LH/GLS contain different ligands inserted at the same site within the AAV VP3 region. The linker sequences used to display these epitopes were also the same. However, the BPV mutant was fully infectious, whereas the LH mutant was completely noninfectious (Table 2). Whether this difference is due to the length of the insertion (11 vs. 15 residues), or the primary amino acid sequence of the insertion, remains to be determined.

Identification of optimal sites for heterologous ligand insertion

Of importance was not only the identification of key positions on the surface of viral particle, but the fact that our mutagenesis strategy simultaneously showed that each of these sites was capable of accepting foreign ligand insertions for retargeting of the particle to alternative receptors. These positions are in the N-terminal region of VP2 (following amino acid 139 or 161), and the loop IV region of VP3 (following amino acid 459, 584, or 587). All of these locations were capable of tolerating peptide insertions of up to 15 amino acids and in most cases allowed the production of recombinant virus at titers that were essentially the same as wild type. In addition, we have shown that there is often a requirement for the inclusion of appropriate linker sequences in the design of the inserted ligands and have identified optimal linkers for this purpose.

Generation of AAV vectors with altered tropism

On the basis of our findings on accessibility of the capsid protein-localized BPV peptides, we hypothesized that positioning LH peptide epitopes at the same sites should make these ligands available for efficient interaction with LH receptors on the cell surface. By using an immunoprecipitation assay, we were able to show efficient display of the LH motifs on mutant virus particles (data not shown). This finding provided the rationale for the generation of a recombinant AAV vector, A139LH/GLS, containing an LH peptide insertion in the AAV VP1 capsid protein ORF, and testing this mutant for its ability to direct gene transfer to receptor-bearing cell lines. The data generated with A139LH/GLS on OVCAR-3 and HeLa cell lines showed that this virus demonstrates a profile of gene transfer significantly different from those of virus with unmodified capsid or with nontargeting capsid modifications. This difference was especially dramatic when LH receptor expression was increased on the target cells by preincubation with progesterone, or when the endogenous HS-dependent cellular interaction was competed with soluble HS. These findings highlight the specificity of the retargeted virus for the LH receptor, but, more importantly, they demonstrate that infection can proceed via an

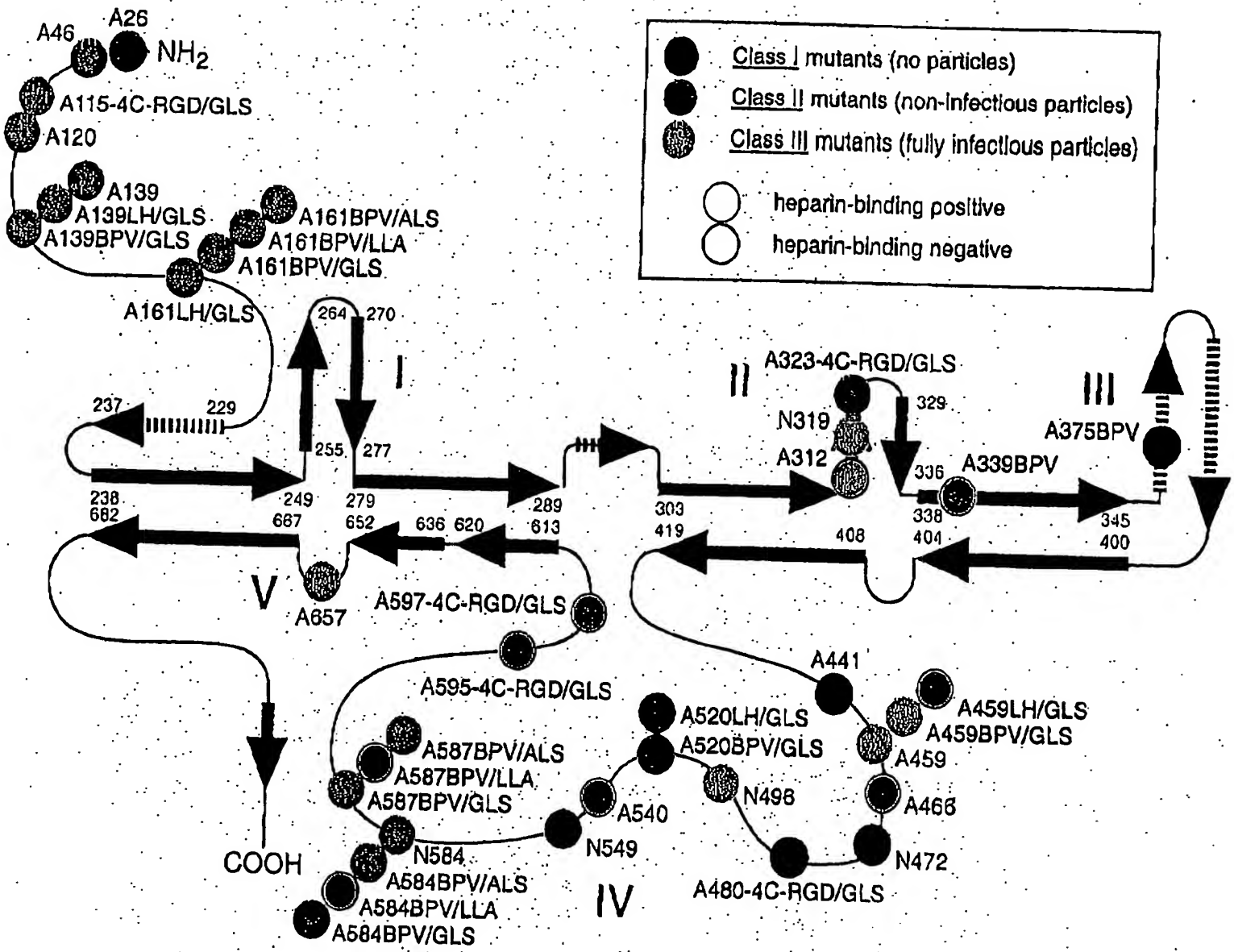

FIG. 4. Distribution of insertion mutants. The positions of the various insertion mutants are shown on a diagram of the computer-generated model of secondary structure of the AAV capsid protein. Amino acid positions are illustrated in light blue. Heavy arrows represent strongly predicted β sheets, whereas dashed arrows represent weakly predicted β sheets. The five putative loop regions are numbered I–V. The colors of the circles indicate the phenotypes of the mutants as described in the legend.

alternative receptor and show that infection can occur in the absence of the endogenous HSPG interaction.

Successful utilization of the LH peptide incorporated into the AAV capsid protein for the purposes of vector retargeting suggests that other peptide ligands may work just as well in the same context. In this regard, the rapidly emerging technology of phage display libraries has proved its utility as a means to identify peptides that are able to bind specifically to certain molecules on a cell surface *in vivo*. This high-throughput method is based on the capability of small peptide ligands to target a bacteriophage particle to previously characterized as well as uncharacterized structures on a cell membrane. Successes in phage biopanning in an *in vivo* context (Arap *et al.*, 1998; Johns *et al.*, 2000) strongly suggest that this novel technology may prove a useful source of targeting peptides to be used for modification of endogenous tropism of recombinant AAV vectors.

Although we have demonstrated the utility of small peptides to be incorporated into a number of preferred sites within the AAV capsid protein, the size restrictions of these locales have not been fully defined. In this regard, the compatibility of the capsid structure with protein ligands of a larger size, such as, for example, single-chain antibodies (scFv), would significantly expand the range of potential targeting applications. Furthermore, although we have demonstrated that including appropriate residues on either side of the displayed heterologous motif is a viable approach to promote particle stability and epitope display, our attempts to similarly minimize distortion of the local capsid structure by inclusion of disulfide linkages were unsuccessful. It is clear that a more detailed understanding of AAV capsid structure is needed to aid in the development of this technology.

ACKNOWLEDGMENTS

We thank Dr. J. Kleinschmidt for kindly providing us with the monoclonal antibodies A20 and B1. We also thank Dr. R.J. Samulski for providing pACG2 and pXX6 plasmid. We acknowledge the Vector Core Laboratory at the Children's Research Institute, Children's Hospital (Columbus, OH) and Dr. K.R. Clark for technical assistance on recombinant AAV production and titering. We also thank Angela Young for help on this project. This work was supported by grants from the National Institutes of Health (R21 DK55557) and the Children's Research Institute (Columbus, OH).

REFERENCES

ABRAHAMSSON, G., JANSON, P.O., and KULLANDER, S. (1997). Steroid release from two human epithelial ovarian tumors: Evidence for an intrinsic production in vitro. Gynecol. Oncol. 64, 99–104.

AGBANDJE, M., KAJIGAYA, S., McKENNA, R., YOUNG, N.S., and ROSSMANN, M.G. (1994). The structure of human parvovirus B19 at 8 Å resolution. Virology 203, 106–115.

AGBANDJE-McKENNA, M., LLAMAS-SAIZ, A.L., WANG, F., TATTERSALL, P., and ROSSMANN, M.G. (1998). Functional implications of the structure of the murine parvovirus, minute virus of mice. Structure 6, 1369–1381.

ARAP, W., PASQUALINI, R., and RUOSLAHTI, E. (1998). Cancer treatment by targeted drug delivery to tumor vasculature in a mouse model. Science 279, 377–380.

BARTLETT, J.S. (1999). Prospects for the development of targeted adeno-associated virus (AAV) vector systems. Tumor Targeting 4, 143–149.

BARTLETT, J.S., SAMULSKI, R.J., and McCOWN, T.J. (1998). Selective and rapid uptake of adeno-associated virus type 2 in brain. Hum. Gene Ther. 9, 1181–1186.

BARTLETT, J.S., KLEINSCHMIDT, J., BOUCHER, R.C., and SAMULSKI, R.J. (1999a). Targeted adeno-associated virus vector transduction of nonpermissive cells mediated by a bispecific F(ab'γ)$_2$ antibody [published erratum appears in Nat. Biotechnol. 1999;17:393]. Nat. Biotechnol. 17, 181–186.

BARTLETT, J.S., WILCHER, R., and SAMULSKI, R.J. (1999b). Infectious entry pathway of adeno-associated virus and adeno-associated virus vectors. J. Virol. 74, 2777–2785.

CHAPMAN, M.S., and ROSSMANN, M.G. (1993). Structure, sequence, and function correlations among parvoviruses. Virology 194, 491–508.

CHIORINI, J.A., YANG, L., LIU, Y., SAFER, B., and KOTIN, R.M. (1997). Cloning of adeno-associated virus type 4 (AAV4) and generation of recombinant AAV4 particles. J. Virol. 71, 6823–6833.

CHOU, P.Y., and FASMAN, G.D. (1978). Prediction of the secondary structure of proteins from their amino acid sequence. Adv. Enzymol. Relat. Areas Mol. Biol. 47, 45–148.

CLARK, K., VOULGAROPOULOU, F., and JOHNSON, P. (1996). A stable cell line carrying adenovirus-inducible *rep* and *cap* genes allows for infectivity titration of adeno-associated virus vectors. Gene Ther. 3, 1124–1132.

CLARK, K.R., LIU, X., McGRATH, J.P., and JOHNSON, P.R. (1999). Highly purified recombinant adeno-associated virus vectors are biologically active and free of detectable helper and wild type viruses. Hum. Gene Ther. 10, 1031–1039.

DELEAGE, G., and ROUX, B. (1987). An algorithm for protein secondary structure prediction based on class prediction. Protein Eng. 1, 289–294.

DUAN, D., YUE, Y., YAN, Z., McCRAY, P.B., JR., and ENGELHARDT, J.F. (1998). Polarity influences the efficiency of recombinant adenoassociated virus infection in differentiated airway epithelia. Hum. Gene Ther. 9, 2761–2776.

GARNIER, J., GIBRAT, J.F., and ROBSON, B. (1996). GOR method for predicting protein secondary structure from amino acid sequence. Methods Enzymol. 266, 540–553.

GIROD, A., RIED, M., WOBUS, C., LAHM, H., LEIKE, K., KLEINSCHMIDT, J., DELEAGE, G., and HALLEK, M. (1999). Genetic capsid modifications allow efficient re-targeting of adeno-associated virus type 2 [published erratum appears in Nat. Med. 1999;5:1438]. Nat. Med. 5, 1052–1056.

GOODMAN, S., XIAO, X., DONAHUE, R.E., MOULTON, A., MILLER, J., WALSH, C., YOUNG, N.S., SAMULSKI, R.J., and NIENHUIS, A.W. (1994). Recombinant adeno-associated virus-mediated gene transfer into hematopoietic progenitor cells. Blood 84, 1492–1500.

GRAHAM, F.L., SMILEY, J., RUSSELL, W.C., and NAIRN, R. (1977). Characteristics of a human cell line transformed by DNA from human adenovirus type 5. J. Gen. Virol. 36, 59–74.

GRIMM, D., KERN, A., PAWLITA, M., FERRARI, F., SAMULSKI, R., and KLEINSCHMIDT, J. (1999). Titration of AAV-2 particles via a novel capsid ELISA: Packaging of genomes can limit production of recombinant AAV-2. Gene Ther. 6, 1322–1330.

HAMILTON, T.C., YOUNG, R.C., and OZOLS, R.F. (1984). Experimental model systems of ovarian cancer: Applications to the design and evaluation of new treatment approaches. Semin. Oncol. 11, 285–298.

HERMONAT, P.L., LABOW, M.A., WRIGHT, R., BERNS, K.I., and MUZYCZKA, N. (1984). Genetics of adeno-associated virus: Isola-

tion and preliminary characterization of adeno-associated virus type 2 mutants. J. Virol. 51, 329–333.

JANIK, J.E., HUSTON, M.M., and ROSE, J.A. (1984). Adeno-associated virus proteins: Origin of the capsid components. J. Virol. 52, 591–597.

JI, T.H., RYU, K.S., GILCHRIST, R., and JI, I. (1997). Interaction, signal generation, signal divergence, and signal transduction of LH/CG and the receptor. Recent Prog. Horm. Res. 52, 431–453.

JOHNS, M., GEORGE, A.J., and RITTER, M.A. (2000). In vivo selection of sFv from phage display libraries. J. Immunol. Methods 239, 137–151.

KAY, M.A., MANNO, C.S., RAGNI, M.V., LARSON, P.J., COUTO, L.B., McCLELLAND, A., GLADER, B., CHEW, A.J., TAI, S.J., HERZOG, R.W., ARRUDA, V., JOHNSON, F., SCALLAN, C., SKARSGARD, E., FLAKE, A.W., and HIGH, K.A. (2000). Evidence for gene transfer and expression of factor IX in haemophilia B patients treated with an AAV vector. Nat. Genet. 24, 257–261.

KONISHI, I., KURODA, H., and MANDAI, M. (1999). Review: Gonadotropins and development of ovarian cancer. Oncology 57(Suppl. 2), 45–48.

LI, J., SAMULSKI, R.J., and XIAO, X. (1997). Role for highly regulated *rep* gene expression in adeno-associated virus vector production. J. Virol. 71, 5236–5243.

McKENNA, R., OLSON, N.H., CHIPMAN, P.R., BAKER, T.S., BOOTH, T.F., CHRISTENSEN, J., AASTED, B., FOX, J.M., BLOOM, M.E., WOLFINBARGER, J.B., and AGBANDJE-McKENNA, M. (1999). Three-dimensional structure of Aleutian mink disease parvovirus: Implications for disease pathogenicity. J. Virol. 73, 6882–6891.

OKADA, H., MIYAMURA, K., ITOH, T., HAGIWARA, M., WAKABAYASHI, T., MIZUNO, M., COLOSI, P., KURTZMAN, G., and YOSHIDA, J. (1996). Gene therapy against an experimental glioma using adeno-associated virus vectors. Gene Ther. 3, 957–964.

RABINOWITZ, J.E., XIAO, W., and SAMULSKI, R.J. (1999). Insertional mutagenesis of AAV2 capsid and the production of recombinant virus. Virology 265, 274–285.

RUFFING, M., ZENTGRAF, H., and KLEINSCHMIDT, J.A. (1992). Assembly of viruslike particles by recombinant structural proteins of adeno-associated virus type 2 in insect cells. J. Virol. 66, 6922–6930.

SANES, J.R., RUBENSTEIN, J.L.R., and NICOLAS, J.F. (1986). Use of a recombinant retrovirus to study post-implantation cell lineage in mouse embryos. EMBO J. 5, 3133–3142.

SUMMERFORD, C., and SAMULSKI, R.J. (1998). Membrane-associated heparan sulfate proteoglycan is a receptor for adeno-associated virus type 2 virions. J. Virol. 72, 1438–1445.

TRATSCHIN, J.-D., MILLER, I.L., and CARTER, B.J. (1984). Genetic analysis of adeno-associated virus: Properties of deletion mutants constructed in vitro and evidence for an adeno-associated virus replication function. J. Virol. 51, 611–619.

TSAO, J., CHAPMAN, M.S., AGBANDJO, M., KELLER, W., SMITH, K., WU, H., LUO, M., SMITH, T.J., ROSSMAN, M.G., COMPANS, R.W., and PARRISH, C.R. (1991). The three-dimensional structure of canine parvovirus and its functional implications. Science 25, 1456–1464.

WISTUBA, A., WEGER, S., KERN, A., and KLEINSCHMIDT, J.A. (1995). Intermediates of adeno-associated virus type 2 assembly: Identification of soluble complexes containing Rep and Cap proteins. J. Virol. 69, 5311–5319.

WU, P., XIAO, W., CONLON, T., HUGHES, J., AGBANDJE-McKENNA, M., FERKOL, T., FLOTTE, T., and MUZYCZKA, N. (2000). Mutational analysis of the adeno-associated virus type 2 (AAV2) capsid gene and construction of AAV2 vectors with altered tropism. J. Virol. 74, 8635–8647.

XIAO, X., LI, J., and SAMULSKI, R. (1998). Production of high-titer recombinant adeno-associated virus vectors in the absence of helper adenovirus. J. Virol. 72, 2224–2232.

YANG, Q., MAMOUNAS, M., YU, G., KENNEDY, S., LEAKER, B., MERSON, J., WONG-STAAL, F., YU, M., and BARBER, J.R. (1998). Development of novel cell surface CD34-targeted recombinant adeno-associated virus vectors for gene therapy. Hum. Gene Ther. 9, 1929–1937.

ZHOU, X., and MUZYCZKA, N. (1998). In vitro packaging of adeno-associated virus DNA. J. Virol. 72, 3241–3247.

ZOLOTUKHIN, S. (1999). Recombinant adeno-associated virus purification using novel methods improves infectious titer and yield. Gene Ther. 6, 973–985.

Address reprint requests to:
Jeffrey S. Bartlett
Children's Research Institute, Room W531
700 Children's Drive
Columbus, OH 43205

E-mail: BartlettJ@pediatrics.ohio-state.edu

Received for publication March 6, 2001; accepted after revision July 26, 2001.

Published online: August 15, 2001.